

Glucose as a Potent Inducer of Cell Death in Yeast

Sara Raquel Reis de Oliveira

Dissertation to obtain the Master Degree in
Biological Engineering

Jury

Presidente: Prof. Maria Raquel Murias dos Santos Aires Barros,
Departamento de Bioengenharia (DBE)

Orientação: Prof. Isabel Maria de Sá Correia Leite de Almeida,
Departamento de Bioengenharia (DBE)
Dr. Beatriz Monge Bonini, Katholieke Universiteit Leuven

Vogal: Dr. Sandra Sofia Costa dos Santos

October 2011

ACKNOWLEDGEMENTS

Now, that another chapter of my academic formation is written, I would like to thank you to all of those that somehow helped me during this project:

First of all, I would like to thank to the promoters of my work, Prof. Johan Thevelein from KUL and Prof. Isabel Sá-Correia from IST. Without them, it wouldn't be possible. To PhD. Beatriz Monge Bonini, my supervisor, for all the patient guidance and teaching, caring support and friendship. I can't thank you enough.

For the colleagues from the MCB laboratory and new friends: Betty, Alessandro, Georg, Tom, Dries, Nico, Yudi, Jurgen, Bram, Ben, Dorota, Marta and Steijn. I really appreciate all the good moment and valuable knowledge that you gave me. I couldn't forget Ken! To him a special thank you for sharing with me the bench, the knowledge, the traditional Belgium meals, the funny discussions, the worries, the celebrations and much more. Dank u well!

For the friends from all times, I would like to thank you for helping me feeling home even if I was really far away. Would not be fair not mentioning Nuno Bernardes. The reason why I ended up in central Europe (Leuven) and the start of all of these. Thanks for the advices and availability.

The most valuable element during this journey was my family: Obrigada por tudo!

ABSTRACT

The aim of the present work was the study of the apoptotic mechanisms induced by glucose in *Saccharomyces cerevisiae* *TPS1* deletion mutant. The *TPS1* gene encodes the Trehalose-6-phosphate synthase. When cells of this mutant were exposed to glucose, they lost progressively the capacity to proliferate but maintained the membrane integrity for much longer time, what was evaluated by using the fluorescent probes oxonol and propidium iodide. The overexpression of *pPDE2* recovered viability of the *tps1Δ* mutant to a high extent when compared to the wild type. After glucose addition, the presence of apoptotic and/or necrotic phenotypes was analyzed by the detection of accumulated intracellularly reactive oxygen species (ROS), assessed by 2',7'-dichlorodihydrofluorescein diacetate and 123 DihydroRhodamine, by the presence of DNA fragmentation evaluated by TUNEL assay, phosphatidylserine (PS) externalization visualized by the fluorescent Annexin-V binding and finally, by the release of cytochrome c to the cytosol, detected by western blot.

Altogether, the results obtained indicate that exposition of yeast cells with *TPS1* gene deleted to different glucose concentrations, from 5 to 100 mM glucose, results in growth arrest originated by apoptotic cell death, rather than necrotic death.

Keywords: *Saccharomyces cerevisiae*, glucose signaling, cAMP pathway, ROS production, apoptosis and necrosis.

RESUMO

O presente trabalho teve como objectivo o estudo dos mecanismos apoptóticos induzidos por glucose no mutante de eliminação de *TPS1* em *Saccharomyces cerevisiae*. O gene *TPS1* codifica a Trealose-6-fosfato sintase. Quando as células de levedura deste mutante são expostas a glucose, estas perdem progressivamente a capacidade de proliferar contudo mantêm a integridade membranar por um período maior, esta última avaliada pelos flurocromos Bis-oxonol e Iodeto de Propídio. A sobreexpressão de *pPDE2* recuperou extensivamente a viabilidade do mutante *tps1Δ* quando comparado com células de *wt*. Após adição de glucose, a presença dos fenótipos de apoptose e/ou necrose foi analisada, verificando-se a acumulação intracelular de espécies reactivas de oxigénio (ERO), avaliada através de diacetato de 2',7'-dicloro-dihidrofluoresceína e 123 DihidroRodamina, a ocorrência de fragmentação de ADN observada no ensaio TUNEL, a externalização de fosfatidilserina visualizada pela ligação fluorescente de Anexina-V e para finalizar o registo de liberação de citocromo c para o citosol por western blot.

Em conjunto, os resultados obtidos indicam que a exposição de células de levedura com o gene *TPS1* eliminado a diferentes concentrações de glucose, entre 5 a 100 mM de glucose, provoca uma paragem de crescimento originada por morte celular apoptótica, ao invés de morte necrótica.

Palavras-chave: *Saccharomyces cerevisiae*, glucose; sinalização, via do AMP cíclico, produção de ERO, apoptose e necrose.

INDEX

1. LITERATURE OVERVIEW	1
1.1 Nutrient Availability and Yeast Growth	1
1.1.1 S. cerevisiae Growth Curve: Glucose influence.....	1
1.2 Glucose Metabolism Machinery.....	3
1.2.1 Sensing	3
1.2.2 Transporters	4
1.2.3 Signal Transduction	6
1.2.3.1 cAMP-PKA pathway activators.....	6
1.2.3.2 Protein Kinase A role	8
1.2.3.3 cAMP-PKA pathway regulation through cAMP control.....	8
1.3 Trehalose pathway	9
1.3.1 Trehalose synthesis	9
1.3.2 Hxk2 inhibition by trehalose 6-phosphate.....	9
1.3.3 Influence on glycolysis upon TPS1 deletion	10
1.4 Programmed Cell Death Modes	11
1.4.1 Apoptosis.....	12
1.4.1.1 Apoptotic markers in yeast.....	14
1.4.1.1.1 Cytochrome c release.....	15
1.4.1.1.2 Reactive Oxygen Species.....	17
1.4.1.1.3 DNA fragmentation	18
1.4.1.1.4 Phosphatidylserine exposure	19
1.4.1.2 Ras-cAMP-PKA pathway importance in yeast apoptosis.....	20
1.4.2 Necrosis	21
2. MATERIALS AND METHODS	24
2.1 Strains and Growth Conditions	24
2.2 Yeast Genomic DNA Preparation.....	24
2.3 PCR: Polymerase Chain Reaction	24
2.4 Spot Assay/Drop Test	25
2.5 Clonogenic Assay	25
2.6 Isolation of Mitochondrial and Post Mitochondrial Fractions	26
(Cytochrome C Release).....	26
2.7 Immunoprecipitation Assay / S-nitrosylation of GAPDH.....	27
2.7.1 Preparation of Yeast Protein Extracts	27
2.7.2 Immunoprecipitation	27

2.8	Measuring Protein Concentration.....	28
2.9	SDS-PAGE and Western Blotting	28
2.10	Fluorescence Microscopy.....	28
2.10.1	Reactive Oxygen Species Accumulation.....	29
2.10.1.1	Hydrogen Peroxidase Formation.....	29
2.10.1.2	Superoxide Anion Formation	29
2.10.2	Phosphatidylserine Residues Externalization.....	30
2.10.4	DNA Fragmentation (TUNEL Assay)	31
2.10.6	Viability Quantification	31
2.10.6.1	Oxonol staining	32
2.11	Determination of Ras2 Activity.....	32
3.	SOLUTIONS.....	Error! Bookmark not defined.
3.1	TE Buffer.....	67
3.2	TAE Buffer 10x (1% agarose).....	67
3.3	Digestion Buffer (cyt c)	67
3.4	Lyticase Buffer	67
3.5	Annexin Buffer.....	67
3.6	ST-PMSF	67
3.7	Phosphate buffered saline (PBS).....	67
3.8	Lysis Buffer (Immunoprecipitation).....	67
3.9	Wash Buffer (Immunoprecipitation)	67
3.10	Protein sample buffer 5x.....	68
3.11	TBS 10x.....	68
3.12	TBST	68
3.13	MOPS Running buffer	68
	(NuPage® 20x, Invitrogen).....	68
3.14	MOPS Blotting buffer	68
3.15	Milk solution	68
3.16	Lysis buffer (RAS)	68
3.17	Wash buffer (RAS).....	68
4.	RESULTS.....	33
4.1	Deletion of <i>TPS1</i> Causes Growth Defect in Glucose Containing Medium.....	33
4.2	<i>Tps1</i> Deletion Mutant Presents a Glucose Induced Loss Of Viability	35
4.2.1	Proliferation Capacity	35
4.2.2	Cell Membrane Integrity	36
4.3	<i>Tps1</i> Deletion Mutant Presents Apoptotic Markers after Glucose Addition.....	38

4.3.1 ROS	38
4.3.2 Phosphatidyl Serine externalization	41
4.3.3 TUNEL	43
4.3.4 Cytochrome c Release	44
4.4 S-nitrosilation of GAPDH	45
4.5 <i>Tps1</i> Deletion Mutant Presents a High RAS Activity after Glucose Addition	46
4.6 The Deletion of Known Pro-apoptotic Proteins in <i>tps1Δ</i> Background Did not Result in Growth Recover after Glucose Addition	47
5. DISCUSSION	48
5.1 <i>Tps1</i> Deletion Mutant Growth Defect in already 2mM Glucose Containing Medium Can Be Restored by Overexpression of <i>PDE2</i>	48
5.2 Glucose Induces Loss of Viability in <i>tps1Δ</i> Deletion Mutant with Cell Membrane Integrity Maintenance	49
5.3 <i>TPS1</i> Deletion Mutant Undergoes Apoptosis after Glucose Addition	50
5.4 <i>Tps1</i> Deletion Mutant Pathway Disorder	51
5.5 Ras Activation Role in Regulating the Apoptotic Phenotype	51
5.6 Limit Between Apoptosis and Necrosis in <i>tps1Δ</i> Strain Seems Higher than 100 mM Glucose	52
6. CONCLUSIONS	54
BIBLIOGRAPHY	55

TABLES INDEX

Table 1 – Yeast strains used in the present work, respective relative genotypes and references.	24
Table 2 – Primers used in the present work.	25
Table 3 – PCR general program followed in the present work.....	25

FIGURES INDEX

Figure 1 – Typical growth curve Typical Yeast Growth Curve. <i>Saccharomydes cerevisiae</i> grown in YPD media at 30°C for 12 hours with data measurements every 2 minutes (Held, 2010).....	2
Figure 2 – Galactose metabolism. Pathway of extracellular galactose and glucose leading to glycolysis. Note that galactose enters the glycolytic mainstream bypassing the hexokinase step via the Leloir pathway (adapted from Bustamante and Pedersen, 1977).	2
Figure 3 – Glucose sensing by Snf3 and Rgt2 in <i>S. cerevisiae</i> and respective gene repression. Low extracellular glucose concentrations are sensed by Snf3 and high concentrations of glucose are sensed by Rgt2 (Filip Rolland, Joris Winderickx, and Johan M Thevelein 2002).....	4
Figure 4 - Structure of yeast sugar transporters. Generally, these proteins in yeasts have 12 hydrophobic transmembrane domains (represented as cylinders: 1-12) with both the N- and C-termini intracellularly disposed. The position of the five conserved sequence motifs that have been recognized in sugar transporters is represented in the figure by the letters (A-E). N-linked glycosylation can occur in the extracellular loop between helices 1 and 2 as shown (Leandro, Fonseca, and Gonçalves 2009).	6
Figure 5 – Glucose sensing and signaling in yeast (Rolland et al., 2001).	7
Figure 6 – cAMP-PKA pathway fraction (adapted from Santangelo, 2006).	8
Figure 7 - Pathways of glycogen and trehalose metabolism (Silva-udawatta and Cannon, 2001).....	10
Figure 8 - Temporal order of events occurring during acetic acid induced death in <i>S. cerevisiae</i> W303 strain (Pereira et al., 2008).	11
Figure 9 - Physiological scenarios of yeast apoptosis (Carmona-Gutierrez et al., 2010).	13
Figure 10 - Assays routinely used in the field of yeast PCD. (adapted from Carmona-Gutierrez et al., 2010).	15

Figure 11 - Models for the release of cytochrome c from mitochondria into cytosol. The outer mitochondrial membrane (OMM) ruptures as a result of the mitochondrial matrix swelling, allowing cytochrome c to escape from mitochondria (a, b). Model a involves the permeability-transition pore (PTP) opening whereas model b involves the voltage-dependent anion channel (VDAC) closure and inner mitochondrial membrane. A large channel forms in the OMM, allowing cytochrome c release, but mitochondria are not damaged (c–e). ANT, adenine-nucleotide translocator (Martinou, Desagher, and Antonsson 2000).....	16
Figure 12 – Oxidative stress severity and respective cell fade (Scherz-Shouval and Elazar, 2007).	18
Figure 13 - Schematic representation of the loss of membrane lipid asymmetry during apoptosis and specific binding of Annexin-V (van Engeland et al., 1998).....	20
Figure 14 - Yeast cells undergo apoptosis through hyperactivation of the Ras/cAMP/PKA signalling pathway upon several stimuli (adapted from Leadsham et al., 2010).....	21
Figure 15 - Schematic view of stimuli and cellular processes that interfere with yeast necrosis (Eisenberg et al., 2010).	22
Figure 16 - Apoptosis versus necrosis. A healthy cell (A) shrinks and its DNA - which usually is dispersed throughout the nucleus - starts to clump around the nucleus' edge (B). The nucleus and cell quickly break up, becoming apoptotic bodies (C), which are ingested by healthy cells nearby (D). Swelling and inflammation (E) is characteristic from necrosis. When a necrotic cell ruptures (F) it can damage nearby healthy tissue (Purdy, 1997).	23
Figure 17 – H2DCFDA-AM uptake and subsequent modifications (adapted from Held, 2010).....	30
Figure 18 – Growth of wt (left), <i>tps1Δ</i> (center) and <i>tps1Δ+pPDE2</i> (right) on 100 mM galactose (top) and several glucose concentrations (from 1 mM to 100 mM) in YP medium.	33
Figure 19 – Growth curves on 100 mM galactose medium (a) and several glucose concentrations: 1 mM (b), 2 mM (c), 5 mM (d), 20 mM (e), 50 mM (f) and 100 mM (g); of wt (full line), <i>tps1Δ</i> (dotted line), <i>tps1Δ+pPDE2</i> (dashed orange line). Cells were grown in galactose-containing medium until mid-exponential phase and transferred to fresh glucose-containing medium at an initial OD ₆₀₀ of 0.05. OD ₆₀₀ measurements were performed in a Bioscreen C apparatus (LabSystems).	34
Figure 20 – Clonogenic assay for wt (full line), <i>tps1Δ</i> (dotted line), <i>tps1Δ+pPDE2</i> (dashed line). Cells were grown until mid-exponential phase in YPGal and glucose was added, at time zero, to obtain different final concentrations: 5 mM (a), 20 mM (b), 50 mM (c) and 100 mM (d). Samples were collected at the time indicated, sequentially diluted to a final concentration corresponding to an	

OD ₆₀₀ of 0.0001 for the wt and <i>tps1Δ+pPDE2</i> and 0.001 for the <i>tps1Δ</i> and then plated on YPGal (in triplicate). Viability was estimated by c.f.u. counts. Are presented the most representative results from at least three independent experiments.....	36
Figure 21 - Oxonol molecule estructure.....	36
Figure 22 – Cell membrane integrity of wt (full line), <i>tps1Δ</i> (dotted line), <i>tps1Δ+pPDE2</i> (dashed line) during exposure to glucose. Cells were grown until mid-exponential phase in YPGal and glucose was added, at time zero, to several final concentrations: 20 mM (a), 50 mM (b) and 100 mM (c). Samples were collected at the times indicated and properly diluted. Viability was estimated by depolarized cells: evaluation of loss of plasma membrane integrity assessed with the fluorescent probe, DiBAC4(3) (Oxonol). Are presented the mean values from at least three independent experiments.....	38
Figure 23 – Representative image for comparison of different ROS type production in <i>tps1Δ</i> mutants. ROS accumulation was assessed by loading the cells with 123DHR and 2,7-CDCHF after glucose addition to final concentration of 50 mM. Wt always showed an insignificant level of ROS with both dyes as well as the <i>tps1Δ+pPDE2</i> cells (not shown). Fluorescent micrographs (a, c); DIC (phase contrast) image of the same cells (b, d).....	39
Figure 24 – Visualization of ROS production in wt, <i>tps1Δ</i> , <i>tps1Δ+pPDE2</i> and <i>tps1Δ Hxk2Δ</i> mutants. ROS accumulation was assessed by loading the cells with 123DHR after glucose addition to two different final concentrations (20 mM and 50 mM) and samples were visualized each 2h up to 8h. Here we just present the micrografs taken at 2h after glucose addition as in the succeeding hours there is no detectable difference (fluorescence is maintained). Wt showed always an insignificant level of ROS (a, b) as well as the <i>tps1Δ+pPDE2</i> and <i>tps1Δ Hxk2Δ</i> mutants. Meanwhile the <i>tps1Δ</i> showed an unequivocal increase in ROS levels with nearly all cells exhibiting ROS accumulation at all concentrations, maintaining it up to 8h post glucose addition (c, d). A specific field was selected to better observe the ROS accumulation after 2h in 50 mM glucose. Fluorescent micrographs were observed with filter set FITC (a, c); DIC (phase contrast) image of the same cells (b, d)	40
Figure 25 – Exposition of phosphatidylserines (PS) in the outer leaflet of the cytoplasmatic membrane with Annexin V – FLOUS (green) and necrotic cells with PI (orange-red), 4h and 7h after glucose addition to a final concentration of 50 mM. This double staining allowed us to realize that the wt (top panels) did not show a significant staining level at all conditions tested, whereas the <i>tps1Δ</i> (lower panels). A specific field was selected to better observe the cellular membrane fluorescence of <i>tps1Δ</i> after 4h in 50 mM glucose. Apoptotic cell (A), primary necrotic cell (PN) and	

secondary necrotic cells (SN). Fluorescent micrographs were observed with filter set FITC (a, c, e); DIC (phase contrast) image of the same cells (b, d, f).	42
Figure 26 – TUNEL assay, 4h after glucose addition to final different concentrations: 1 mM (a), 2 mM (b), 5 mM (c), 10 mM (d), 20 mM (e), 50 mM (f), 100 mM (g), wt (h), negative control (i), positive control (j). Fluorescent micrographs (left panels); DIC (phase contrast) image of the same cells (right panels).	43
Figure 27 –Immunodetection of cytochrome c (full line) and COX (dashed line) from time zero up to 5h post glucose addition in mitochondria (M) and in postmitochondrial supernatant (PMS) of wt (top panels), <i>tps1Δ</i> (middle panels) and <i>tps1Δ+pPDE2</i> (bottom panels). Two different glucose concentrations were evaluated: 20 mM (left panels) and 50 mM (right panels). The gel was loaded with 20 µg of protein from mitochondria samples and 100 µg of protein from postmitochondrial supernatant samples.	44
Figure 28- GAPDH is S-nitrosilated during glucose-induced apoptosis. Quantification of band intensity from western blot assay by densitometry. Band intensities were normalized to the intensity of IgG bands. Data express the GAPDH/IgG fold change in comparison to control (lane 1). Immunoprecipitation of S-nitrosilated GAPDH with an anti-CSNO antibody from cellular extracts of untreated, either glucose (100 mM) and DETA/NO-treated cell of wt (lanes 4 and 5) and <i>tps1Δ</i> (lanes 1 to 3).	45
Figure 29 – Ras2 is activated during glucose-induced apoptosis. Quantification of band intensity from a Western blot assay by densitometry. Band intensities were normalized to the intensity of pure protein bands. Data express the Ras activity fold change in comparison to control. Detection of Ras activity with an anti-Ras antibody from cellular extracts of untreated (100 mM galactose) and glucose-treated cell of <i>tps1Δ</i> (left bars) and <i>tps1Δ+pPDE2</i> (central bars) and wt (right bars) with different final concentrations. (1 mM, 2 mM, 5 mM, 20 mM, 50 mM, 100 mM).	46
Figure 30 – Growth of wt (column 1), <i>tps1Δ</i> (column 2) and several double deletion mutants (column 3 - 6) on 100 mM galactose (top) and several glucose concentrations (from 1 mM to 100 mM).	47

LIST OF ABBREVIATIONS

AIDA	advanced image data analyzer
AIDS	acquired immune deficiency syndrome
AMP	adenosine monophosphate
ANT	adenine-nucleotide translocator
ATP	adenosine triphosphate
BSA	bovine serum albumine
cAMP	cyclic adenosine monophosphate
DCDHF-DA	2,7-dichlorodihydrofluorescein diacetate
DCDHF	dichlorodihydrofluorescein
DCF	dichlorofluorescein
DHR 123	dihydrorhodamine 123
°C	Celsius degrees
c.f.u.	colony-forming units
Cyt c	cytochrome c
CSNO	S-nitrosocysteine
DAPI	4',6-diamidino-2-phenylindole
dATP	deoxyadenosine triphosphate
DDT	dichlorodiphenyltrichloroethane
DETA/NO	diethylenetriamine/nitric oxide
DHR123	dihydrorhodamine 123
DIC	differential interference contrast
DNA	deoxyribonucleic acid
dNTP	deoxyribonucleotide
EDTA	ácido etilenodiamino tetra-acético
e.g.	<i>exempli gratia</i>
et al.,	<i>et alii</i>
FACS	Fluorescence Activated Cell Sorting
FITC	fluorescein isothiocyanate
Fru1,6bP	fructose-1,6-biphosphate
FSC	forward scatter
GAPDH	Glyceraldehyde 3-phosphate dehydrogenase
Glu6P	Glucose-6-phosphate
GTP	guanine triphosphate
HEPES	4-(2-hydroxyethyl)-1-piperazineethanesulfonic acid
MOMP	mitochondrial outer membrane permeabilization
MOPS	3-(N-morpholino)propanesulfonic acid

mRNA	messenger ribonucleic acid
NAD	nicotinamide adenine dinucleotide
Nonidet P-40	octylphenoxypolyethoxyethanol
PBS	phosphate buffered saline
PCD	Programmed Cell Death
PCR	polymerase chain reaction
PI	propidium iodide
Pi	phosphate
PKA	protein kinase A
PMS	post-motichondrial supernatant
PMSF	phenylmethanesulfonylfluoride
PN	primary necrosis
PS	phosphatidylserine
PTP	permeability-transition pore
OD ₆₀₀	optical density measured at wave lenght 600 nm
OD ₆₆₀	optical density measured at wave lenght 660 nm
o.n.	over night
R123	rodamina 123
RBD	Ras binding domain
ROS	Reactive Oxygen Species
rpm	round per minute
RT-PCR	real time polymerase chain reaction
SDS-PAGE	sodium dodecyl sulfate polyacrylamide gel electrophoresis
SN	secondary necrosis
SSC	side scatter
STRE-genes	stress-responsive genes
TAE	tris acetate EDTA
TBS	tris-buffered saline
TdT	terminal deoxynucleotidyl transferase
TE	Tris-EDTA
Tris	2-amino-2-hidroximetil-1,3-propanodiol
Triton X-100	polyoxyethylene octyl phenyl ether
TUNEL	TdT-mediated dUTP nick end labeling
URA	uracil
UV	ultra violet
VDAC	voltagedependent anion channel
V _{max}	maximum velocity
YPD	yeast extract peptone dextrose

YPGal yeast extract peptone galactose
wt wild-type
w/v weight per volume

INTRODUCTION

Programmed cell death (PDC) defines all modes of death under molecular control and carried out in a controlled manner. Apoptosis has been classified as PCD and the role of apoptosis in multi-cellular organisms has been documented extensively. Apoptosis has a logical function in numerous developmental processes, for example cell death shapes the digits in fetal hands. In microorganisms, the functional role of apoptosis is less evident. The molecular hallmarks of apoptosis in cells of higher eukaryotes have also been discovered in cells of microbial microorganisms such as yeast. This has led to suggestions for a functional role of apoptosis in colonies or multicellular aggregates of single-celled microorganisms. The apoptotic markers in yeast can be triggered by a rather diverse array of unrelated compounds (for a review see (reviewed in Carmona-Gutierrez *et al.*, 2010; Sharon *et al.*, 2009). Recently, evidence suggested that necrosis, first described as an accidental uncontrolled form of death, can be regulated in yeast and also occurs under normal physiological conditions like aging. A variety of agents capable of inducing yeast apoptosis at low doses could shift cell death to a rather necrotic phenotype when used at higher concentrations (for a review see Eisenberg *et al.*, 2010).

Our previous results show that glucose, the most-preferred carbon substrate of many microorganisms, is a potent inducer of apoptosis in yeast cells in which downregulation of hexokinase activity is compromised. Yeast hexokinase is inhibited by trehalose-6-phosphate, the product of the *Tps1* enzyme. Absence of the inhibitor causes rapid expression of classical apoptotic markers followed by cell death upon addition of glucose. Deletion of the *HXK2* gene, encoding the major yeast hexokinase, prevents the glucose-induced apoptotic cascade. Also treatments or mutations inactivating respiration, counteracts to some extent apoptosis and cell death in *tps1* mutants. Interestingly, this suggests a process in yeast very similar to the well-known involvement of hexokinase and mitochondrial respiration in the control of apoptosis in mammalian cells. Our results also show that downregulation of the yeast Ras-cAMP-PKA pathway suppresses to some extent apoptosis and cell death in the *tps1* mutant. This suggests that hyperphosphorylation of sugar by hexokinase triggers apoptosis by overactivation of this signaling pathway. The Ras-cAMP-PKA pathway is well known to act as trigger of apoptosis and cell death in yeast (Hlavatá *et al.*, 2003; Gourlay and Ayscough, 2006).

The *Tps1* control of hexokinase was discovered because of the inability of *tps1* mutants to grow on glucose and related rapidly-fermented sugars. *Tps1* mutants grow on galactose, which is phosphorylated by galactokinase. Addition of only 1% glucose to galactose already causes a detectable growth inhibition, indicating extreme sensitivity of *tps1* mutants to glucose. Addition of glucose to *tps1* mutants causes hyperaccumulation of sugar phosphates, especially fructose-1,6-bisphosphate, and depletion of ATP and free phosphate (Neves *et al.*, 1995). This metabolic deregulation has logically been thought off as the reason why *tps1* mutants arrest growth after addition of glucose but it poorly explains the extreme sensitivity to even low levels of glucose. Our results show that glucose addition to cells of a *tps1Δ* mutant growing on galactose, not only causes growth arrest but rapid loss of viability. This loss of

viability is associated with rapid and strong expression of classical apoptotic markers: cytochrome c release from the mitochondria, dramatic formation of reactive oxygen species (ROS), phosphatidylserine (PS) exposure and chromatin fragmentation.

Deletion of *HXK2*, the gene encoding the most active isoenzyme in glucose phosphorylation, suppresses the glucose growth defect of the *tps1* mutant (Hohmann *et al.*, 1993) and also suppresses the appearance of all apoptotic markers tested. This indicates that glucose triggers apoptosis in the *tps1* mutant by causing Hxk2 hyperactivity.

Yeast mutants with an overactive Ras-cAMP-PKA pathway are well known to rapidly loose viability under conditions of slow growth or growth arrest. This is associated with appearance of typical apoptotic markers. This finding has identified the Ras-cAMP-PKA pathway as a central controller of yeast apoptosis but the connection with glucose as a trigger of this pathway (Longo 2004; Hlavatá *et al.*, 2008) has never been made. Glucose stimulates cAMP synthesis in yeast through a glucose-sensing G-protein coupled receptor Gpr1, which activates Gpa2, a second G-protein that in addition to Ras activates adenylate cyclase. Interestingly, rapid glucose-induced cAMP signaling through this GPCR system also requires glucose phosphorylation (Beullens *et al.*, 1988; Tamaki 2007). In the absence of the GPCR system, glucose is able to trigger partial cAMP signaling through this glucose phosphorylation-dependent pathway (S Colombo *et al.*, 1998; Kraakman *et al.*, 1999). Although the mechanism involved is unclear it may be due to a partial stimulation of Ras activity being required for sensitization of adenylate cyclase to stimulation by Gpa2 (S Colombo *et al.*, 1998). The growth defect on glucose of the *tps1* mutant can be suppressed by lowering the activity of the cAMP-PKA pathway. This was accomplished by overexpression of the high-affinity cAMP phosphodiesterase, encoded by *PDE2*, in the *tps1Δ* mutant. These results suggest that unbridled hexokinase activity triggers apoptosis by overstimulation of the cAMP-PKA pathway, possibly by enhancing Ras activity.

The objective of this research is to study the correlation between glucose, Ras activation and apoptosis in the yeast *Saccharomyces cerevisiae*. It will be also interesting to investigate if necrotic cell death is involved, knowing that the Ras2/PKA signalling belongs to one of the major pro aging pathways conserved in various organisms and regulates yeast chronological life span, where necrotic cell death is prominent as a physiological cause of cell death (reviewed in Eisenberg *et al.*, 2010). In the present work, we will use methods described in the literature to detect the presence of apoptotic markers in different strains after addition of glucose. For this purpose, fluorescent microscopy will be used to visualize the presence of apoptotic markers in the *Saccharomyces cerevisiae* strains wild type, *tps1Δ* and *tps1Δ* overexpressing the *PDE2* gene, by cell staining with propidium iodide (cell viability), annexin-V (phosphatidyl serine exposure), and dihydrorhodamine 123 (ROS accumulation). Apoptotic DNA fragmentation will be assessed by the TUNEL assay and Immunodetection through the Western blot method will be used to determine cytochrome c release from mitochondria. The activity of the Ras2 proteins (GTP/GDP loading state) involved in the cAMP-PKA pathway will be also determined as

previously described (Colombo *et al.*, 2004). Other proteins of the fungal apoptotic network already described as key proteins in regulating apoptotic-like cell death (ex. endonuclease G), will be studied as well, new deletions mutants will be constructed for this purpose.

1. LITERATURE OVERVIEW

1.1 Nutrient Availability and Yeast Growth

As a free-living microorganism, the characteristics of the surrounding environment are crucial for *Saccharomyces cerevisiae* growth, more specifically nutrient availability which is the factor that most influences the growth pattern. Yeast cells are capable of adapting their metabolism according to the nutrients that are present or absent. Nutritional conditions deeply affect cell growth. An example of this is nutrient starvation having the most dramatic effect in micro-organisms (Rolland *et al.*, 2002). Yeast cells undergoing a nutritional shift-up from a poor to a rich carbon source take several hours to adapt to the novel, richer carbon source, consequently in proliferation mode (Querin *et al.*, 2008). On the other way, by shutting down their metabolic activity and entering in cell cycle arrest, yeast cells can survive for long periods in a poor nutritional environment.

1.1.1 *S. cerevisiae* Growth Curve: Glucose influence

Depending on the characteristics of the medium, yeast cells show a specific growth pattern, although some general common phases can be identified (Figure 1).

When a culture of yeast cells is pinched in a fresh growth medium, they enter lag phase where they are biochemically active but not dividing. This phase refers the initial growth phase, when the number of cells remains relatively constant prior to rapid growth, also known as adaptation time. Here individual cells are actively metabolizing, in preparation for cell division. The cells usually activate the metabolic pathways to make enough essential nutrients to begin active growth. The extent of this phase depends on firstly the initial population size and physiological state, and secondly environmental conditions like temperature, pH, oxygen, salt concentration, nutrients and others.

Once the cell starts actively metabolizing, they begin DNA replication and shortly after cell division. This begins the second phase of growth called the exponential phase of growth. This is the period in which cell growth is the fastest. The time it takes the culture to double is called generation time. This exponential phase depends on several factors: the organism itself, the growth medium, and the temperature are all important factors in determining the generation time. The budding index is a physiologically relevant “global” parameter that reflects the complex links between cell growth and division that are both coordinately and deeply affected by nutritional conditions (Querin *et al.*, 2008).

The third major phase in growth of yeast is stationary phase when metabolism slows and the cells stop rapid cell division. The factors that cause cells to enter stationary phase are related to change in the environment typically caused by high cell density or nutrient exhaustion (Asaduzzaman, 2007). Here cells are characterized mainly by cell wall resistance to degrading enzymes (zymolyase, glusulase and

lyticase), they better resist some environmental stresses (as high temperatures and osmolarity), autophagy is prompted and reserve carbohydrates are vastly accumulated.

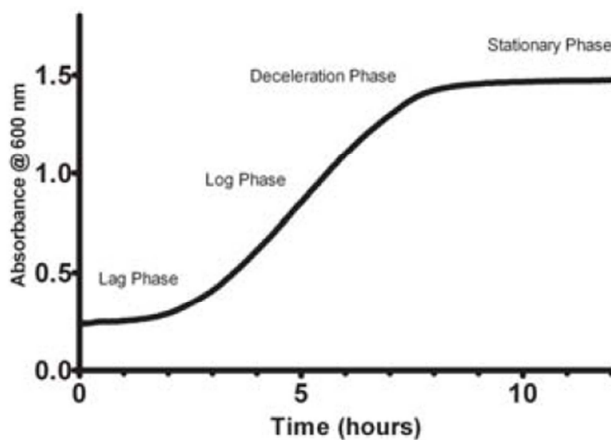


Figure 1 – Typical Yeast Growth Curve. *Saccharomyces cerevisiae* grown in YPD media at 30°C for 12 hours with data measurements every 2 minutes (Held, 2010).

The addition of glucose to *Saccharomyces cerevisiae* triggers a variety of regulatory phenomena: changes in the intracellular metabolites concentration and in proteins and mRNAs stability; modifications occur in the activity of enzymes as well as in the transcription rate of a large number of genes, some of the genes being induced while others are repressed (reviewed in Gancedo, 2008). Initial glucose metabolism is required for the induction of most of them as well as for producing energy.

Being a facultative anaerobic organism, *S. cerevisiae* is able to grow in a respirative or in a fermentative way. Some sugars induce the fermentative pathway as glucose does, which are instantly directed to the glycolysis. Some others, wherein galactose is included, are also fermentative sugars although they need extra conversion steps in order to enter glycolysis (Figure 2). The utilization of galactose requires the Leloir pathway (reviewed in Carlson, 1987). The usage of this group of sugars results in a fermentation rate slower than with rapidly fermentable sugars. This means that yeast cells will metabolize other sources of carbon, e.g., glucose, in preference to galactose even if a mixture of glucose and galactose is available to the cell (Holden *et al.*, 2004).

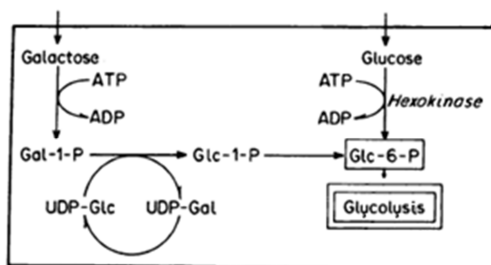


Figure 2 – Galactose metabolism. Pathway of extracellular galactose and glucose leading to glycolysis. Note that galactose enters the glycolytic mainstream bypassing the hexokinase step via the Leloir pathway (adapted from Bustamante and Pedersen, 1977).

Adding a rapidly fermentable sugar (glucose, for example) to carbon-starved yeast cells or cells growing on a nonfermentable carbon source such as ethanol (derepressed cells) triggers a notable variety of regulatory phenomena: Crabtree effect. A major role of glucose induced signalling is to switch metabolism from a gluconeogenic/respiratory mode to a fermentative mode. L-Gluconeogenic/respirative metabolism is switched off through glucose-induced inactivation of gluconeogenic enzymes (such as fructose-1,6-bisphosphatase) and repression by glucose of the genes encoding the enzymes of gluconeogenesis and respiration (such as cytochrome oxidase). Glucose also activates glycolysis by inducing the expression of genes encoding glycolytic enzymes (such as pyruvate decarboxylase) and by allosterically activating key glycolytic enzymes (Thevelein and Hohmann, 1995).

By the time the fermentable sugars are exhausted, cells switch to respiration mode after an adaptation period, referred as diauxic shift. Since ethanol was produced in the previous stage, now it can be used as carbon source.

1.2 Glucose Metabolism Machinery

Glucose related pathways present strong induction and repression controls. This is a sign of glucose's essential role in yeast adaptative behavior, being this sugar the yeast preference. Although these pathways have been studied for many years, only recently significant progress has been made in elucidating the upstream sugar sensing mechanisms that control activation of these pathways (Rolland *et al.*, 2000). Furthermore, a major issue is defining if sensing occurs at the cell surface by membrane-localized receptors or internally; that is, at the level of metabolism. Both seem to exist in yeast (Rolland *et al.*, 2002).

1.2.1 Sensing

A glucose-sensing mechanism has been described in *S. cerevisiae* that regulates expression of glucose transporter genes. The sensor proteins Snf3 and Rgt2 are homologous to the transporters they regulate. Snf3 and Rgt2 are integral plasma membrane proteins with unique carboxy-terminal domains that are predicted to be localized in the cytoplasm. There is evidence that the cytoplasmic domains of Snf3 and Rgt2 are required to transmit a glucose signal (Özcan *et al.*, 1998). This reinforces the idea that glucose transport via Snf3 and Rgt2 is not only involved in glucose sensing but, rather, that these proteins behave like glucose receptors. The identification of this class of nutrient sensors is an important step in elucidating the complex of regulatory mechanisms that leads to adaptation of fungi to different environments (Kruckeberg *et al.*, 1998).

In the absence of glucose, Rgt1-represses transcription of HXT1-4. When analyzing in a condition with low amounts of glucose, inhibition of the Rgt1-repressing activity occurs, a process triggered by Snf3 via Grr1-mediated ubiquitination. At high concentrations of glucose, Rgt2 triggers HXT1 expression. This involves Grr1-dependent conversion of Rgt1 into a transcriptional activator and another mechanism in which several components of the main glucose-repression pathway are involved. The Snf3- and Rgt2-mediated derepression of the HXT genes also involves sequestering at the plasma membrane of the transcriptional repressors Mth1 and Std1. Moreover, at high glucose concentrations HXT2, HXT4, HXT6, HXT7 and SNF3 are repressed by Mig1 via the main glucose-repression pathway. In addition, Snf3 is involved in a second pathway leading to the high-glucose-induced repression of HXT6 (Figure 3).

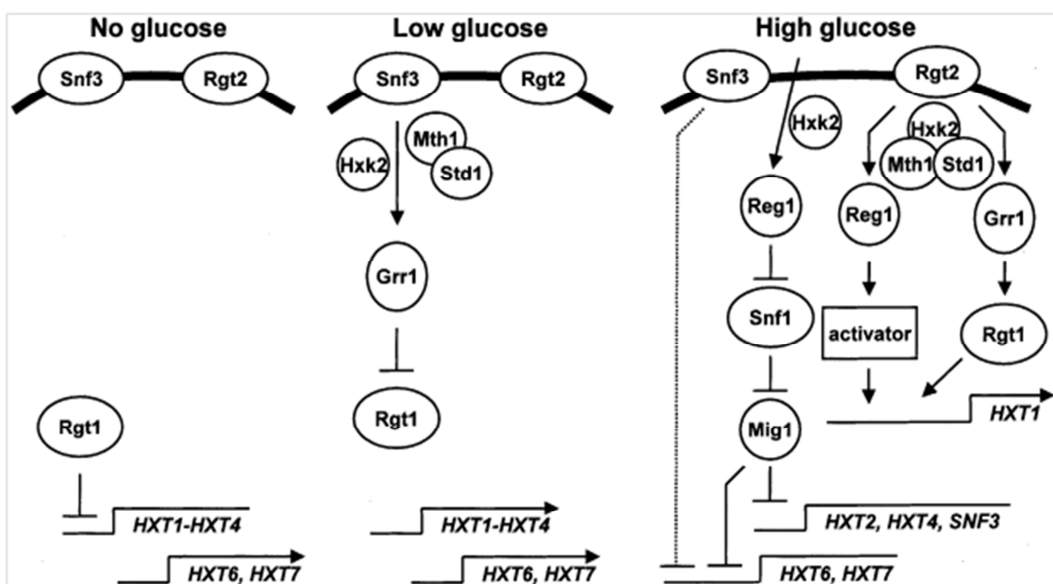


Figure 3 – Glucose sensing by Snf3 and Rgt2 in *S. cerevisiae* and respective gene repression. Low extracellular glucose concentrations are sensed by Snf3 and high concentrations of glucose are sensed by Rgt2 (Rolland *et al.*, 2002).

1.2.2 Transporters

Yeast cells have a preference for mono- and disaccharides over any other carbon source. Since biological membranes are not permeable to sugars, cellular uptake of these compounds is helped by 'transporters'.

Given the importance of glucose transport as a site of control of glycolytic flux, the regulation of glucose transporters is necessarily complex. The question of the actual role of all of these proteins in sugar catabolism have been raised, as some appear to be lowly expressed, and point mutations of these genes may confer pleiotropic phenotypes, inconsistent with a simple role as catabolic transporters. About a decade ago new findings started appearing relating the intimate involvement of carriers with the process of sensing glucose, a model for which there was growing support (reviewed in Bisson *et al.*, 1993). Nowadays it is established that glucose sensing involves the plasma membrane proteins Snf3, Rgt2 and

Gpr1 and the glucose phosphorylating enzyme Hxk2, as well as other regulatory elements whose functions are not totally understood (reviewed in Gancedo, 2008).

Hexoses uptake is mediated by a large family of related transporter proteins. Just in *Saccharomyces cerevisiae*, twenty different hexose transporter-related proteins genes have been identified (HXT1-17, GAL2, SNF3, RGT2): six of these transmembrane proteins (Hxt1-4, 6-7) mediate the metabolically relevant glucose, fructose and mannose uptake for growth, two others (Hxt5, Hxt8) catalyze the transport of only small amounts of these sugars, one protein (Gal2) is a galactose transporter but also able of glucose transportation, other two (Snf3, Rgt2) have a glucose sensor action, another two (Hxt9, Hxt11) are involved in the multi-drug resistance process, and the functions of the remaining hexose transporter-related proteins are not yet known (Rintala *et al.*, 2008). The catabolic hexose carriers exhibit different affinity for their substrates and expression of their corresponding genes is controlled by the glucose sensors according to the availability of carbon sources. Multigene family further characterization of these hexose transporters was needed in order to reveal the role of transport in yeast sugar metabolism (reviewed in Boles and Hollenberg, 1997). More recently the observation of transcriptome-wide up-regulation and downregulation of gene expression in response to activated Ras disclosed several genes that respond equally to both glucose addition and Ras2 activation (Santangelo, 2006). This was an important contribute to better understand the role of multigene family in transport versus sugar metabolism in yeast.

More specifically, yeast cells present two transporters for monosaccharides, the so-called glucose and galactose transporters that act by a facilitated diffusion mechanism. In the case of glucose transport (Figure 4), two components with high- and low-affinity constants have been identified kinetically. Activity of the high-affinity component is dependent on the presence of active kinases whereas activity of the low-affinity component is independent of the presence of these enzymes. Two genes, HXT1 and HXT2, encode two different glucose transporters with high affinity and are repressed by high glucose medium concentrations. Kinetic studies suggest that at least one additional gene exist, encoding a transporter with a low affinity and is expressed constitutively. Encoded by the gene GAL2, the Galactose transporter has D-galactose as main natural substrate. Expression of this gene is induced by galactose and repressed by glucose.

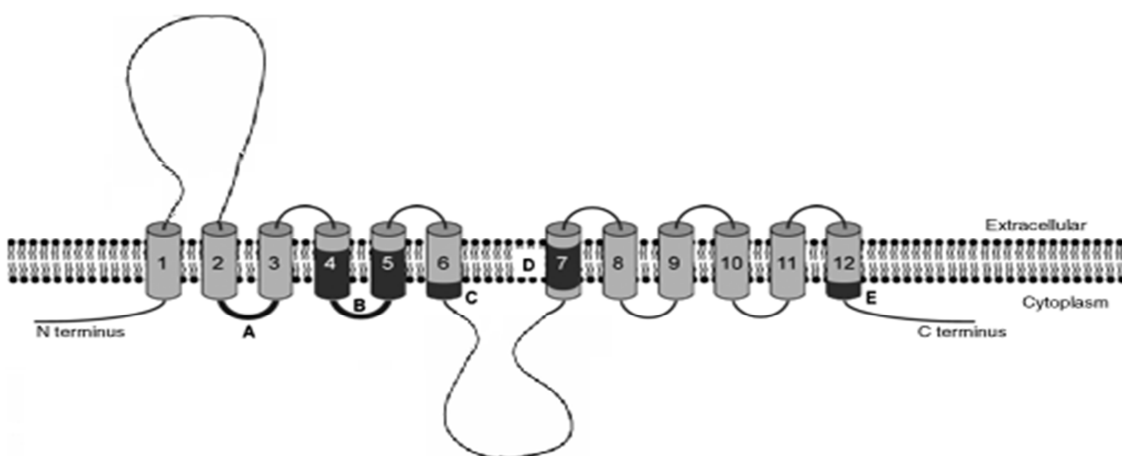


Figure 4 - Structure of yeast sugar transporters. Generally, these proteins in yeasts have 12 hydrophobic transmembrane domains (represented as cylinders: 1-12) with both the N- and C-termini intracellularly disposed. The position of the five conserved sequence motifs that have been recognized in sugar transporters is represented in the figure by the letters (A-E). N-linked glycosylation can occur in the extracellular loop between helices 1 and 2 as shown (Leandro et al., 2009).

The rate of sugar utilization in yeast cells is often dictated by the activity and transporters concentration in the plasma membrane and also controlled by changes in affinity of the corresponding transporters as well as by an irreversible inactivation that affects their V_{max} (Lagunas, 1993).

The primary targets of high glucose signaling are low-affinity glucose transporter genes such as HXT1, and the primary targets of low glucose signaling are high-affinity transporter genes such as HXT2; however, the two signaling pathways are probably not entirely discrete (Kruckeberg et al., 1998).

1.2.3 Signal Transduction

Numerous mechanisms have evolved to transduct glucose-induced signal, including those that act at the gene transcription levels, mRNA stability, mRNA translation and protein stability (Johnston, 1999). However, it is known that the majority of glucose effects call for some level of metabolism, indicating that glucose binding to a receptor is often not enough to signal glucose presence in yeast (reviewed in Gancedo, 2008). cAMP, as an intermediate metabolite, plays an essential role in glucose signaling, which in its turn activates PKA, which is sufficient to induce the gene transcription characteristic from glucose sensing (Wang et al., 2004).

1.2.3.1 cAMP-PKA pathway activators

Nutrients sensing research has revealed a pathway closely related and probably also involving protein kinase A (PKA) for its targets regulation as a nutrient status function. To the 'fermentable-growth-medium' induced pathway be continually activated, it requires both a fermentable carbon source, like glucose, and all essential nutrients. The nutrient-sensing and signal-transmission components of this

pathway investigation showed that active nutrient carriers, like the Pho84 phosphate transporter, the Gap1 amino acid permease and the Mep2 ammonium permease act as sensors for phosphate, amino acid and ammonium activation, respectively, of the PKA targets.

The glucose-induced cAMP signaling studies have led to the identification of a G-protein coupled receptor (GPCR) system, consisting of Gpr1 (a 7-transmembrane receptor) and Gpa2 (a G alpha protein), that mediates sucrose and glucose activation of cAMP synthesis (Figure 5). Nutrient-sensing G-protein coupled receptor system was the first identified in eukaryotes. Moreover, it was found that two Gpa2-associated kelch-repeat proteins (Krh1 and Krh2), directly regulate PKA, thereby bypassing adenylate cyclase stimulation (Rolland *et al.*, 2001).

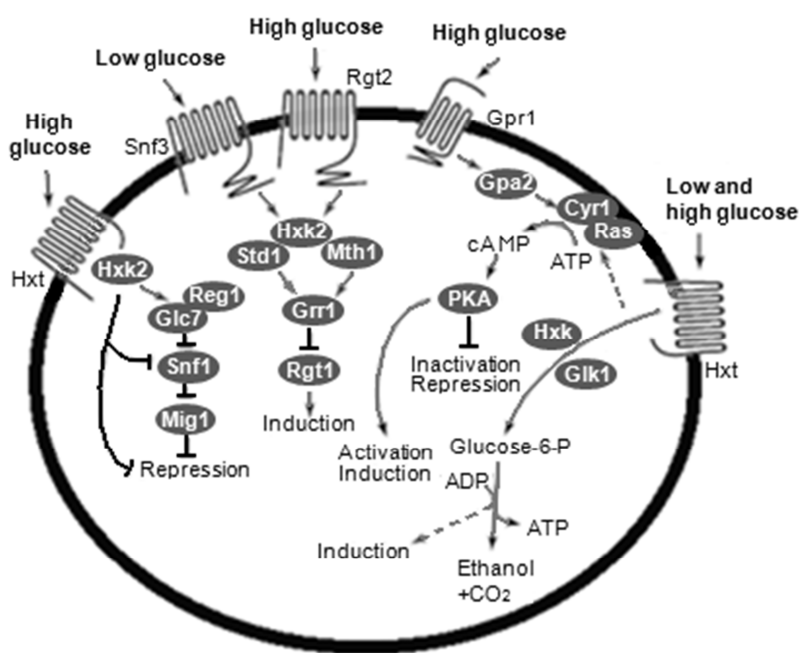


Figure 5 – Glucose sensing and signaling in yeast (Rolland *et al.*, 2001).

Glucose phosphorylation is catalysed by hexokinase I (Hxk1), hexokinase II (Hxk2) and a specific glucokinase (Glk1). Either Hxk1 or Hxk2 is sufficient for a fast, sugar-induced disappearance of catabolite-repressible mRNAs (short-term catabolite repression). Hxk2 is particularly required and sufficient for long-term glucose repression.

The main component of this signaling transduction pathway is adenylate cyclase, which catalyzes the synthesis of cAMP. The rise of cAMP levels is mostly due to the activation of this plasma membrane-bound adenylate cyclase mediated by different G proteins: Ras1, Ras2 and Gpa2. In *S. cerevisiae*, adenylate cyclase activity is controlled by the Ras proteins. These proteins are members of the small GTPase superfamily, which are active in the GTP-bound form and inactive in the GDP-bound form. Glucose addition triggers a rapid increase in the GTP loading state of Ras2 related with the glucose

induced increase in cAMP (Colombo *et al.*, 2004). It was shown that GTP loading is dependent on Cdc25 and that Ira proteins deletion causes constitutively high GTP loading. This means that Ira1 and Ira2 negatively regulate the Ras2 Protein activation state and are required for the glucose-induced increase in Ras2 GTP loading (Figure 6) (Tanaka *et al.*, 1990).

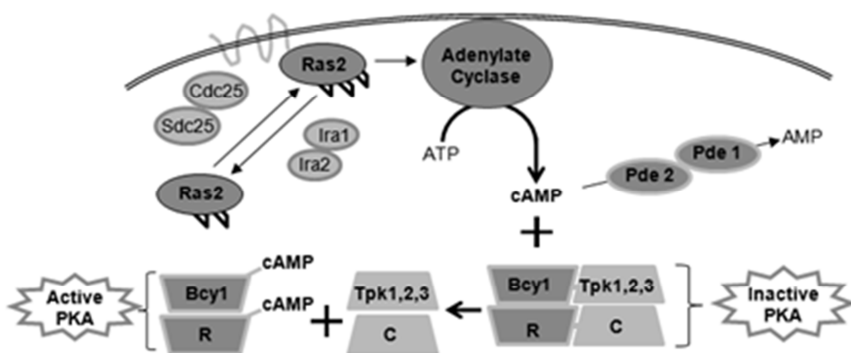


Figure 6 – cAMP-PKA pathway fraction (adapted from Santangelo, 2006).

1.2.3.2 Protein Kinase A role

It seems that the rapid spike of cAMP after glucose addition is mainly created in order to activate PKA. Protein kinase A is constituted by two regulatory monomers (Bcy1) and two other with catalytic function (Tpk1,2,3) (Fig 6). Each individual subunit presents some unique targets, for example, it was newly shown that the loss of Tpk3p function has the particular consequence of significantly reduction in respiratory function (Chevtzoff *et al.*, 2005). This supports the link between Ras signaling and mitochondrial function, which in turn influence the oxidative stress management and the regulation of yeast aging (Gourlay and Ayscough, 2006).

Adding to the active PKA function of phosphorylate proteins involved in transcription, energy metabolism and growth and proliferation (Santangelo, 2006), the Ras/cAMP/PKA pathway also plays a role in aging (Longo, 2003), thermotolerance (Zhu *et al.*, 2000), bud site selection, actin repolarization (Schneper *et al.*, 2004), trehalose and glycogen accumulation (Smith *et al.*, 1998), stress resistance (expression STRE-genes) (Wang *et al.*, 2004), and sporulation (Cameron *et al.*, 1988); it might also regulate pseudohyphal differentiation in response to nutrient limitation.

1.2.3.3 cAMP-PKA pathway regulation through cAMP control

In yeast, the cAMP intracellular concentration depends on the respective activities of Cyr1 (adenylate cyclase) and of the phosphodiesterases Pde1 and Pde2. Pde2 is the high affinity phosphodiesterase, being responsible for a much more relevant action while Pde1 is the low affinity one, acting in a very soft way (Thevelein *et al.*, 2000). When the *PDE2* gene is overexpressed, the cAMP

content suffers a decrease (Noubhani *et al.*, 2009). *PDE2* negative regulation of Ras signaling, is due to cAMP hydrolysis catalyzation to AMP, thereby downregulating signal transduction through the Ras pathway (Gourlay and Ayscough, 2006).

1.3 Trehalose pathway

The discovery about the key role of a subunit of the trehalose synthase complex in the glucose influx control into glycolysis was the first indication of this pathway importance. After several studies of genetic suppressors, it is believed that the inability to grow on glucose is due to unlimited influx of sugar into glycolysis and subsequent overflow of this pathway (Blázquez *et al.*, 1993; Thevelein and Hohmann, 1995; Ernandes *et al.*, 1998; Bonini *et al.*, 2004).

1.3.1 Trehalose synthesis

The disaccharide trehalose (α -D-glucopyranosyl-1,1- α -D-glucopyranoside), a non-reducing disaccharide, has a widespread occurrence in nature. In addition to its role as a carbohydrate storage compound, it is present in particularly large quantities in many survival forms, as it is an important stress protectant (Dijk *et al.*, 1995). Trehalose is also involved in metabolic signaling and regulation of carbohydrate metabolism. When the proliferation mode is activated, the accumulated trehalose is mobilized by the trehalase to two glucose molecules (Thevelein, 1984).

S. cerevisiae synthesizes trehalose by two consecutive enzymatic reactions catalyzed by a multimeric enzymatic complex: trehalose-6-phosphate synthase (encoded by the genes *TPS1*), trehalose 6-phosphate phosphatase (encoded by *TPS2*) and two redundant regulatory subunits *Tps3* and *Ts1* (Figure 7).

1.3.2 *Hxk2* inhibition by trehalose 6-phosphate

Trehalose metabolism is linked to the control of glucose influx, mainly through hexokinase activity inhibition by trehalose 6-phosphate (Figure 7). Yeast hexokinase II (the most abundant isoenzyme of hexokinase during growth of *S. cerevisiae* on glucose) was reported to be inhibited *in vitro* by 40 μ M of trehalose 6-phosphate (Blázquez *et al.*, 1993). Supporting this is the fact that *HXK2* deletion restores growth on glucose of mutants with nonfunctioning trehalose-6-P (Hohmann *et al.*, 1993).

1.3.3 Influence on glycolysis upon *TPS1* deletion

Mutations in the *TPS1* gene originate a trehalose and Tre6P synthesis defect but also a specific growth deficiency on rapidly fermented sugars like glucose. Growth on galactose or on nonfermentable carbon sources like glycerol or ethanol is normal. Glucose addition to *TPS1* deletion mutant cells growing on glucose results in hyperaccumulation of the sugar phosphate intermediates (glucose 6-phosphate, fructose 6-phosphate, and fructose 1,6-bisphosphate) in the first part of glycolysis and rapid depletion of ATP and phosphate, as well as all intermediates of glycolysis downstream of glyceraldehyde-3-phosphate dehydrogenase. This severe glycolysis deregulation is believed to be the cause of the glucose growth defect (Thevelein and Hohmann, 1995). The sugar phosphates hyperaccumulation in the *tps1Δ* after addition of glucose is consistent with overactive hexokinase activity (Figure 7). Several mutations have been described that suppress the growth defect of *TPS1Δ*, apparently by reducing sugar influx into glycolysis or by redirecting the excess sugar phosphate into glycerol synthesis through overexpression of the GPD1-encoded NAD-dependent glycerol-3-phosphate dehydrogenase (Noubhani et al., 2009). As previously mentioned, deletion of the *HXK2* gene, which encodes the most active hexokinase isoenzyme, restores the ability of the *tps1Δ* mutant to grow on glucose, supporting this conclusion (Hohmann et al., 1993).

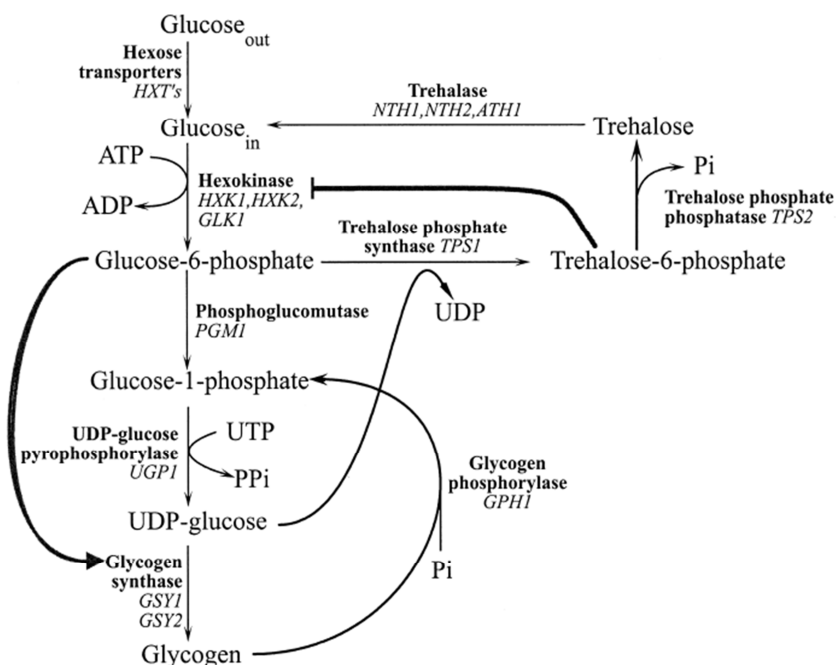


Figure 7 - Pathways of glycogen and trehalose metabolism (Silva-udawatta and Cannon, 2001).

1.4 Programmed Cell Death Modes

Programmed cell death (PCD) defines all modes of death, whose execution is carried out in a regulated fashion and is therefore under molecular control. This requires that the process follows a specific and well organized sequence, as for example in the acetic acid induced apoptosis (

Figure 8), in which one event is triggered by another (like, for instance, during the caspase cascade in mammalian cells). Particularly apoptosis has been classified as PCD, as it is the most regulated one, nonetheless, cell death can manifest non-apoptotic features. This means that other types of death are, indeed, involved in a cell's programmed end, as necrosis does (reviewed in Eisenberg *et al.*, 2010).

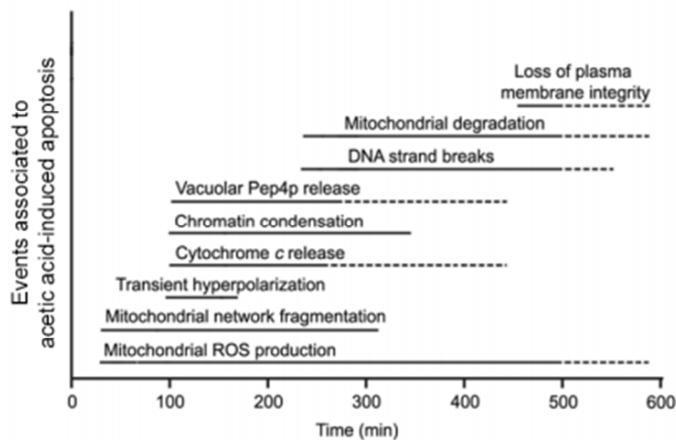


Figure 8 - Temporal order of events occurring during acetic acid induced death in *S. cerevisiae* W303 strain (Pereira *et al.*, 2008).

Some authors categorize PCD in two main types: apoptosis and autophagy. In apoptosis (type I PCD) both mitochondria-dependent and -independent signaling pathways are effective. Autophagy (type II PCD) represents a 'self-eating' mechanism of damaged cells and organelles, as a result of lysosome activity. However, autophagy is also one of the major degradation and recycling systems within cells, promoting survival during nutrient starvation (reviewed in Hamann *et al.*, 2008).

Whole population benefit is the ultimate goal of single cells death. This altruistic behavior is still discussed. However, PCD in yeast is the first experimental evidence for the so-called group selection theory: apoptotic genes became selected during evolution as a tool for population advantage (Ruckenstuhl *et al.*, 2010).

1.4.1 Apoptosis

Apoptosis has been defined as a highly regulated mechanism of PCD in metazoan, resulting in the homeostatic removal of mutated, injured, infected or basically dispensable cells (reviewed in Fröhlich and Madeo, 2000).

A wide range of stress conditions and drugs can induce an apoptotic phenotype in *S. cerevisiae*: low doses of H₂O₂, acetic acid, HOCl, Amiodarone, and aspirin, hyperosmotic and temperature stress, the DNA damaging drug adozelesin as well as amphotericin B, UV radiation, low levels of valproic acid and even high concentrations of glucose and NaCl and others; with the first two being the most popular triggers (reviewed in Fröhlich *et al.*, 2007). In addition to the conditions mentioned above, internal features like aging and decrease of actin mobility also contribute to yeast cells undergoing apoptosis (Gourlay *et al.*, 2004).

Glucose signaling had been recently demonstrated to have a progeriatric effect on chronologically aged yeast cells: glucose addition ends up in a reduced efficacy of cells to enter quiescence, finally causing superoxide-mediated replication stress and apoptosis (Ruckenstuhl *et al.*, 2010). Two forms of cellular ageing occur in yeast. Replicative ageing, also referred as mother cell specific ageing is based on how many progenies a single mother cell has produced. The maximum generation number that a mother cell can undergo is referred to as the Hayflick limit (Hayflick, 1965). After this, the cell is no longer capable of replicating and undergoes program cell death (PCD). Chronological ageing, also called postmitotic ageing, is defined by survival rates during long-term cultivation (reviewed in Fröhlich *et al.*, 2007). During failed mating, mating-type pheromones trigger cell death to prevent the culture from infertile or otherwise damaged haploid cells (reviewed in Carmona-Gutierrez *et al.*, 2010). In addition, apoptosis can also happen during meiosis of diploid cells, which might guarantee that only genetic recombinants that are adapted to their surroundings live on (Knorre *et al.*, 2005). Cell aging follows a degeneration process resulting in the end in cell death (Figure 9). This phenomenon is evolutionary conserved and present in unicellular eukaryotes as well, making yeast a treasured model (reviewed in Carmona-Gutierrez *et al.*, 2010), as many anti-aging stimuli that have been discovered in the yeast chronological aging system had their later confirmation in higher cells or organisms (Ruckenstuhl *et al.*, 2010).

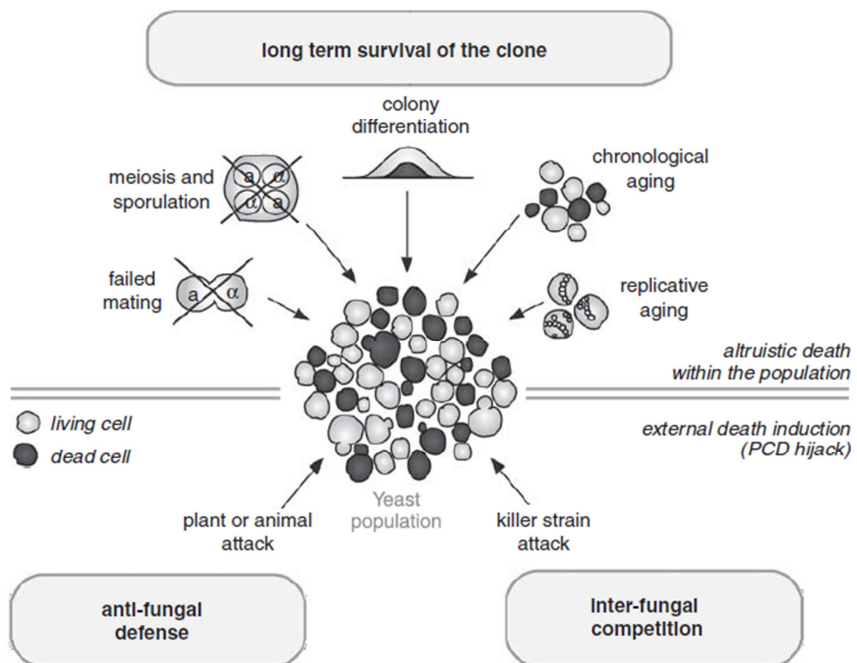


Figure 9 - Physiological scenarios of yeast apoptosis (reviewed in Carmona-Gutierrez et al., 2010).

Apoptosis in yeast cells has been exploited by bacteria in order to achieve a competitive advantage, by releasing oxidative burst and/or release of other pro-apoptotic substances, inducing this way the host and/or in the pathogen to undergo apoptosis (reviewed in Hamann *et al.*, 2008). On the other hand, it was already reported that in an attempt of mimicking natural environment, superoxide partially mediates the premature death program in order to promote the release of nutrients and therefore the regrowth of a subpopulation of better-adapted mutants (Fabrizio *et al.*, 2004).

Apoptosis caught scientist's attention when they realized how crucial its role was for many fundamental processes in humans (reviewed in Fröhlick and Madeo, 2001). Deregulations at the apoptotic pathway's level contributes to the pathogenesis of multiple prevalent diseases of today (reviewed in Carmona-Gutierrez *et al.*, 2010). Apoptosis down regulation is associated with cancer, atherosclerosis, neoplastic disorders, autoimmune disorders (e.g. multiple sclerosis) and spreading of viral infections (e.g. AIDS), while up regulation is linked to neurodegenerative disorders (e.g. Alzheimer's disease), and ischaemic injury (e.g. myocardial infarction), bacterial infections (e.g. *Neisseria meningitidis*), haematological disorders (e.g. myelodysplastic syndromes), and toxin-induced diseases (e.g. alcohol-induced hepatitis) (Vermeulen *et al.*, 2005).

Currently is completely accepted that mitochondria is a precious puzzle piece in apoptosis orchestra, since numerous conserved mechanisms for mitochondrial involvement in apoptosis have been proposed. More specifically, involvement of fusion and fission proteins in the mitochondrial pathway of cell death seems to be a more conserved event between mammals, flies, worms, and yeast. In addition,

mitochondrial fragmentation has been documented to be a feature of mammalian and non-mammalian eukaryotic apoptosis. What is left to know about mitochondrial death pathways may explain the differences between various species. Thus, more genetic and biochemical analyses might elucidate the sophisticated mitochondrial mechanisms regulating the decision whether a eukaryotic cell lives or dies. Furthermore, yeast have been shown to be powerful models to understand the mechanisms of human disease as they relate to the mitochondrial pathway of cell death. Thus, continued research into the mitochondrial contribution to cell death in model organisms is likely to provide important insight in the future (reviewed in Abdelwahid *et al.*, 2011).

1.4.1.1 Apoptotic markers in yeast

Dying yeast shares with mammalian cells many or all of the following apoptotic events (both at morphological and molecular terms): on one hand, morphological apoptotic markers, such as chromatin condensation, nuclear DNA digestion, cytoplasmic condensation, cell shrinkage, loss of mitochondrial membrane potential, 'blebbing' of the cell surface, phospholipid phosphatidylserine exposure in the outer leaflet of the plasma membrane and the generation of reactive oxygen species (ROS), were already registered in yeast. On the other hand, apoptosis fundamental molecular regulators in yeast have been identified by different groups, including core executors like a caspase, the apoptosis-inducing factor (AIF), endonuclease G or the serine protease OMI, as well as pivotal inhibitors like the AAA-ATPase CDC48 (p97/VCP) or the IAP (inhibitor of apoptosis protein) BIR1 (Ruckenstein *et al.*, 2010). The key feature of apoptosis is that many of these events alone could kill a cell; in fact all of them take place as an organized programme (Fraser and James, 1998).

The indispensable test for cell death in yeast is the clonogenic assay. In contrast to cultured mammalian cells, viable individual yeast cells give rise to a colony. Stain based methods can also be applied, but in general the clonogenic assay is the preferred one. DNA fragmentation is measured with the TUNEL assay. Annexin V staining is used to visualize the exposition of phosphatidyl serine simultaneously with propidium iodine in order to test sphaeroplasts integrity, as they are sensitive and easily damaged by harsh treatment. Intracellular ROS accumulation is a reliable and easily testable marker of yeast apoptosis; furthermore it is often used as the first apoptotic clue. Cells are incubated by dihydrorhodamine 123 or similar, and fluorescent cells counted under a microscope or quantified in an appropriate fluorescent reader after a short incubation time. Meanwhile, ROS and Annexin V staining plus propidium iodine are routinely used in FACS analysis. Chromatin condensation and margination can be identified after DAPI staining or in the electron microscope (reviewed in Fröhlich *et al.*, 2007) (Figure 10).

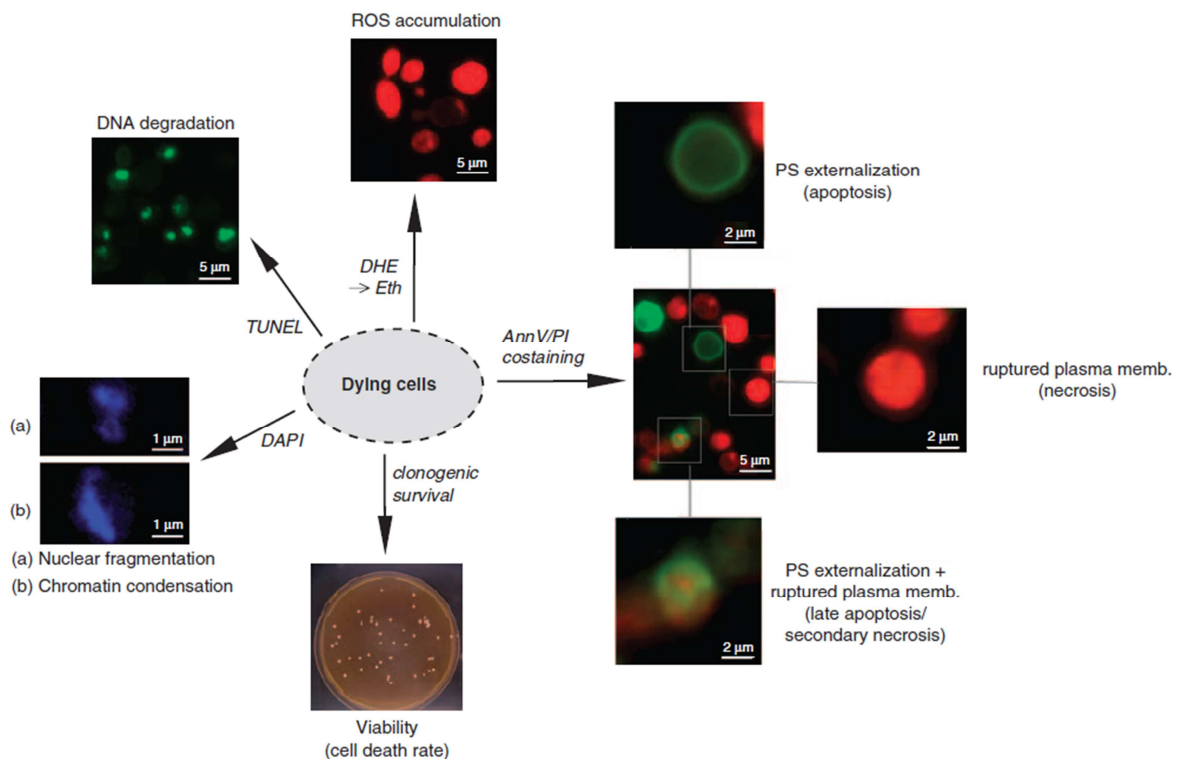


Figure 10 - Assays routinely used in the field of yeast PCD (adapted from Carmona-Gutierrez *et al.*, 2010).

1.4.1.1.1 Cytochrome c release

Release of cytochrome c is an essential apoptotic signal in both human and *S. cerevisiae* cells. This was established since respiratory deficient strains and cytochrome c deleted strains showed diminished apoptosis upon acetic acid and partially heterologous bax induced apoptosis (Kai-uwe *et al.*, 2007).

Mitochondrial cytochrome c, known for its electron carrier role in the respiratory chain, translocates to the cytosol in apoptotic cells, where it participates in the activation of specific steps in the apoptotic cascade. The mechanism responsible for the release of cytochrome c from mitochondria during apoptosis is unknown. However, it was already reported that cytochrome c release from mitochondria is an early event in the apoptotic process (Bossy-Wetzel *et al.*, 1998).

As oxygen radicals are normal byproducts of respiration, a specific modulation of the respiratory chain may have been developed to increase the output of ROS as needed. Some believe that the cytochrome c release is a result of that modulation. Nowadays, cytochrome c release itself became an apoptotic marker, possibly in order to make the regulatory cascade less dependent on the redox state of the cell (reviewed in Fröhlich and Madeo, 2000).

A puzzling fact is the mitochondrial membrane potential maintenance following depletion of cytochrome c. Two pools of cytochrome c can be assumed: a major pool freely placed in the intermembrane space and which could be available for release after MOMP (mitochondrial outer membrane permeabilization), and another pool adherent to the respiratory chain, carrying electrons between complexes III and IV of this chain. The latter pool would be sufficient to maintain mitochondrial respiration and polarization when the former pool has been released. It is also feasible that released cytochrome c return in to the inner-membrane space and participate in electron transport. This may allow mitochondria to temporarily sustain ATP production in particular, in order to ensure normal caspase activation, which requires ATP or dATP. Permeabilization of mitochondrial membranes seems to occur in many forms of cell death. However, the mechanisms underlying this process may differ according to the specific ‘death’ stimuli, presumably to cell type and to cell death mode: apoptosis versus necrosis (reviewed in Gogvadze *et al.*, 2006). The difficulty of the precise mechanisms identification that contribute to the release of cytochrome c and other proteins from the intermembrane space can be explained by the complexity of events at the mitochondrial level during cell death (Figure 11). The use of cell-free systems might be very helpful.

The precise understanding of these mechanisms urges as they may be a precious key for the identification of therapeutic targets for drugs development that will modulate cell death associated with many pathological states (Martinou *et al.*, 2000).

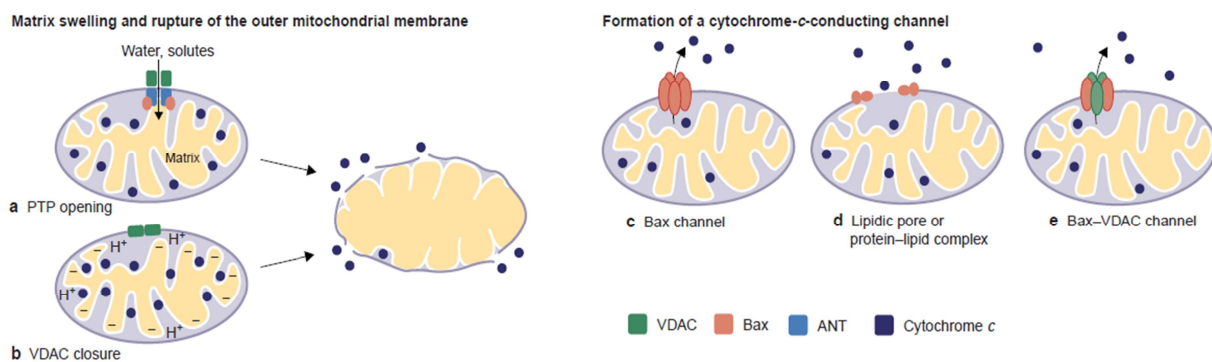


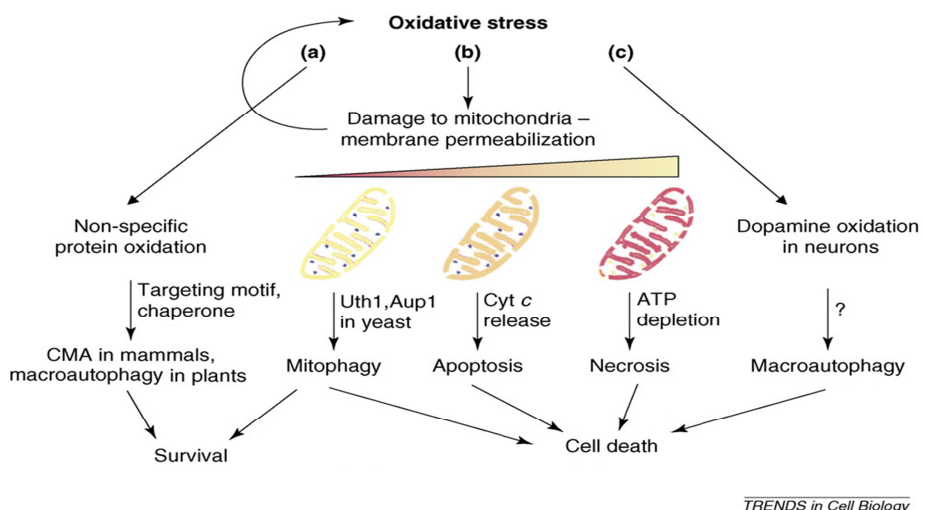
Figure 11 - Models for the release of cytochrome c from mitochondria into cytosol. The outer mitochondrial membrane (OMM) ruptures as a result of the mitochondrial matrix swelling, allowing cytochrome c to escape from mitochondria (a, b). Model a involves the permeability-transition pore (PTP) opening whereas model b involves the voltage-dependent anion channel (VDAC) closure and inner mitochondrial membrane. A large channel forms in the OMM, allowing cytochrome c release, but mitochondria are not damaged (c–e). ANT, adenine-nucleotide translocator (Martinou *et al.*, 2000).

1.4.1.1.2 Reactive Oxygen Species

Another evidence of mitochondria importance and involvement in apoptosis is the Reactive Oxygen Species (ROS) key role in dying cells. There are several forms of ROS, namely: superoxide, hydrogen peroxide and others. The effects of ROS on cellular processes depend on severity and duration of exposure.

ROS accumulation was proven to occur in yeast cells after induction of apoptotic death by various stimuli. Moreover, there is evidence that they are necessary and sufficient to induce an apoptotic phenotype in yeast. Some authors suggest that the formation of ROS, a well characterized class of apoptotic inducers, is a crucial event in the evolutionary original apoptotic mechanism (Madeo *et al.*, 1999). ROS have long been known to be a killing response element of immune cells to microbial invasion. New evidence reinforced ROS key role as a messenger in cell signal transduction, including: apoptosis, gene expression, cell cycling and the activation of cell signaling cascades. It is worth to note that ROS serve as both intra- and inter-cellular messengers. These reactive molecules are formed by several different mechanisms and can be detected by a significant amount of techniques (Held, 2010).

Depending on the stress nature, ROS cause loss of essential cellular functions or toxic functions gain. ROS vital targets consist of membrane lipid integrity and activity of ROS-susceptible proteins, including proteins required for accurate translation of mRNA. Protein oxidation can result in toxic proteic aggregates accumulation or induction of apoptosis (reviewed in Avery, 2011). Depending on the harshness of the ROS production stimuli, the cells fate can be survival or a necrotic collapse (Figure 12). ROS (such as $O_2^- \bullet$, H_2O_2 and OH^\bullet) play a fundamental regulatory role in early as well as late steps in apoptosis. It was showed that oxygen radicals are indeed a promoter in yeast and mammalian apoptosis and not a byproduct as initially thought (reviewed in Fröhlich *et al.*, 2007). In every studied situations of cell death induction by exogenous stimuli, ROS accumulation occurs and is necessary for cell death to occur, as oxygen stress triggers the apoptotic cascade by itself (reviewed in Fröhlich and Madeo, 2000).



TRENDS in Cell Biology

Figure 12 – Oxidative stress severity and respective cell fate (Scherz-Shouval and Elazar, 2007).

Probably, the regulatory pathways complexity is a consequence of basic mechanism evolution, often ending up in contradictory behavior in different apoptotic models. Some apoptotic pathways preserved the usage of ROS in early regulatory steps, while others use them in late steps. Furthermore, a number of unconventional pathways lacking the involvement of ROS emerged, as is the case of ROS-independent apoptotic pathway via CD95 (a mammalian protein) (Hug *et al.*, 1994). However, even at this alternative pathway, the expression of the proapoptotic CD95 ligand is still induced by ROS (Hug *et al.*, 1997).

This mounting understanding of the principal ROS targets will offer new possibilities for therapy of ROS related diseases (Madeo *et al.*, 1999). Recent research addressed whether the mechanism downstream of this signal uses conserved elements. Interestingly, it was proved that functional conservation is shared with worms such as *Caenorhabditis elegans*, plants, unicellular eukaryotes and even bacteria (reviewed in Carmona-Gutierrez *et al.*, 2010).

1.4.1.1.3 DNA fragmentation

Is a well-known fact among researchers that genomic DNA cleavage at regularly spaced sites into histone-associated DNA fragments of mono or oligonucleosomal lengths occurs in cells undergoing apoptosis. DNA damage and replication failure can stimulate the activation of yeast cell death programs having oxygen metabolism and ROS generation the major causes of DNA damages. In *S. cerevisiae*, several players involved in DNA-damage-regulated apoptosis have been found (reviewed in Carmona-Gutierrez *et al.*, 2010) Besides this characteristic feature, distinctive nucleus and cytoplasm morphologic changes were observed in apoptotic cell. The morphologic alterations due to apoptosis take place in three phases, however the main nuclear changes occur in the first one: chromatin condensation into crescentic

caps at the nuclear periphery, nuclear disintegration and reduction in nuclear size between others. The second phase (which might overlap phase 1) is characterized by apoptotic bodies' formation. In phase 3 a progressive degeneration of residual nuclear and cytoplasmic structures occurs (Arends *et al.*, 1990).

Despite of oligonucleosomal fragmentation not being a required feature of apoptosis, nucleosomal particles in cytoplasmic fractions or cell culture supernatants are still measured, since DNA degradation is extremely common varying between a great or less extent in apoptotic cells. The majority of techniques for DNA strand breaks detection rely on enzymatic labelling of the 3*-hydroxyl ends using modified nucleotides. In fact there are two enzymatic labeling methods: *in situ* nick translation and *in situ* end labeling (TUNEL). The former method relies on the specific binding of the large (Klenow) fragment of DNA polymerase I to nicked DNA, and catalyses the template-dependent addition of nucleotides. The latter method relies on the binding of terminal deoxynucleotidyl transferase (TdT) to free 3*-hydroxyl ends of double- or single-strand DNA breaks, catalysing the incorporation of labelled and unlabelled nucleotides independent of a template (Alison, 1999).

Both methods do not discriminate between apoptotic and necrotic cells, but given that random fragmentation is more related to necrosis, the TUNEL (TdT-mediated-dUTP nick end labelling) method is considered to be more specific for apoptosis, particularly in its early stages (Alison, 1999).

1.4.1.1.4 Phosphatidylserine exposure

The aminophospholipid phosphatidylserine (PS) localizes chiefly in membrane leaflets facing the cytosol. This PS plasma membrane asymmetry is maintained by an aminophospholipid translocase (also known as flippases), which transports selectively aminophospholipids from the outer to the inner leaflet (van Heerde *et al.*, 2000).

Blood platelets were the first cells where the change of PS asymmetry was observed (E M Bevers *et al.*, 1982), but soon was confirmed that apoptotic nucleated cells also share this characteristic. Is given to the scramblase activation the reason of this phenomenon, which scrambles the PS symmetrically over the two leaflets (Williamson *et al.*, 1995). This mechanism operates during apoptosis resulting in the cell surface exposure of PS (Figure 13) and is independent of cell type and specie or apoptosis induction system used. Moreover, it occurs in an early execution phase, even before nuclear and cytoplasmic morphologic changes (reviewed in van Engeland *et al.*, 1998). In mammalian cells, surface exposed PS is recognized, hence removal or phagocytosis of senescent and dying cells occurs (Fadok *et al.*, 1992).

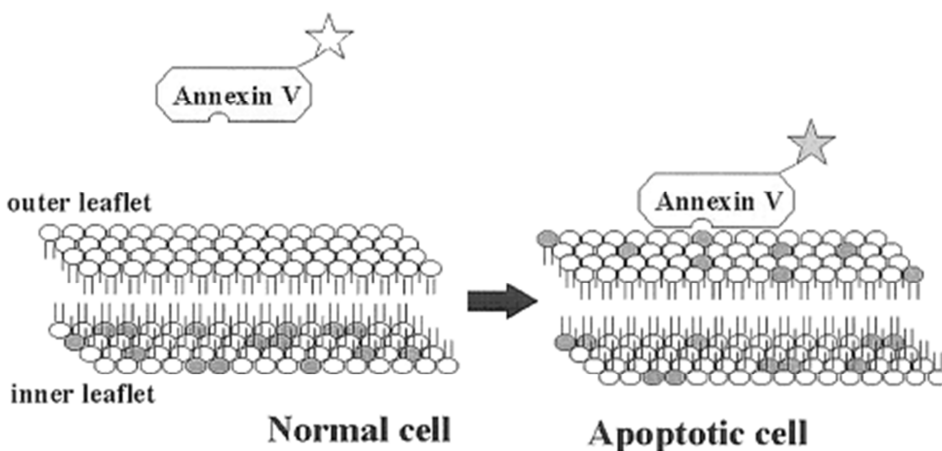


Figure 13 - Schematic representation of the loss of membrane lipid asymmetry during apoptosis and specific binding of Annexin-V (van Engeland et al., 1998).

PS externalization is detected by Annexin-V, which together with PI can give another information: segregation between apoptotic and necrotic cells, since the referred process presents a green fluorescence while the plasma membrane integrity is still intact and a red fluorescence when that integrity is compromised in simultaneous presence of both dyes.

1.4.1.2 Ras-cAMP-PKA pathway importance in yeast apoptosis

The Ras/cAMP/PKA is a key signaling mechanism that coordinates cell growth and proliferation according to nutrient availability (Thevelein and De Winde, 1999). Entering in the diauxic shift means Ras activity downregulation. This leads to a range of responses including cell-cycle exit, upregulation of stress response factors and enhanced carbohydrate storage. Instead of being downregulated, if the RAS/cAMP/PKA pathway is maintained active, a consequence, for example, of the constitutively active oncogenic *RAS2^{Val19}* allele, results in mitochondria collapse and so ROS production. These cells life-span is shortened in a PCD way, featuring apoptosis (Hlavatá et al., 2003). Ras activation also takes part in ageing as cells with overactive RAS/PKA signaling, as registered in *RAS2^{Val19}* cells, display reduced proliferation rates and accelerated replicative senescence fading in an apoptotic mode. It was demonstrated that Ras signaling is involved in proliferation rate and replicative lifespan by two unlike, ROS-dependent, routes. While the decrease in generation time is linked to the specifically inactivation of the mitochondrial nucleotide carrier, longevity is affected by other, and newly discovered, target(s) of ROS attack (Hlavatá et al., 2008).

In yeast cells expression of constitutively active Ras signaling pathway and consequent rise in cyclic AMP (cAMP) levels leads to the mitochondrial membrane potential loss, ROS accumulation and cell death. Stabilization of the actin cytoskeleton ends up in hyperactivation of Ras2p (Gourlay and Ayscough, 2006). Therefore, this phenomenon was termed as actin-mediated apoptosis (ActMAP). Srv2p/CAP (actin

regulatory protein) connects actin and Ras signalling by binding to adenylate cyclase (Cyr1p) that catalyses cAMP production thus PKA activation (Leadsham *et al.*, 2010). Actin is linked to the sensing of nutritional signals, by Whi2p. It was found that upon PKA activation, its subunit Tpk3p is the responsible for the linking of actin aggregation and cAMP formation to apoptosis (reviewed in Fröhlich *et al.*, 2007). PKA activation and mitochondrial dysfunction leads to ROS accumulation, however, a protective mechanism exists that can shield actin from the ravages of oxidative stress by the function of the oxidoreductase Oye2 (Leadsham *et al.*, 2010).

Adding to actin upregulation effect on Ras, there are other substances that exert the same result, contributing for Ras involvement in yeast apoptosis: osmotin, acetic acid, H₂O₂ and others (Pereira *et al.*, 2008) (Figure 14).

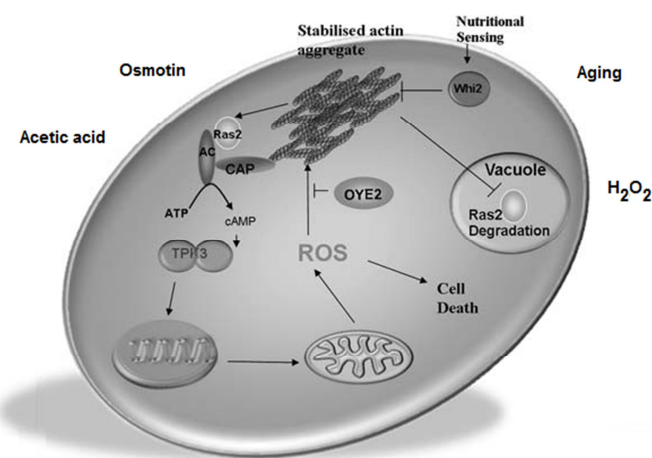


Figure 14 - Yeast cells undergo apoptosis through hyperactivation of the Ras/cAMP/PKA signalling pathway upon several stimuli (adapted from Leadsham *et al.*, 2010).

1.4.2 Necrosis

Necrosis was long considered an accidental cell death process, much less orderly than apoptosis due to extremely cellular injury such as chemical or physical disruption of the plasma membrane. It was believed that massive corruption of cellular structures and metabolism prevented the collaboration of the cell in its death process. As an example, high concentrations of H₂O₂ result in cell death associated with disintegration of intracellular structures but without the phenotypic markers of apoptosis (Madeo *et al.*, 1999). Such a definition, though, proved to be unsuitable to many necrotic scenarios. The discovery that genetic manipulation of several proteins either prevented or enhanced necrotic cell death argued in favor of a molecular regulation through signal transduction pathways and catabolic mechanisms in necrotic execution, which controls longevity and whose physiological function may be aging. For instance, calpains, cathepsins and cyclophilin D are frequently necessary for necrotic cell death (reviewed in

Golstein and Kroemer, 2007; reviewed in Festjens *et al.*, 2006; Syntichaki and Tavernarakis, 2003) and a decisive role for the serine/threonine kinases RIP1 and RIP3 has been proven (reviewed in Galluzzi *et al.*, 2006).

For more than a decade, yeast has been an apoptosis research model. Nowadays, evidence also points out to the existence of a necrotic program. In one hand there are mitochondria, aging and low pH as positive regulators of this process, on the other hand there are cellular polyamines (e.g. spermidine) and endonuclease G as well as homeostatic organelles (e.g. vacuole or peroxisomes) as potent inhibitors of necrosis (Figure 15). Physiological necrosis is thought to stimulate intercellular signaling via the release of necrotic factors that stimulate viability of healthy cells and, therefore, guarantee survival of the clone (reviewed in Eisenberg *et al.*, 2010).

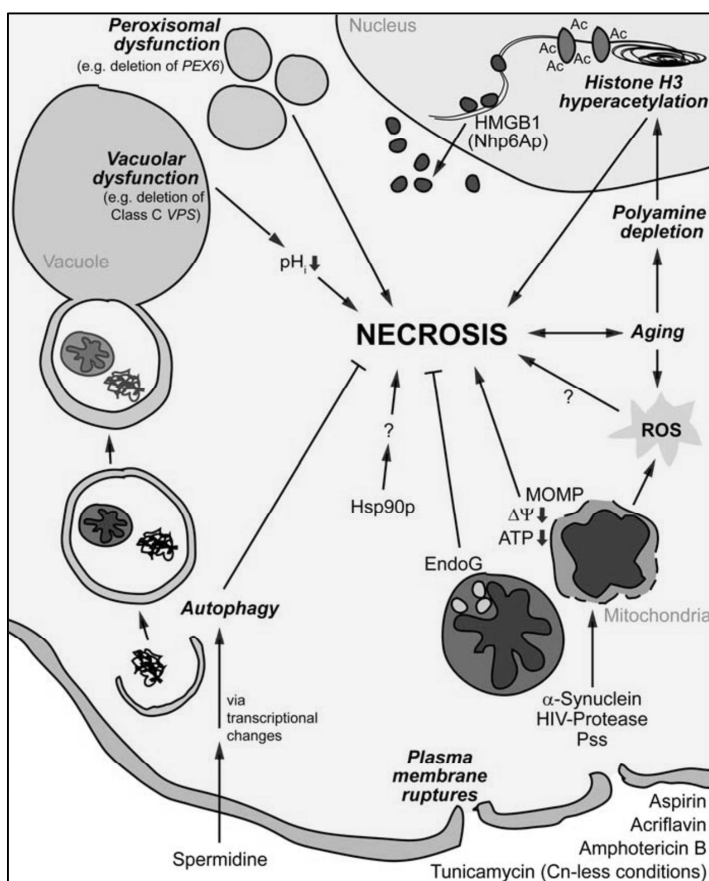


Figure 15 - Schematic view of stimuli and cellular processes that interfere with yeast necrosis (Eisenberg *et al.*, 2010).

Necrotic cell death presents the following morphological characteristics: cell volume increase (oncrosis), organelle swelling and plasma membrane rupture and consequently loss of intracellular contents. In addition, it shows bioenergetic impairment and random DNA degradation (reviewed in

Eisenberg *et al.*, 2010). In contrast with the organized energy-dependent apoptotic process, the plasma membrane integrity is maintained, intracellular content (like DNA) undergoes ordered degradation, and exposure or secretion of diverse factors promotes phagocytic cell elimination or acts as an immuno-suppressant (Figure 16).

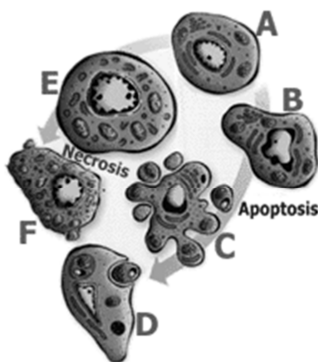


Figure 16 - Apoptosis versus necrosis. A healthy cell (A) shrinks and its DNA - which usually is dispersed throughout the nucleus - starts to clump around the nucleus' edge (B). The nucleus and cell quickly break up, becoming apoptotic bodies (C), which are ingested by healthy cells nearby (D). Swelling and inflammation (E) is characteristic from necrosis. When a necrotic cell ruptures (F) it can damage nearby healthy tissue (Purdy, 1997).

Necrosis was already linked to several diseases such as ischemia, trauma and possibly some forms of neurodegeneration (Vanlangenakker *et al.*, 2008; Akiyama *et al.*, 2000) as well as various cardiovascular disorders (Tavernarakis, 2007). In addition, some viruses, bacteria and protozoa can induce necrosis (Proskuryakov *et al.*, 2003). Hence, further biochemical understanding of the necrotic mechanisms is mandatory to develop new strategies for therapeutic intervention of these disorders or pathological conditions (reviewed in Eisenberg *et al.*, 2010).

In a closer perspective, it could be stated that an apoptotic yeast cell will inevitably undergo necrosis (loss of plasma membrane integrity) since phagocytosis by neighboring yeast cells is improbable. In the end, an apoptotic ‘dead cell’ will present a metabolic breakdown leading to the collapse of plasma membrane integrity and hence necrotic morphology (Ludovico *et al.*, 2005). This phenomenon is called “secondary necrosis” as it results from a preceding type of cell death, which can be apoptosis. Its detailed characteristics and precise moment in which this occurs are still unknown. However there are evidences suggesting that secondary necrosis (SN) occurs very quickly, within 2–3 h after the beginning of primary apoptotic death (Phillips *et al.*, 2006). But another form of necrosis needed to be proposed, since necrotic markers appear without apoptotic characteristics, which can be distinguished from SN, being referred to as “primary necrosis” (PN). In order to detect PN, a combination of assays targeting several markers is indispensable to detect typical necrotic features. Meanwhile apoptotic markers (Fig. 10) should not be overlooked (reviewed in Eisenberg *et al.*, 2010).

Despite of the already known necrosis facts, the study of this PCD form is still in its infancy and much more is needed to uncover.

2. MATERIALS AND METHODS

2.1 Strains and Growth Conditions

S. cerevisiae strains used in this work are listed below (Table 1). The YEplac 195 expression vector contains the promoter and terminator sequences of the 5' and 3' regions of the *PDE2* gene.

Yeast cells were grown at 30°C on rich medium (YP) containing 1% yeast extract (Merck) and 2% bactopeptone (Oxoid) or on selective synthetic minimal media appropriated for the auxotrophic marker (composition: 0,077% (w/v) CSM-URA (formedium), 0,17% (w/v) Yeast Nitrogen base w/o amino acids and ammonium sulfate (Remel) and 0,5% (w/v) ammonium sulfate (Sigma-Aldrich), pH 5,5) supplemented with galactose or glucose both from Sigma. For solid media, 1,5% (w/v) Bacto-agar (Difco) was added, and in the case of minimal media, the pH was adjusted to 6,5.

Table 1 – Yeast strains used in the present work, respective relative genotypes and references.

Yeast strains	Relative Genotype	Reference
W303 – 1A	<i>Mata leu2-3, 112 ura3-1 trp1-1 his3-11,15 ade2-1 Can1-100 GAL SUC</i>	Thomas and Rothstein (1989)
<i>tps1Δ</i>	<i>W303-1A Mat a tps1::TRP1</i>	Hohmann <i>et al.</i> , 1993
<i>tps1Δ+pPDE2</i>	<i>W303-1A Mat a tps1::TRP1 + YEplac195 PDE2</i>	Bonini, Beatriz (unpublished results)
<i>tps1Δ hxp2Δ</i>	<i>W303-1A Mat a tps1::TRP1 hxp2::LEU2</i>	Hohmann <i>et al.</i> , 1993

2.2 Yeast Genomic DNA Preparation

Cells were grown on appropriate medium, collected and transferred to 2 ml tube with approximately 0.3 g of glass beads and 200 µl of TE buffer (see 3.1). 200 µl of PCI (phenol-chloroform-isoamylalcohol – 25:24:1) were added and cells were disrupted for 20 s in a fast prep apparatus (Precellys 24 – Bertin Technologies). The extracts were centrifuged for 10 min at 20000 g and the aqueous phase (the supernatant) collected. DNA was precipitated by the addition of 500 µl of ethanol 100%.

2.3 PCR: Polymerase Chain Reaction

PCR was used in this work to verify proper deletion of genes in the *tps1Δ* strain. All genes were deleted by replacing their open reading frame by a Kanamycin cassette (Bonini, unpublished results). The forward primers used to check the deletions are specific for each gene and the reverse primer is specific for the Kanamycin cassette (table 2).

Table 2 – Primers used in the present work.

Gene Name	Primer sequence
NMA111	5'-AACACAGCAGTCGTTCATGC-3'
NUC1	5'-GATTCCCTTATCGCAGGCAAG-3'
ESP1	5'-TCGGCAATCACTCTAGTGTCC-3'
MCA 1	5'-AACCTTAAGCCAACGAGGTAG-3'
KAN	5,- CCCATATAAATCAGCATCC-3'

The final volume of the PCR mixture was 20 µl per reaction and its composition was: 1 µl of template DNA (around 100 ng genomic DNA), 2 µl of each specific primer (forward and reverse; 60 ng/ µl), 2.5 µM of each dNTP (2 µl of dNTP mixture solution 4x25 µM in a dilution 1:10), 0.5 µl of TaqE polymerase (1.25 U), 2 µl of buffer with MgCl₂ and distilled water to 20 µl.

PCR products were visualized in a 1% agarose gel. TAE buffer (1x) was used as running buffer at 100 V for 35 min, and the DNA was stained with SYBR Safe TM DNA gel stain (Invitrogen) solution.

DNA was visualized with a UV Bioimaging System (Invitrogen) and images captured using the internal camera. The general PCR program used is shown in Table 3.

Table 3 – PCR general program followed in the present work.

Step	Temperature (°C)	Time
1	94	4 min
2	94	1 min
3	From 48 to 52	30 s
4	72	1 min*
5	72	10 min
6	10	~

* elongation: 30 cycles from step 2 until step 4.

2.4 Spot Assay/Drop Test

Cells were grown until mid exponential phase in YPGal and diluted in 1 ml of water to an OD₆₀₀ of 1. The suspension was sequentially diluted (10 times each dilution) until reach an OD₆₀₀ of 0.001 and 5 µl of each dilution was spotted on YPGal and YPD solid media containing different concentrations of the carbon source (from 1, 2, 5, 10, 20, 50, 100 mM). Plates were then incubated at 30°C for 2 to 3 days.

2.5 Clonogenic Assay

Cells were grown in YPGal medium until mid exponential phase. Samples were taken after 0h, 2h, 4h, 6h, 8h and 24h of glucose addition (glucose final concentration of 5, 20, 50 and 100 mM) and diluted

in 1 ml with medium to an OD₆₀₀ of 0.1. The suspension was sequentially diluted until reach an OD₆₀₀ of 0.001. Then 100 µl of the most diluted suspension were plated in YPGal (three replicates) and incubated for 3 days at 30°C and formed colonies were counted. The percentage of viable cells was calculated using the number of colony-forming units (c.f.u.) at zero time as reference (100%). The values are the average of three independent experiments.

2.6 Isolation of Mitochondrial and Post Mitochondrial Fractions

(Cytochrome C Release)

Cells were inoculated in a 50 ml pre-culture at 30°C and 200 rpm. This pre-culture was used to inoculate 1 L YPGal. After an over night (o.n.) incubation at 30°C, 100 mM of glucose was added and the culture was further incubated for the desired time according to the experiment. The procedure was adapted from the Tzagoloff method (Tzagoloff *et al.*, 1975).

After incubation with glucose, cells were harvested by centrifugation at 2500 g for 10 min and washed once with 1.2 M sorbitol. The cells were weighted and resuspended in 5 ml of Digestion buffer (see 3.3) per g of cells (wet weight) and the suspension was incubated for 40 min to 1 h at 30°C to digest the cell wall. The spheroplasts were collected by centrifugation at 1000 g for 10 min with soft brake, gently washed two times with 1.2 M sorbitol and resuspended in 2.5 ml of ST-PMSF buffer (see 3.6) per g cell (wet weight). The suspension was transferred to a 30 ml Wheaton dounce and stroked with a tight-fitting pestle until the spheroplasts were broken by the shear force. Cell debris were removed by centrifugation at 2500 g for 10 min and the supernatant was centrifuged once more. Then, the supernatant was collected and centrifuged at 12000 g for 15 min at 4°C to sediment mitochondria. The post-mitochondrial supernatant (PMS) was transferred to new tube and the mitochondrial pellet was resuspended in 500 µl ST-PMSF buffer. Samples were centrifuged again at 12000 g for 15 min and the final mitochondrial pellet resuspended in 250 µl ST-PMSF buffer. Both PMS and mitochondrial fraction were used to detect cytochrome c by Western Blotting (see 2.9). The primary antibody anti cytochrome c was custom made (Eurogentec, 1:5000 dilution (v/v) in 5% milk in TBST), and the primary antibody anti the mitochondrial protein Cox II was from Mitosciences (MS419, dilution of 1:200 (v/v) in 5% milk). Cox II was detected in both mitochondrial fraction and post mitochondrial supernatant to normalize protein loading and assure that the supernatant was free of mitochondrial contamination. The secondary antibody is anti-rabbit for cytochrome c and anti-mouse for Cox II, horseradish peroxidase-conjugated anti IgG, used at a dilution of 1:5000 and detected by enhanced chemiluminescence (Western Blotting, see 2.9).

2.7 Immunoprecipitation Assay / S-nitrosylation of GAPDH

Cells were inoculated in a 3 ml pre-culture at 30°C and 200 rpm. This pre-culture was used to inoculate 10 ml per sample of YPGal. After an o.n. incubation at 30°C, 100 mM glucose or 2 mM DETA/NO donor were added to the proper samples and the culture was further incubated for 2 hours.

2.7.1 Preparation of Yeast Protein Extracts

Cells were harvested by vacuum filtration and washed with ice-cold PBS 1x (see 3.7). The cells were immediately frozen in liquid nitrogen after being collected in an eppendorf. The pellets were left to thaw in ice and 500 µl of lysis buffer (see 3.8) were added. The pellets were resuspended and one volume of glass beads was added. Cells were broken using the vortex, seven times for 1 min each with intervals of 1 min on ice. The homogenate was then centrifuged at 2000 g for 5 min at 4°C. The supernatant was transferred to fresh 1.5 ml tubes and centrifuged again at 20000 g for 30 min at 4°C. The supernatants were transferred to new 1.5 ml tubes and protein concentrations were quantified (see 2.9). The used volume in subsequently step corresponded to 500 µg of protein per 500 µl of buffer.

2.7.2 Immunoprecipitation

For the immunoprecipitation of nitrosilated proteins, 3 µl of the antibody rabbit anti-S-nitrosocysteine (Sigma-Aldrich) were added to 500 µg of protein lysate in a total volume of 500 µl. The suspensions were incubated for 4h at 4°C with rotation (as a negative control, 500 µl of lysate were incubated without antibody). The samples were then transferred to a tube having 20 µl of washed protein G plus/protein A-agarose beads. The cell lysates were gently rocked with the beads-Ab complex o.n. at 4°C. The agarose beads were collected by centrifugation at 1000 g for 1 min at 4°C and washed two times with 1 ml ice-cold lysis buffer (see 3.8) and two times with 1 ml ice-cold wash buffer (see 3.9). The elution of the beads was performed in 20 µl of sample buffer (see 3.10). To dissociate the immunocomplexes from the beads, they were boiled for 5 min. The beads were collected by centrifugation at 20000 g for 1 min and the supernatant loaded on a SDS-PAGE gel and transferred to a nitrocellulose membrane before being probed o.n. with a monoclonal mouse anti-GAPDH antibody (MAB374, Chemicon) at a dilution of 1:200 (v/v). Horseradish peroxidase-conjugated anti-mouse IgG secondary antibody was used at a dilution of 1:5000 and detected by enhanced chemiluminescence (Western Blotting, see 2.9).

2.8 Measuring Protein Concentration

The protein concentration of the samples was determined by the Thermo Scientific Pierce 660 nm Protein Assay. The standard curve was designed by different known concentrations of a BSA (Bovine Serum Albumine) solutions and water was used as blank. 300 µl of Pierce® reagent was added to 20 µl of sample (two replicates) and absorbance was measured at 660 nm using Spectra Max Plus 384 (Molecular Devices, Brussels) after 5 min incubation in a 96 well plate.

2.9 SDS-PAGE and Western Blotting

Protein samples with the dye were boiled for 5 min and pulled down before applying on gel. Protein samples were resolved by pre-prepared SDS-PAGE (NuPAGE® 4-12% Bis-Tris gel 1.0 mm x 10 wells, Invitrogen) in a vertical electrophoresis chamber (Novex Mini-Cell, Invitrogen) with 1xSDS Running buffer (see 3.13) at 150V (Power PAC 300) for 1.5 h and blotted on nitrocellulose membrane (Hybond-C Extra, Amersham Biosciences, UK) in a blotting buffer (see 3.14) at 300 mA for 1.5 h, placed inside a western blot chamber (BIO-RAD Mini Protean®3Cell). The membranes were washed one time with TBS (see 3.11) and blocked for 2 h with 5% milk in TBST buffer (see 3.12) at room temperature. Then they were incubated overnight with the primary antibody in milk TBST solution at 4°C with gentle shaking. On the next day, the membranes were washed three times with TBST buffer (see 3.12) for 10 min each and incubated for 1 h with secondary antibody solution (1:5000 dilution (v/v) in 5% milk solution) at room temperature with gentle shaking. Once more, the membranes were washed three times with TBST buffer 10 min each. The detection was achieved by rapidly incubating the membranes with SuperSignal® WestPico Chemiluminescent (Pierce Chemical, Rockford), 1:1 peroxide and luminal solution. Subsequently visualization was performed using Las-4000 mini Luminescent Image Analyzer apparatus (Fuji Film) and the software Las-4000 image reader. The data obtained was then analyzed through the program AIDA (advanced image data analyzer) version 4.22.034.

2.10 Fluorescence Microscopy

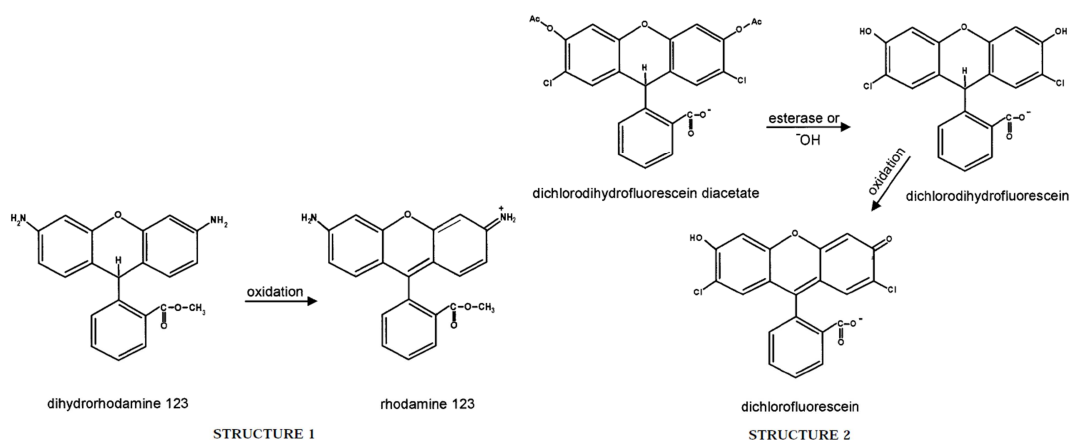
The observation of the apoptotic markers was achieved by detecting reactive oxygen species (ROS) accumulation, externalization of phosphatidylserine residues, DNA fragmentation and cell viability, assayed by the use of fluorescent dyes.

2.10.1 Reactive Oxygen Species Accumulation

The sequential reduction of oxygen through the addition of electrons leads to the formation of a number of ROS, which have been documented, namely: superoxide, hydrogen peroxide, hydroxyl radical, hydroxyl ion. Two different ROS types formation were visualized by adding appropriate dyes. Both used dyes are cell permeant indicators for ROS. DCDHF-diacetate, DCDHF and DHR are lipophilic and ONOO^- readily diffuse across cell membranes.

2.10.1.1 Hydrogen Peroxidase Formation

This oxygen specie was detected by using Dihydrorhodamine 123 (DHR 123, Invitrogen). Dihydrorhodamine 123 (DHR), a structural analog of DCDHF, lacks the diacetate and dichloro substituents of DCDHF and has amino groups in place of the two hydroxyl groups of DCDHF (see Structures 1 and 2). Upon oxidation of DHR to fluorescent rhodamine, one of the two equivalent amino groups tautomerizes to a charged imino, effectively trapping rhodamine within cells (Crow, 1997).



Cells were grown in YPGal medium until mid exponential phase, and samples of OD_{600} of 1 were prepared. Different glucose concentrations and 2 $\mu\text{l/ml}$ of DHR 123 were added and the culture was further incubated at 30°C for the desired time according to the experiment. ROS accumulation was visualized through Axioplan 2 imaging from Zeiss, using the filter set 10 (excitation BP 450-490 nm, emission BP 515-565 nm).

2.10.1.2 Superoxide Anion Formation

The detection was made by using 2'7'-dichlorodihydrofluorescein diacetate (H_2DCFDA , Invitrogen). Intracellular esterases remove the lipophilic blocking groups converting the probe H_2DCFDA into H_2DCF , a non-fluorescent and charged form of the dye that is much better retained by the cells than

the parent compound; in the presence of oxygen species, H₂DCF is oxidized to the high fluorescent 2',7'-dichlorofluorescein (Figure 17) (Tarpey *et al.*, 2004).

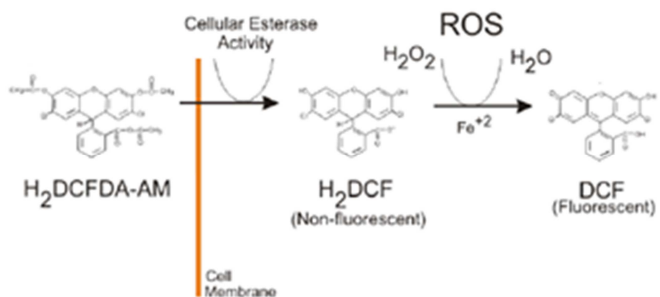


Figure 17 – H₂DCFDA-AM uptake and subsequent modifications (adapted from Held, 2010).

Cells were grown in YPGal medium until mid exponential phase, and samples of OD₆₀₀ of 1 were prepared. Different glucose concentrations and 1 µl/ml of H₂DCFDA were added and the culture was further incubated at 30°C for the desired time according to the experiment. ROS accumulation was visualized through Axioplan 2 imaging from Zeiss, using the filter set 10 (excitation 495 nm and emission 515 nm).

2.10.2 Phosphatidylserine Residues Externalization

Cells were grown until mid exponential phase in YPGal medium (3 ml inoculum) and 50 ml YPGal were inoculated with this suspension in order to obtain OD₆₀₀ of 0.1 and then further incubated o.n. at 30°C. Different concentrations of glucose were added to the cultures according to the experiment and the cells were incubated at 30°C for the desired time. Then the samples were transferred to a 50 ml pre-weighted falcon and centrifuged at 2500 g for 10 min. The supernatant was discarded and the cell pellets were washed with sorbitol 1,2 M. The supernatants were discarded, the falcons dried and the cells weighted. The cells were resuspended in 5 ml of Lyticase buffer (see 3.4) per g of cells and the suspension was incubated for 40 min to 1 h at 30°C to digest the cell wall. The spheroplasts were collected by centrifugation at 1000 g for 10 min with soft break, gently washed one time with 50 ml of sorbitol 1.2 M and centrifuged once more at 1500 g for 5 min. The supernatants were discarded with a tip and washed with 500 µl Annexin buffer. The pellets were then resuspended in 250 µl Annexin buffer and 38 µl of this suspension were transferred to new eppendorfs, and 2 µl Annexin-V-FLUOS and 2 µl PI were added (staining kit from Roche). This mixture was left in the dark for 20 min and centrifuged at 1500 g for 2 min. The cells were washed with Annexin buffer, resuspended and 5 µl were applied to an ethanol cleaned slide (Madeo *et al.*, 1997). Externalization of phosphatidylserine residues was visualized through Axioplan 2 imaging from Zeiss (AxioVisio 4.6). Annexin-V-FLUOS excitation and emission wavelengths are 488 nm 518 nm, respectively. Propidium iodide excitation and emission wavelengths range are 488 to 540 nm and 617 nm, respectively.

2.10.4 DNA Fragmentation (TUNEL Assay)

The detection of DNA fragmentation was made by Terminal deoxynucleotidyl transferase dUTP Nick End Labeling (TUNEL) assay. Cells were inoculated in a 3 ml pre-culture at 30°C and 200 rpm. This pre-culture was used to inoculate 5 ml YPGal. After an o.n. incubation at 30°C, glucose was added in different concentrations and the cultures were further incubated for 4h. Cell fixation was done by adding 268 µl of formaldehyde 37% (w/v) and samples were incubated for an extra hour. Cellular suspensions were centrifuged at 2500 g for 5 min, supernatants discarded and pellets washed one time with 5 ml of 0.1 M potassium phosphate buffer pH 7.5 containing 1.2 M sorbitol. Then the pellets were resuspended in the same buffer with 1.5 µl 2-mercaptoethanol and 1 mg zymolyase 20T per ml and incubated for 40 min at 30°C. The cells were collected after centrifugation at 1000 g for 5 min with low break and washed once with PBS containing 1.2 M sorbitol and resuspended in 1 ml of the same buffer. A cell sample of 30 µl was transferred to a polylysine treated glass slide (Poly-L-Lysine 10 min, washed with water and air dried) and incubated at room temperature for 10 min. After washed three times with 30 µl PBS 1x, 30 µl of sodium citrate were added and samples were incubated on ice for 2 min, washed two times with PBS 1x and incubated again for 1 h at 37°C with 30 µl of reaction mix (450 µl Label solution with 50 µl Enzyme solution, In Situ Cell Death Detection kit, Roche). Visualization was achieved by fluorescent microscopy (filter set 40 (BP360)51, BP485)17, BP560)18) from Zeiss, excitation filter BP 450-490, beam splitter FT510 and emission filter LP520) after having the samples washed three times with PBS 1x.

As a positive control wt cells were treated with DNase I in tris HCl pH 7.5, 10 mM MgCl₂ and BSA. The negative control was obtained by incubating wt cells with label solution without terminal transferase.

2.10.6 Viability Quantification

In order to have a quantitative result about the percentage of live and dead cells in a population after glucose addition, a flowcytometry study was performed using FACScan flow cytometer (FACSCalibur cytometer, Becton Dickinson) equipped with a 488 nm argon lazer at low flow rate. This is possible by simultaneous scattering and fluorescence signal measurements. An optimized sheath fluid was used (BD FACSFlowTM, BD Biosciences) and the setting were setup: Threshold was set on FSC at 500 V and FSC and SSC detector voltages were E00 and 300 V, respectively. Fluorescence detectors were adjusted to 600 V.

Cells were grown at 30°C in YPGal medium until mid exponential phase. After glucose was added the culture was further incubated for the desired time according to the experiment and samples were taken each 2h.

2.10.6.1 Oxonol staining

Bis-(1,3-dibutylbarbituric acid) trimethine oxonol (DiBAC4(3)) (FlouroPure™, Molecular Probes, USA), also known as oxonol dye, has an absorbance at 493 nm and emission at 516 nm. A FL1 filter was applied (530/30 nm).

Each sample was diluted in milliQ water until a good flow rate is reached (approximately 100 cells per second). After the blanks had been measured (samples without dye), 460 µl of these suspensions were taken and dispensed in a new polystyrene round bottom tube (BD Falcon™, BD Biosciences, USA), where 40 µl of Oxonol was added (1,6 µg/ml of final concentration). Samples were then resuspended in a vortex and measured after being incubated for 15 min in the dark and further vortex-mixed. Data was obtained and analyzed using the program BD Cell Quest™ Pro software version 4.0.2. A dot plot FSC-H vs FL-1H was represented and percentage of dead cells of each region was calculated after the clouds of cells were gated.

2.11 Determination of Ras2 Activity

Cells were grown at 30°C in YPGal medium until mid exponential phase. Then they were harvested (5 mL of the culture) by centrifugation at 2500 g for 10 minutes and washed with MilliQ water. The weight of cells was determined and 500 µL of lysis buffer (see 3.16) was added per 400 mg of cells. The cells were broken by adding 0.3 g of glass beads and 2 times running in Fast prep instrument (Precellys 24) at 25 seconds each. The cells were centrifuged at 7000 g for 5 min and the supernatant was collected. Then, 500 µL of lysis buffer was added and the protein was quantified (see 2.8). Afterwards, 300 µg of protein were taken and 20 µL of RasBindingDomain (RBD)-glutathione-beads (Ras activation assay Biochem Kit™, Cytoskeleton, Inc.) were added and the total volume was adjusted to 500 µL with lysis buffer, followed by incubation with rotation for 1 hour at a cold room. Afterwards, the samples were centrifuged at 1000 g for 1 minute and washed with wash buffer (see 3.17) for 3 times being careful not to disturb the beads pellet. After removing the supernatant to have a final volume of approximately 20 µL, the protein loading buffer was added and the results were obtained by Western Blotting (see 2.9). For the detection of Ras2, Anti-Ras (Santa Cruz Biotechnology, Inc.) with 1:250 v/v dilution was used as primary antibody, while the secondary antibody (anti-goat) was diluted to a concentration of 1:5000 v/v (Santa Cruz Biotechnology, Inc.). The quantification of Ras2 was done by using the Advanced Image Data Analyzer (AIDA version 4.22.034, Raytest Isotopenmessgeräte GmbH).

4. RESULTS

4.1 Deletion of *TPS1* Causes Growth Defect in Glucose Containing Medium

As previously mentioned in chapter 2, the first step of trehalose synthesis is catalyzed by *Tps1*, an enzyme that plays a crucial role in control of glycolysis. The *tps1Δ* strain is sensitive to glucose and does not grow in the presence of this sugar. A spot assay was performed to evidence the high sensitivity of the *tps1Δ* strain upon glucose. Growth is already affected in the presence of just 1 mM glucose; *tps1Δ* mutants did not grow when glucose concentrations exceeded 2 mM (Figure 18 - central panel). Growth of the *tps1Δ* strain was restored when they had the *PDE2* gene overexpressed. However, the overexpression of *PDE2* did not completely restore the growth of *tps1Δ* strain on glucose to the wild type level. In the spot assay, a slight reduced growth of the *tps1Δ* strain overexpressing *PDE2* was still visible in glucose containing medium when compared to its growth in galactose containing medium (Figure 18 - right panel). The WT did not show any evidence of growth alteration (Figure 18 - left panel).

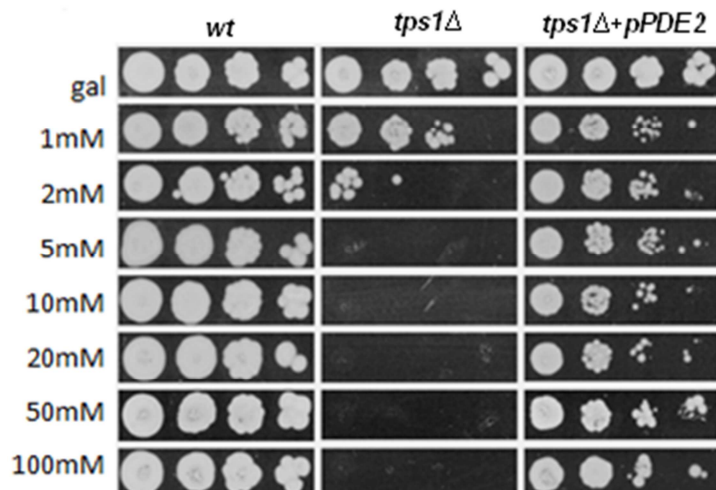


Figure 18 – Growth of wt (left), *tps1Δ* (center) and *tps1Δ+pPDE2* (right) on 100 mM galactose (top) and several glucose concentrations (from 1 mM to 100 mM) in YP medium.

The growth of the above mentioned strains were also characterized in liquid medium. The *tps1Δ* mutant sees its growth restricted as soon as 1 mM of glucose is added to the medium (Figure 19 – b). The *tps1Δ* strain still grew in YP with 2 mM of glucose (Figure 19- c), however its growth was inhibited if glucose concentrations were 5 mM or higher (Figure 19 – b to g). The growth curves also showed us that the *tps1Δ+pPDE2* cell population, although it grows on glucose, has a longer lag phase than the wt. The duration of *tps1Δ+pPDE2* lag phase increases with increasing glucose concentration present in the medium. It changes from approximately 5h (Figure 19 – b) in the presence of 1 mM glucose up to 12h (Figure 19 - g) in presence of 100 mM glucose, while the wt maintained a lag phase of approximately 4h in all conditions. Similar growth for all strains was observed in YPGal medium (Figure 19- a). The *tps1Δ+pPDE2* strain appeared to have a slight delay, when entering the exponential phase. The results obtained in liquid medium matched the observations obtained with the spot assay (Figure 18).

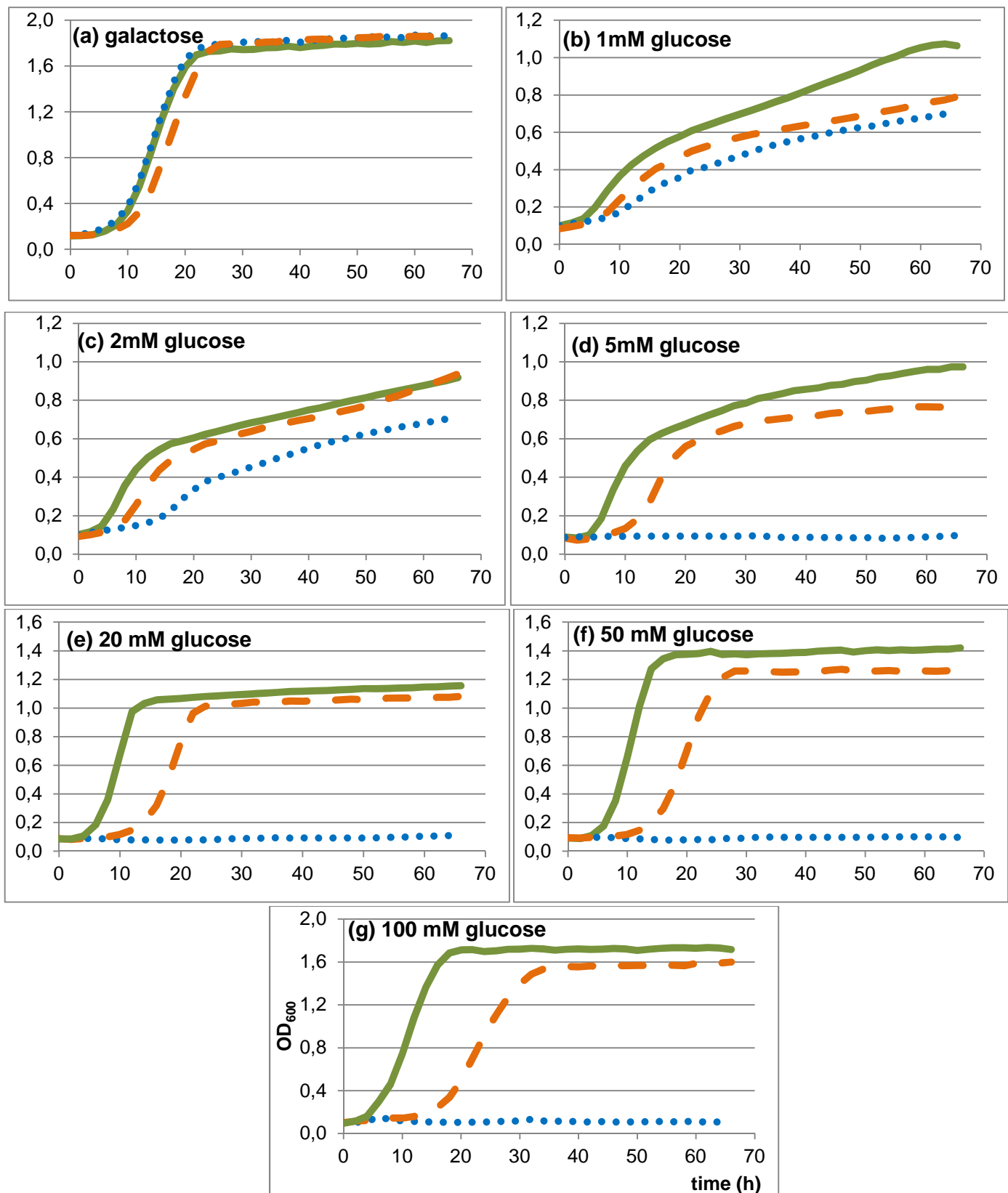


Figure 19 – Growth curves on 100 mM galactose medium (a) and several glucose concentrations: 1 mM (b), 2 mM (c), 5 mM (d), 20 mM (e), 50 mM (f) and 100 mM (g); of wt (full line), *tps1Δ* (dotted line), *tps1Δ+pPDE2* (dashed orange line). Cells were grown in galactose-containing medium until mid-exponential phase and transferred to fresh glucose-containing medium at an initial OD₆₀₀ of 0.05. OD₆₀₀ measurements were performed in a Bioscreen C apparatus (LabSystems).

4.2 *Tps1* Deletion Mutant Presents a Glucose Induced Loss of Viability

To better characterize the glucose induced loss of growth capacity of *tps1Δ*, viability assays were performed. We started to assay proliferation capacity through a conventional spread technique (clonogenic assay).

4.2.1 Proliferation Capacity

Not surprisingly, after 7h, 5h, 4h and 3h of glucose addition to final concentrations of 5 mM, 20 mM, 50 mM and 100 mM, respectively, only 50% of the *tps1Δ* cells retained the capacity to form colonies (Figure 20). The *tps1Δ+pPDE2* cells showed, in every condition, a higher viability than the *tps1* deletion mutant, where at least 75% of the cells were able to form colonies after 24h of glucose addition. In medium with final glucose concentrations of 20 mM and 50 mM, the *tps1Δ+pPDE2* showed a slight decline in the number of c.f.u. already after 4 hours (Figure 20– b, c). At the highest glucose concentration studied, the *tps1Δ+pPDE2* strain showed a more pronounced decline, from 100% to 75% of the cells able to form colonies at 24h after glucose addition (Figure 20 - d). At this time, the *tps1Δ* cells showed, in every condition studied, a percentage of viable cells lower than 7%.

Also at 24h after glucose addition, the number of wt c.f.u. dropped to values between 83% and 60%. Probably the low values can be explained by the presence of cell aggregates, therefore forming a reduced number of colonies. However, at all conditions studied, both the WT and the *tps1Δ+pPDE2* strains maintained a higher c.f.u. capacity 24h after glucose addition, while the *tps1Δ* had a strong decline in the c.f.u. number (Figure 20).

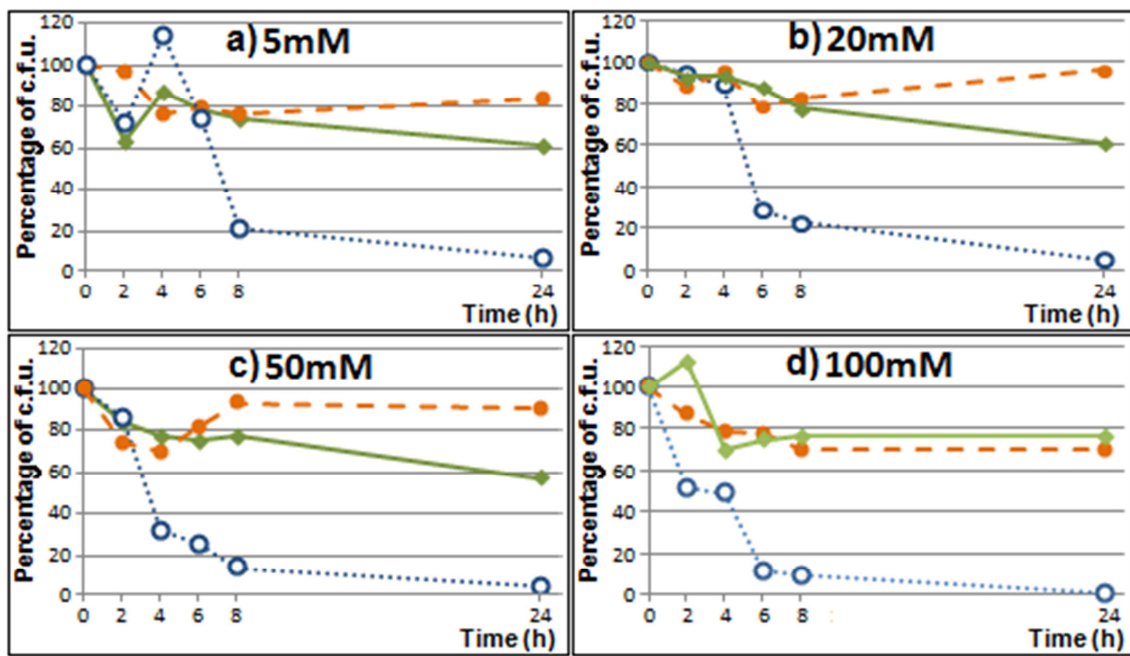


Figure 20 – Clonogenic assay for wt (full line), *tps1* Δ (dotted line), *tps1* Δ +*pPDE2* (dashed line). Cells were grown until mid-exponential phase in YPGal and glucose was added, at time zero, to obtain different final concentrations: 5 mM (a), 20 mM (b), 50 mM (c) and 100 mM (d). Samples were collected at the time indicated, sequentially diluted to a final concentration corresponding to an OD₆₀₀ of 0.0001 for the wt and *tps1* Δ +*pPDE2* and 0.001 for the *tps1* Δ and then plated on YPGal (in triplicate). Viability was estimated by c.f.u. counts. Are presented the most representative results from at least three independent experiments.

4.2.2 Cell Membrane Integrity

The viability was also assessed with Oxonol [DiBAC4(3)] staining by flowcytometry (see 3.11.6.1). Before and after the glucose addition, samples were taken at defined intervals of time as indicated in the figures and the cells were incubated with Oxonol in MilliQ water (in a final concentration of 1,6 μ g/ml).

Viable cells are able to exclude the anionic oxonol (Figure 21), due to transmembrane potential; on the contrary, the fluorescent probe can freely enter cells with a depolarized membrane, where it binds to intracellular proteins or membranes and enhances significantly the green fluorescence (Epps, Wolfe, and Groppi 1994; Dinsdale, Lloyd, and Jarvis 1995).

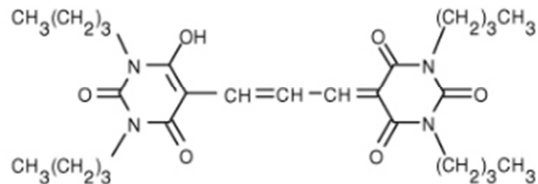


Figure 21 - Oxonol molecule structure.

Conversely, the integrity of *tps1* Δ cell membrane was maintained during the first hours after glucose addition, only decreasing significantly after 8h, until when was kept above 80% and dropping to values of around 45%, 24h after glucose addition. No significant reduction of cell membrane

integrity occurred (merely about 10%) in wt cells exposed to glucose up to 24 h, when evaluated using this dye (Figure 22).

The *tps1Δ+pPDE2* cells showed a slight decrease in viability, which was recovered after 8h of glucose addition when grown in 20 mM glucose medium (Figure 22 - a). In the case of growing cells in 50 mM of glucose-containing medium, the *tps1Δ+pPDE2* cells showed a more prominent decrease in viability between the fourth and eighth hour after glucose addition, although this decrease is also recovered at the end of the experiment (Figure 22 - b). 100 mM of glucose concentration was the only condition, among the ones tested, where *tps1Δ+pPDE2* cells did not recover viability up to the initial values, being observed 80% viable cells after 24h of glucose addition (Figure 22- c). Despite this loss of recovery capacity, the percentage of viable *tps1Δ+pPDE2* cells registered was similar to the wt viability values and significantly different from the *tps1Δ* values.

The comparison of the results obtained by c.f.u. counting and by the fluorescent dye shows that after 8 h of growth on glucose, although the majority of the cells in all three strains retained their membrane integrity (>80%), the *tps1Δ* cells are no longer able to form colonies on solid YPGal medium, presenting a viability lower than 19% at that time (Figure 20). On the other hand, *tps1Δ+pPDE2* cells presented similar values in both assays at the same time (8h). The only difference was the absence of a decline in cell integrity loss in 100 mM of glucose-containing medium (Figure 22 - c), observed in the c.f.u. counting results (Figure 20 - c). At 24h after glucose addition, *tps1Δ* cells presented a loss of proliferation capacity about 7 times bigger than loss of membrane integrity. The wt cells had a higher percentage of cells with preserved membrane integrity (81%) after 24 h of glucose addition than the proliferation capacity value (60%) in the presence of 50 mM of glucose. However, in the other two glucose concentrations the values of cells showing preserved membrane integrity were very similar to the ones showing capacity of proliferation.

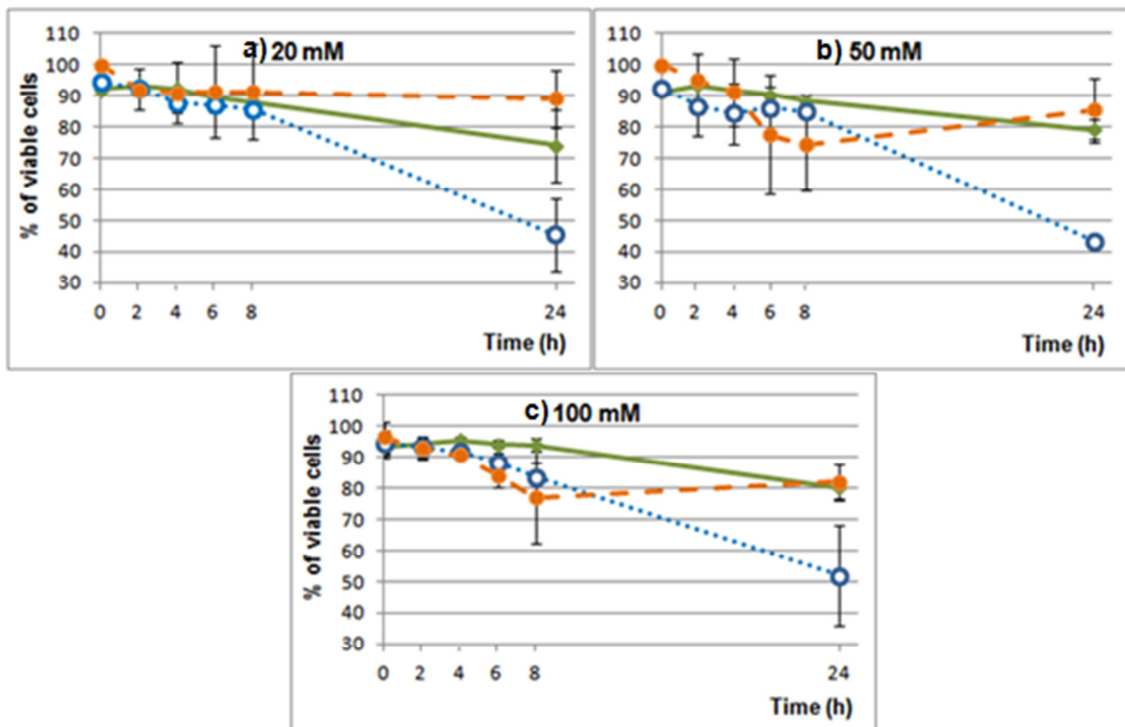


Figure 22 – Cell membrane integrity of wt (full line), *tps1Δ* (dotted line), *tps1Δ+pPDE2* (dashed line) during exposure to glucose. Cells were grown until mid-exponential phase in YPGal and glucose was added, at time zero, to several final concentrations: 20 mM (a), 50 mM (b) and 100 mM (c). Samples were collected at the times indicated and properly diluted. Viability was estimated by depolarized cells: evaluation of loss of plasma membrane integrity assessed with the fluorescent probe, DiBAC4(3) (Oxonol). Are presented the mean values from at least three independent experiments.

4.3 *Tps1* Deletion Mutant Presents Apoptotic Markers after Glucose Addition

4.3.1 ROS

It has already been shown that glucose addition causes a severe deregulation in the early steps of glycolysis in the *tps1Δ* mutant instigating total absence of growth in glucose containing medium (Thevelein and Hohmann, 1995). Natural *petite* mutations in this mutant reducing its mitochondrial activity were shown to partially overcome this problem and tests with mutants without mitochondrial DNA (*rho*⁰) showed the ability to restore growth in glucose containing media, to some extent. Lately, has been described mitochondria implication in certain apoptotic processes which involved release of cytochrome c from this organelle (see 1.4.1.1.1) and Reactive Oxygen Species (ROS) production (see 1.4.1.1.2). Additionally, ROS also act as cell death regulators and their presence has been linked to apoptotic phenomena. It has already been published that ROS plays an important role in the induction of apoptosis in mammalian (Ahamed *et al.*, 2011) as well as in yeast cells (reviewed in Carmona-Gutierrez *et al.*, 2010). It is well documented that the intracellular accumulation of ROS leads to cell damage (reviewed in Avery, 2011) by perturbing the external redox potential of cell structures (Madeo *et al.*, 1997; Ludovico *et al.*, 2001).

With the help of H₂DCFDA and 123-DHR, it was observed that glucose induced the intracellular accumulation of ROS (Figure 22). The appearance of yeast cells with a strong green

fluorescence indicates that cells sustained considerable amounts of ROS (Figure 24- c); conversely, control cells, wt cells (at all conditions) and *tps1Δ* (incubated in the absence of glucose, with 100 mM galactose instead), evidenced no fluorescence and appeared dark against the faint fluorescent background (Figure 24- a). The presence of ROS accumulation in the *tps1Δ hxa2Δ* double deletion mutant was also tested, since it is known that the deletion of HXA2 gene in the *tps1Δ* background recovers growth on glucose (Blázquez *et al.*, 1993; Hohmann *et al.*, 1993). As expected, it showed no ROS production, similar to the wt situation. Since this strain showed no growth problem on glucose, neither ROS accumulation, it was not studied in further detail.

Only *tps1Δ* cells incubated in presence of glucose, during 8 h, presented ROS accumulation. To evidence the staining, a specific field containing a group of cells was selected (Figure 24).

Since this is a qualitative method, this staining protocol did not allow us to quantify the difference between *tps1Δ* cells treated with 20 mM and 50 mM of glucose. Between *tps1Δ* cells there was no detected difference among different incubation times. The same results were obtained with 100 mM glucose (not shown).

In the case of H₂DCFDA's usage, the results obtained indicate that the type of ROS responsible for oxidizing this molecule are produced in a minor quantity, consequently less cells appear fluorescent.

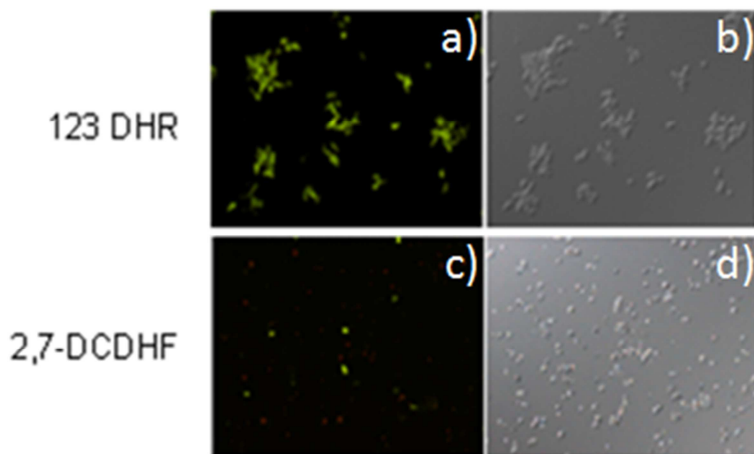


Figure 23 – Representative image for comparison of different ROS type production in *tps1Δ* mutants. ROS accumulation was assessed by loading the cells with 123DHR and 2,7-CDCHF after glucose addition to final concentration of 50 mM. Wt always showed an insignificant level of ROS with both dyes as well as the *tps1Δ+pPDE2* cells (not shown). Fluorescent micrographs (a, c); DIC image of the same cells (b, d).

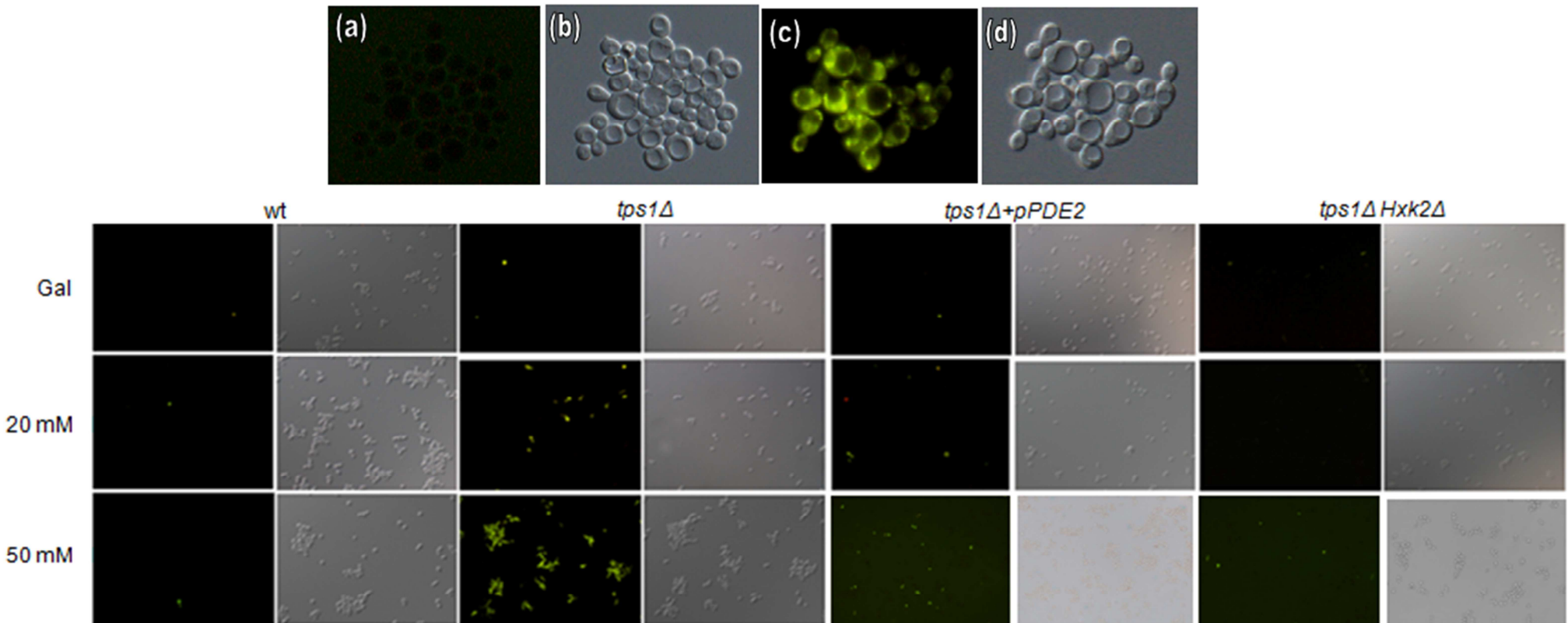


Figure 24 – Visualization of ROS production in wt, *tps1* Δ , *tps1* Δ +*pPDE2* and *tps1* Δ *Hxk2* Δ mutants. ROS accumulation was assessed by loading the cells with 123DHR after glucose addition to two different final concentrations (20 mM and 50 mM) and samples were visualized each 2h up to 8h. Here we just present the micrographs taken at 2h after glucose addition as in the succeeding hours there is no detectable difference (fluorescence is maintained). Wt showed always an insignificant level of ROS (a, b) as well as the *tps1* Δ +*pPDE2* and *tps1* Δ *Hxk2* Δ mutants. Meanwhile the *tps1* Δ showed an unequivocal increase in ROS levels with nearly all cells exhibiting ROS accumulation at all concentrations, maintaining it up to 8h post glucose addition (c, d). A specific field was selected to better observe the ROS accumulation after 2h in 50 mM glucose. Fluorescent micrographs were observed with filter set FITC (a, c); DIC image of the same cells (b, d).

4.3.2 Phosphatidyl Serine externalization

Glucose induced apoptosis in the *tps1Δ* mutant is characterized by exhibition of other specific markers documented in mammalian cells and already for other cases of apoptosis in yeast. Externalization of phosphatidylserines (PS) was assayed by staining with Annexin V – FLUOS (green). Furthermore cells were also treated with Propidium iodide, PI (orange-red). Due to its capacity to bind exclusively to DNA (by intercalating bases) of leaky necrotic cells, which have their plasma membrane compromised (Haugland, 2005), this allows to distinguish between apoptotic and necrotic cells as it is membrane impermeable, hence is not incorporated by viable cells.

After knowing that in the *tps1Δ* the viability loss occurs 4h after glucose addition (Figure 20), cells were incubated in glucose containing medium during at least 4 h. *tps1Δ* cells presented an apoptotic phenotype by having their membranes stained in green in a much higher number (Figure 25 - a) than the wt did. Green cells were also present in higher number than red cells. Conversely, control cells (wt cells at all conditions and *tps1Δ* incubated in the presence of 100 mM galactose), evidenced no significant number of green fluorescent cells neither red cells. Some isolated fluorescent cells randomly pop up, probably due to natural apoptotic/necrotic events, while the rest of the cells appeared no fluorescent (Figure 25). In addition, although it was rare to see, double red and green stained cells could also be visualized. The presence of only green fluorescence means that cells have retained their membrane integrity, as they were not able to incorporate PI, but the plasma membrane asymmetry is no longer present (early apoptotic cells). The opposite, when PI was exclusively taken, pointing out the primary necrotic phenotype, red fluorescence was visualized. The very few cells that do present both red and green fluorescence are most likely in an advance apoptotic or secondary necrotic state

We could clearly show *tps1Δ* apoptotic cells with their membranes stained in green (Figure 25 - a), some cells presenting double staining (Figure 25 - e) and one cell stained in red with compromised cytoplasmatic membrane that, therefore, has already entered in a necrotic stage (Figure 25 - c).

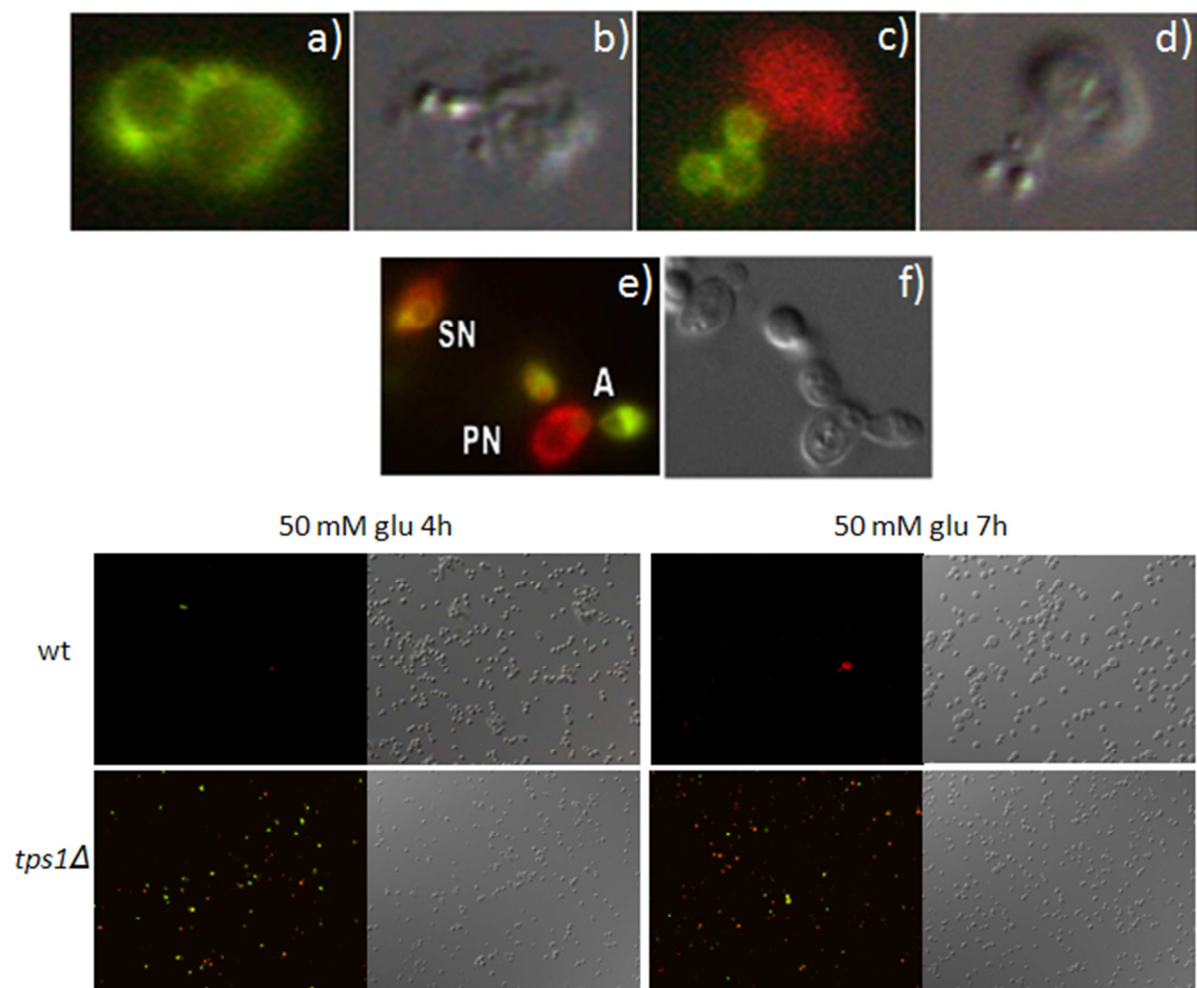


Figure 25 – Exposition of phosphatidylserines (PS) in the outer leaflet of the cytoplasmatic membrane with Annexin V – FLOUS (green) and necrotic cells with PI (orange-red), 4h and 7h after glucose addition to a final concentration of 50 mM. This double staining allowed us to realize that the wt (top panels) did not show a significant staining level at all conditions tested, whereas the *tpslΔ* (lower panels) did. A specific field was selected to better observe the cellular membrane fluorescence of *tpslΔ* after 4h in 50 mM glucose. Apoptotic cell (A), primary necrotic cell (PN) and secondary necrotic cells (SN). Fluorescent micrographs were observed with filter set FITC (a, c, e); DIC (phase contrast) image of the same cells (b, d, f).

4.3.3 TUNEL

Treatment of *tps1* deletion mutant with 2, 5, 10, 20, 50 and 100 mM glucose resulted in a TUNEL-positive result (green fluorescence), indicating the occurrence of DNA strand breaks (Figure 26 - b to g). The positive control (Figure 26 - j) was prepared by adding DNase I to the label solution, while the negative control (Figure 26 - i) was obtained by excluding the terminal transferase from label solution. There is a noticeable increase in stained cells as the glucose concentration increases. Fluorescence intensity seems stronger in *tps1Δ* cells treated with 100 mM glucose (Figure 26 – g) than in the other conditions tested. No detectable TUNEL staining was seen in *tps1* cells after addition of 1 mM glucose, as well in wt glucose treated cells (Figure 26 - a and h). Comparing the glucose addition effect with the controls, we found that fluorescence is as strong as the positive control only with 50 and 100 mM of glucose.

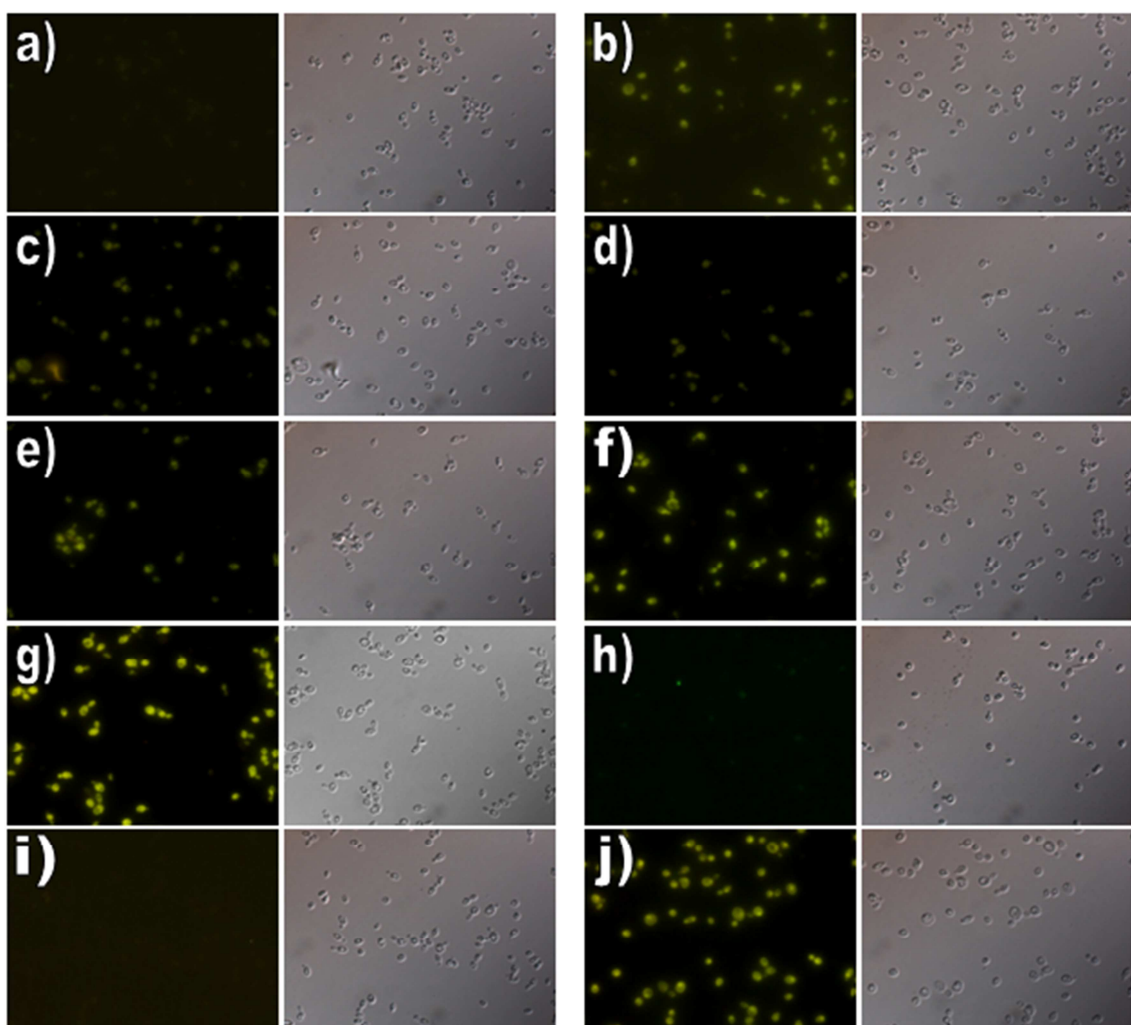


Figure 26 – TUNEL assay, 4h after glucose addition to final different concentrations: 1 mM (a), 2 mM (b), 5 mM (c), 10 mM (d), 20 mM (e), 50 mM (f), 100 mM (g), wt (h), negative control (i), positive control (j). Fluorescent micrographs (left panels); DIC (phase contrast) image of the same cells (right panels).

4.3.4 Cytochrome c Release

Considerable amount of data describes an involvement of mitochondria in the apoptotic mechanism (Liu *et al.*, 1999; Adachi *et al.*, 1997; Kharbanda *et al.*, 1997; Kim *et al.*, 1997; Kluck *et al.*, 1997; Yang *et al.*, 1997; Bossy-Wetzel *et al.*, 1998), and the occurrence of cytochrome c release from the mitochondrial intermembrane space to the cytosol, has also been described in *S. cerevisiae* (Roucou *et al.*, 2000). The detection of cytochrome c in the postmitochondrial supernatant (PMS) was accomplished by Western blot of cellular fractions from wt, *tps1Δ* and *tps1Δ+pPDE2*. As expected, all mitochondrial fractions (M) had cytochrome c and COX II detected, whereas no COX II was detected in PMS fractions, which excludes the possibility of mitochondrial contamination. The following analysis revealed, more importantly that, in fact, cytochrome c is exclusively released into cytoplasm in *tps1Δ* cells subjected to 20 mM (Figure 27 – middle left panel) and 50 mM glucose concentrations (Figure 27 – middle right panel), in contrast to wt cells. Apparently, with 20 mM of glucose, cytochrome c release in *tps1Δ* is only detected after 3h of glucose addition and is maintained up to 5h, while with 50 mM it is already detected 1h after glucose addition, although after 4h it appeared to be no longer detected. Relatively to the *tps1Δ+pPDE2* samples, it was not detectable any cytochrome c release, both for 20 and 50 mM glucose.

Such results are an evidence of mitochondria as an organelle with participation in responses to apoptotic stimuli; in the present case, to glucose presence in the medium.

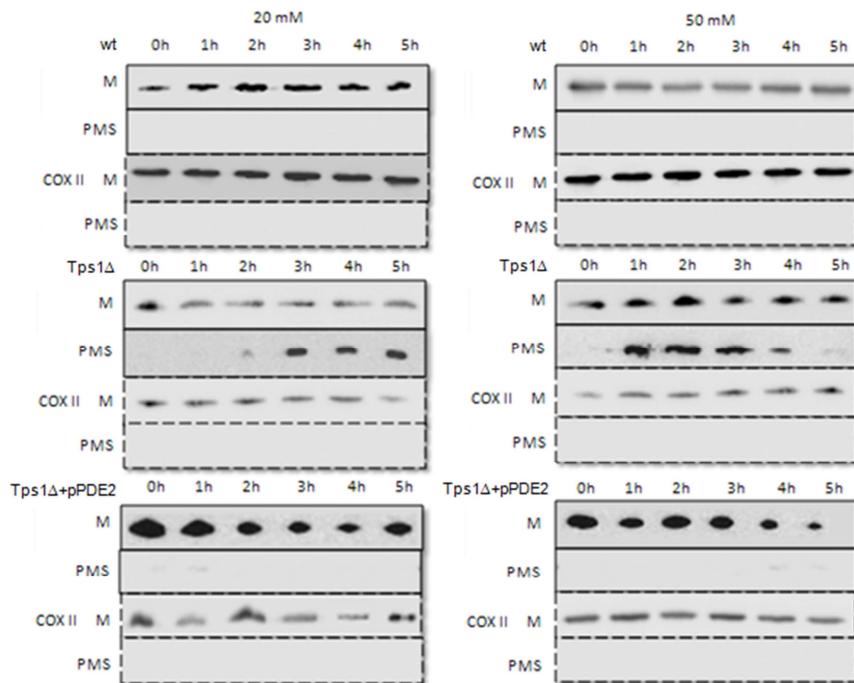


Figure 27 – Immunodetection of cytochrome c (full line) and COX (dashed line) from time zero up to 5h post glucose addition in mitochondria (M) and in postmitochondrial supernatant (PMS) of wt (top panels), *tps1Δ* (middle panels) and *tps1Δ+pPDE2* (bottom panels). Two different glucose concentrations were evaluated: 20 mM (left panels) and 50 mM (right panels). The gel was loaded with 20 µg of protein from mitochondrial samples and 100 µg of protein from postmitochondrial supernatant samples.

As a whole, all the results obtained above shows that glucose is an apoptotic trigger in the *tps1Δ* deletion mutant, with no indication of necrosis being significantly involved in the cell death of this mutant.

4.4 S-nitrosylation of GAPDH

Nitric oxide (NO) is a small molecule with distinct roles in diverse physiological functions in biological systems, among them the control of the apoptotic signaling cascade. It was already demonstrated that NO and glyceraldehyde-3-phosphate dehydrogenase (GAPDH) are crucial mediators of yeast apoptosis. Furthermore, the yeast GAPDH was shown to be a target of extensive proteolysis upon H₂O₂-induced apoptosis and undergoes S-nitrosylation (Almeida *et al.*, 2007). Additionally, in *tps1Δ* strain glycolysis seams blocked in the step where GAPDH participates (Bonini *et al.*, 2004), leading us to investigate if GAPDH nitrosylation also occurs. To assess if NO signaling and GAPDH S-nitrosylation are also linked with glucose-induced apoptotic cell death in *tps1Δ* mutant, we performed an immunoprecipitation of S-nitrosilated GAPDH. Considering the positive control DETA/NO treated cells (Figure 28 – lane 4) a maximum reachable level and the negative control *tps1Δ* cells incubated in the absence of glucose, with 100 mM galactose instead (Figure 28 - lane 1) the basal level, these results gave us some questionable values, since the difference between the basal and the obtained value for glucose incubated *tps1Δ* cells (Figure 28 - lane 2) just differ about half unit. Additionally, upon comparison of *tps1Δ* cells incubated with glucose with the ones incubated with DETA/NO, there was still a difference of one unit, meaning that the higher value could be reached. This did not meet our expectations, as an increase of at least two folds has already been mentioned elsewhere (Almeida *et al.*, 2007), we can just say for now that there is no detectable variation on the level of S-nitrosylation of the glyceraldehyde-3-P dehydrogenase. Further repetitions of this experiment are necessary.

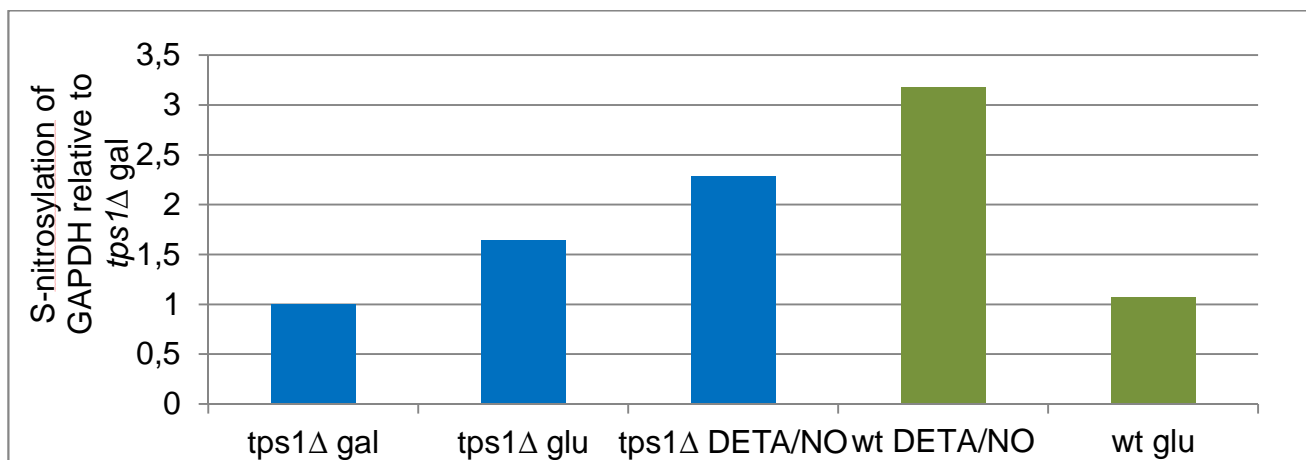


Figure 28- GAPDH is S-nitrosilated during glucose-induced apoptosis. Quantification of band intensity from western blot assay by densitometry. Band intensities were normalized to the intensity of IgG bands. Data express the GAPDH/IgG fold change in comparison to control (lane 1). Immunoprecipitation of S-nitrosilated GAPDH with an anti-CSNO antibody from cellular extracts of untreated, either glucose (100 mM) and DETA/NO-treated cell of wt (lanes 4 and 5) and *tps1Δ* (lanes 1 to 3).

4.5 *Tps1* Deletion Mutant Presents a High RAS Activity after Glucose Addition

Ras is a key regulator of cell growth. In order to verify if there is a correlation between Ras activation, glucose and apoptosis in *S. cerevisiae*, the activity of Ras2 proteins (GTP/GDP loading state), which play an important role in the cAMP-PKA pathway, was quantified (see 2.11). We could demonstrate that the Ras activity was enhanced in *tps1 Δ* cells exposed to glucose (Figure 29 – left bars). The measure of this protein activation in the *tps1* revealed that it can increase up to 8,5 times. In order to increase in a glucose concentration dependent manner, the RAS activation with 5 mM and 20 mM glucose should be between 4 and 8 times the basal level. It was observed an increase of 2,5 fold, 5 fold, 3 fold, 2 fold, 8,5 fold and 6,5 fold for *tps1 Δ* cells incubated in 1 mM, 2 mM, 5 mM, 20 mM, 50 mM and 100 mM, respectively. On the other hand the values of Ras activity in *tps1 Δ +pPDE2* cells was conserved around the wt value in all conditions tested (Figure 29 – right bars).

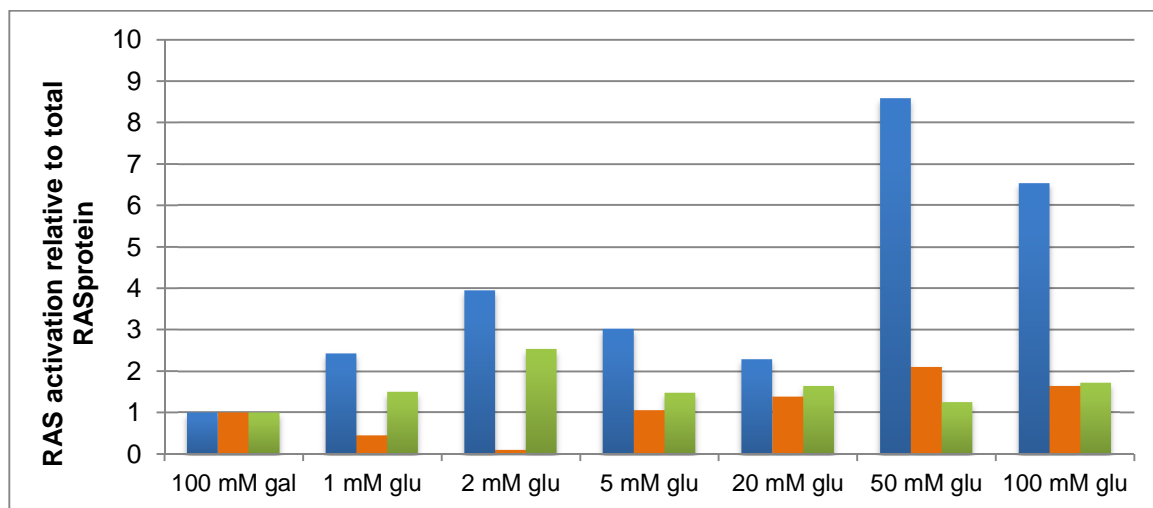


Figure 29 – Ras2 is activated during glucose-induced apoptosis. Quantification of band intensity from a Western blot assay by densitometry. Band intensities were normalized to the intensity of pure protein bands. Data express the Ras activity fold change in comparison to control. Detection of Ras activity with an anti-Ras antibody from cellular extracts of untreated (100 mM galactose) and glucose-treated cell of *tps1 Δ* (left bars) and *tps1 Δ +pPDE2* (central bars) and wt (right bars) with different final concentrations. (1 mM, 2 mM, 5 mM, 20 mM, 50 mM, 100 mM).

4.6 The Deletion of Known Pro-apoptotic Proteins in *tps1Δ* Background Did not Result in Growth Recover after Glucose Addition

Is of interest to study as well other proteins belonging to the fungal apoptotic network already described as key proteins in regulating apoptotic-like cell death (for example, endonuclease G and metacaspase 1) if they are involved in regulating apoptotic-like cell death of the *tps1Δ* mutant after glucose addition. The serine protease *NMA111* (Fahrenkrog, 2011; Fahrenkrog *et al.*, 2004), *NUC1* (Burhans and Weinberger, 2007; Büttner *et al.*, 2007), the caspase-like *ESP1* (Yang *et al.*, 2008), *MAC1* (Mazzoni and Falcone, 2008) genes were deleted in the *tps1Δ* background. A spot assay was performed but the growth of the double mutants was already affected in the presence of very low glucose concentrations similar to the *tps1Δ* single mutant (Figure 30).

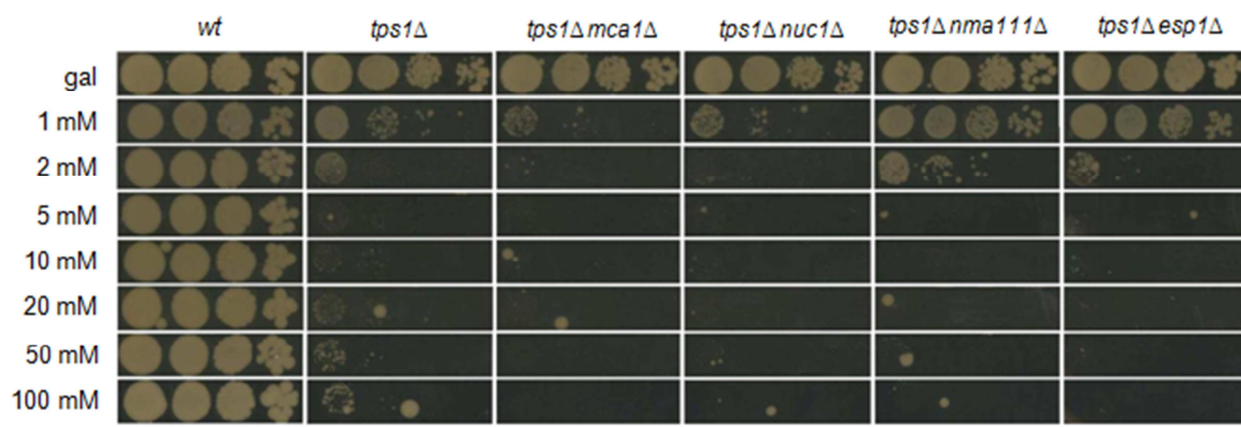


Figure 30 – Growth of *wt* (column 1), *tps1Δ* (column 2) and several double deletion mutants (column 3 - 6) on 100 mM galactose (top) and several glucose concentrations (from 1 mM to 100 mM).

RT-PCR is also interesting to perform in order to evaluate the expression of pro-apoptotic genes in the cells since glucose is added until their collapse. This method would allow us to better understand the apoptotic pathways responsible for the cell death shown by *tps1Δ* cells.

5. DISCUSSION

5.1 *Tps1* Deletion Mutant Growth Defect in already 2mM Glucose Containing Medium Can Be Restored by Overexpression of *PDE2*

cAMP is a “second messenger” in glucose signaling contributing to a fast response to external stimuli. After glucose addition, a rapid but transient spike in cAMP concentration occurs (Thevelein and De Winde, 1999), leading to the activation of PKA. Activation of PKA leads to degradation of trehalose and glycogen, playing a role in stress resistance, expression of STRE-genes and in growth and proliferation. Trehalose by itself has a huge impact in the way yeast cells successfully adapt to changes in the environment by being a reserve carbohydrate which also serves as a stress protectant. Trehalose is particular important in surviving forms, like spores, where it is virtually the only carbon and energy source. Through deletion of *TPS1* a perturbation on trehalose synthesis is induced. We have demonstrated that the *tps1Δ* mutant has a high sensitivity to glucose, as its growth is affected with only 1 mM of glucose concentration (Figure 18 – central panel and Figure 19 - b) and did not grow at all already with 5 mM of glucose (Figure 18 – central panel and Figure 19 - d). This specific growth defect on glucose or other rapidly fermentable carbon sources occurs accompanied by hyperaccumulation of the sugar phosphate intermediates from the first steps of glycolysis and rapid depletion of ATP and Pi (Hohmann *et al.*, 1993; Bonini *et al.*, 2000), which can be the reason for this high sensitivity. Together with hexokinase overactivity and both ATP and free phosphate depletion, *tps1Δ* cells are left with a totally unbalanced metabolism and they are no longer able to proliferate. This occurs mainly due to the lack of glucose repression on glycolysis, which becomes enable to generate ATP. Furthermore, the Ras is also overactive, PKA catalytic subunits are released. Ras overactivation will enhance the need of glycolysis. However, as this pathway is malfunctioning, the cell cannot survive any longer.

Nevertheless, the loss of growth capacity mentioned above is abolished in every glucose concentration tested by overexpressing *PDE2* (Figure 18 – right panel and Figure 19). The gap between *tps1Δ* and *tps1Δ+pPDE2* OD₆₀₀ values in the growth curves shows an increase directly proportional to the glucose concentration. So, the biggest difference (1,5 of OD₆₀₀) is achieved with 100 mM glucose (Figure 19 - g). The most probable explanation for this growth rescue is the intervention of *PDE2* in the cAMP pathway. This enzyme hydrolyses cAMP (Thevelein *et al.*, 2000) counteracting the overactive Ras effect (Figure 29 – left bars) in the *tps1Δ* phenotype in glucose containing medium. By this way, PKA is not activated, so it cannot initiate the apoptotic process that is responsible for (reviewed in Fröhlich *et al.*, 2007), thus *tps1Δ+pPDE2* survives upon glucose addition. Although, growth isn't fully restored, pointing out to the involvement of another pathway in this glucose effect. When the major glucose phosphotransferase *HXK2* is deleted in *tps1Δ* (Hohmann *et al.*, 1993) the accumulation of sugar phosphates intermediates and depletion of ATP and Pi no longer occurs, not being sensed the lack of *TPS1*. As this double mutant growth is totally restored, here can reside the explanation.

As the glucose concentration increase, the *tps1Δ+pPDE2* stationary phase is reached at a higher OD₆₀₀ value accompanying the wt growth curve (Figure 19), however in terms of viability this strain present a better growth improvement at lower glucose concentrations. In order to further understand this glucose concentration dependence in the *tps1Δ+pPDE2* cells recovery, more testes are necessary.

5.2 Glucose Induces Loss of Viability in *tps1Δ* Deletion Mutant with Cell Membrane Integrity Maintenance

There are several methods employed to ascertain quantitatively yeast viability. Yeast cells are generally considered to be dead when they irreversibly lose their ability to proliferate, however they can continue to be metabolically active. After coming across with the growth patterns of the working strains (Figure 19), the viability test showed how fast the capacity to proliferate was lost by the *tps1Δ* strain and how is the adaptation of *tps1Δ+pPDE2* cells profile in order to recover from glucose addition. It is obvious that the difference between the viability of *tps1Δ* cells and both *tps1Δ+pPDE2* cells and wt, mostly after 4h of glucose addition (Figure 20). The viability of *tps1Δ* cells decreased in a glucose concentration dependent manner. Below 100 mM of final glucose concentration *tps1Δ+pPDE2* cells recovered without problems. Apparently, *tps1Δ+pPDE2* and *tps1Δ* have their viability most apart in 20 mM of final glucose concentration in both assays: 95 percentual points in the clonogenic (Figure 20 – top right plot) and 55 percentual points in the cell membrane integrity (Figure 22). On the other hand, the *tps1Δ+pPDE2* strain appeared to decline more with 100 mM glucose as the difference in viability between this mutant and *tps1Δ* at the referred concentration was the lowest (70 percentual points) of all conditions tested. Although, to better describe its recovery in the highest glucose concentration tested it needs to be accompanied for longer in order to figure out when the *tps1Δ+pPDE2* cells reach the original viability values. 24h after glucose addition to a final concentration lower than 100 mM, the wt cells showed a viability of 70% (Figure 20 – b, c) or even lower (Figure 20 - a). This value is lower than expected, although the most probable explanation arises from the OD₆₀₀ measurements. Several factors may have contributed to variations in absorbance, whereas we believe that these are the two main reasons: as the wt presents high cell concentration after 8h of glucose addition (approximately 18 of OD₆₀₀), cells tend to get together, named flocculation phenomenon (Verstrepen *et al.*, 2003); the other one is the fact that wt cells had already entered the stationary phase for more than 5 h by that time, which is accompanied by cell wall thickening (Hao *et al.*, 1997) and cell size enlargement. Both events lead to OD₆₀₀ value given by excess (Am. Soc. Brew. Chem., 1980). The second one can be verified by evaluating the alterations at cell wall thickness level.

By comparing the vital staining with the plate count results, it was evident that the loss of cell membrane integrity was a consequence of viability loss. Apoptosis is a irreversible process, therefore those that enter in the apoptotic state lose their proliferaitaion capacity to prevent aberrant offspring. Since the membrane integrity in the *tps1* strain is maintained up to 8h after glucose addition (in some cases, 50% of cell population had lost their proliferation capacity after 4 hours of glucose addition

without losing membrane integrity), it means that this feature is not a characteristic of early apoptotic state. It still remains largely obscure if this phenomenon is more linked to necrosis than to apoptosis.

5.3 *TPS1* Deletion Mutant Undergoes Apoptosis after Glucose Addition

Apoptotic events were firstly described in mammalian cells, but sooner they were also documented in several yeast strains. *S. cerevisiae* cells undergo apoptosis as a response to exogenous and endogenous stimuli as different as triggers like chemical and physical stresses. It is not a novelty that glucose sends *TPS1* deletion mutant into growth arrest (Bonini *et al.*, 2000). The present work confirms that this specific growth defect in presence of glucose is accompanied by apoptotic markers disclosure: ROS accumulation, externalization of phosphatidylserines (PS), DNA fragmentation and cytochrome c release to the cytosol (Figure 24, Figure 25, Figure 26 and Figure 27).

The ROS accumulation phenomenon had already been described in several other yeast mutants and/or triggered by some other stimuli: low doses of H₂O₂ or acetic acid (Madeo *et al.*, 1999; Ludovico *et al.*, 2001), sugar- or salt-stress (NaCl), plant antifungal peptides, like Osmotin (Narasimhan *et al.*, 2001), Aspirin (Balzan *et al.*, 2004), HOCl (King *et al.*, 2004), or simply sugar itself (Granot *et al.*, 2003). *S. cerevisiae* is not the only yeast, which undergoes apoptosis: Sphingosines have recently been shown to induce apoptosis in *Aspergillus nidulans* (Cheng *et al.*, 2003), *Aspergillus fumigatus* also undergoes apoptosis after entering stationary phase (Mousavi and Robson, 2003) and Amphotericin B kills *Candida albicans* (Phillips *et al.*, 2003) by apoptosis. By now, the pathway responsible for the undergoing of *tps1Δ* mutant into apoptosis is still not completely known, although oxygen radicals seem to be key elements of apoptotic execution, conserved during evolution, since they are undoubtedly produced as the first step in the apoptotic behavior. This phenomenon is certainly and also a glucose dependent event as its occurrence in a cell population is more frequent as glucose concentration rises. Knowing that *tps1Δ* cells present a growth defect with just 5 mM glucose and show apoptotic markers with 20 mM glucose, is expected that with 100 mM glucose (5 times stronger than the lowest glucose concentration that originates ROS) is already a stimulus that induces necrosis. Unfortunately, we could not confirm that theory because this is only suitable to detect presence or absence of the referred marker.

A non-apoptotic cell is able to keep its plasma membrane phospholipid asymmetry (Bretscher, 1972) through flippase action (Higgins, 1994). On the contrary, apoptotic cells seem to lose this capacity, allowing Annexin-V to bind to PS in the outer membrane. Hence, it was possible to follow the apoptotic phenotype of *tps1Δ* cells in glucose containing medium. There was a clear difference between wt (control) and this deletion mutant after 4h of glucose addition (Figure 25): there were much more green-stained *tps1Δ* cells than wt. Some green fluorescent cells could be visualized in wt samples, but as they were in reduced number, it is most likely due to either natural apoptosis occurrence or cell wall digestion, as it is a harsh condition supported by cells, which can cause some stress. And if so, they succumb by primary necrosis (reviewed in Eisenberg *et al.*, 2010). The second

reason mentioned above can also be the answer to the quantity of dead cells in such an early apoptotic state. Unfortunately, this method does not allow quantitative results, which leads to inconclusive extent of necrosis involvement. In order to evaluate that, it is necessary to analyze Annexin-V incubated cells in a flow cytometer.

As part of the mitochondrial electron transport chain, cytochrome c has a very well defined and specific role in electron transfer from complex III to complex IV (Martinou *et al.*, 2000). When the *tps1Δ* cells enter in apoptosis, their cytochrome c no longer stays attached to the inner mitochondrial membrane and the mitochondrial outer membrane becomes permeable. This scenario was never observed in wt or *tps1Δ+pPDE2* cells (Figure 27). It is clear that cytochrome c release is a critical early event in apoptosis. The detection of COX II was never registered, giving the confidence that the cytochrome c detected bands were from the released pool and not from the mitochondria niche.

Taken altogether, these results clearly showed that *tps1Δ* cells undergo apoptosis when exposed to glucose in a concentration equal or higher than 20 mM.

5.4 *Tps1* Deletion Mutant Pathway Disorder

As previously mentioned, the deletion of the *TPS1* gene causes a severe glycolysis deregulation. In an attempt to reveal the key points in the trehalose synthesis and/or glycolysis pathways where the lack of *Tps1* most interfere, a S-nitrosilated GAPDH immunoprecipitation was performed. The results puzzled us as there was no significant increase of this GAPDH form in *tps1Δ* cells extracts after glucose addition (Figure 28). Presently, we are trying to understand if S-nitrosilation of GAPDH is either not linked to glucose-induced apoptotic cell death as was observed for H₂O₂ (Almeida *et al.*, 2007), or was simply a time dependent event. The relation between S-nitrosilated GAPDH and apoptosis is highly important to further understand the involved mechanisms.

5.5 Ras Activation Role in Regulating the Apoptotic Phenotype

The RAS genes family, highly conserved in evolution, was found to be activated in perhaps 20-25% of all human tumors and up to 90% in specific tumor types (reviewed in Downward, 2003). The existence of mammalian RAS homologues in the *S. cerevisiae* (RAS1 and RAS2) has already been described (Powers *et al.*, 1984). Both human and yeast RAS proteins can stimulate the magnesium and guanine nucleotide-dependent adenylate cyclase activity present in yeast cytoplasmatic membranes. Other studies indicate that although RAS proteins are essential controlling elements of adenylate cyclase in yeast, they have other essential functions in that organism (Toda *et al.*, 1986).

In this work we detected that RAS activation in *tps1Δ* cells could be dependent of glucose concentration. In the *TPS1* deletion mutant the activation of RAS, which can be almost 9 times higher than in the same cells incubated in galactose only (Figure 29), increases proportionally to the increase of glucose concentration, what evidences the importance of RAS as a glucose sensing system. However, this assay urges for repetitions with the aim of confirming this observation.

Furthermore, it was recently showed that deregulated Ras signaling compromises DNA damage checkpoint recovery (Wood and Sanchez, 2010). In *tps1Δ+pPDE2* cells, cAMP is hydrolyzed to AMP, resulting in a down-regulation of the signal cascade. However, the non activation of RAS due to this mechanism has remained unclear. Normally Ras is inhibited by Ira proteins, which are regulated by Kelch proteins Gpb1 (negatively regulates Ira2 by promoting its ubiquitin-dependent proteolysis) and Gpb2 (positively regulates Ira2) through Ira1 and Ira2 stabilization. RAS inhibition can also be performed by Krh proteins, as well as gpa2 (which influences the production of cAMP) or Tfs1 (Gombault *et al.*, 2007). GAP and GEF (GDP/GTP exchange factor) proteins, key regulators of Ras, together with its phosphorylation present an involvement of extreme importance in the feedback regulation of the Ras-cAMP pathway (Tamanoi, 2011). The regulation of RAS activity is somehow complex. In order to reveal in which extent each of these players contribute to maintain the wild type activation of the *tps1Δ+pPDE2* further investigation has to be done.

5.6 Limit Between Apoptosis and Necrosis in *tps1Δ* Strain Seems Higher than 100 mM Glucose

As already mentioned (see 1.4.2), high doses of the apoptotic inducer can trigger necrosis. Defining a range of glucose concentrations that is responsible for an apop-

totic phenotype and the boundary between these two cell death modes is of extreme relevance. After having these frontiers established becomes easier studying both and better characterize them.

It was yet possible to define this line that separates apoptosis from necrosis in some stress conditions and drugs. In the case of acetic acid presence, despite of a very small population with apoptotic markers appears at 120 mM, the necrotic process is the predominant cell death mode in samples exposed for 200 min to acetic acid at concentrations above 80 mM (120 to 200 mM). This was suggested by TUNEL assay results for these concentrations and ultimate cell disorganization with most intracellular structures destroyed (Ludovico *et al.*, 2001). When *S. cerevisiae* cells are treated with H₂O₂ in a concentration that belong to the interval of 0,3 – 15 mM, they undergo apoptosis (Madeo *et al.*, 1999). Relatively to metal ions, cells susceptibility is higher, so necrotic phenotype occurs at lower doses than at doses of other environmental toxins, such as H₂O₂ or acetic acid. Effects of Cu²⁺ and Mn²⁺ on cells are highly dosage sensitive. Yeast cells start losing viability between 4-6 mM Cu²⁺ and between 4-8 mM Mn²⁺, however TUNEL-positive result just occurs at the last value of the ranges mentioned. With 10 mM and 12 mM of Cu²⁺ and Mn²⁺, respectively, necrosis is triggered.

Some assays were already identified as good contributors in differentiating apoptosis from necrosis. An example of that is the TUNEL assay. When cells undergo necrosis the DNA fragmentation is random, thus these cells present a TUNEL-negative result similar to the negative control. Additionally, inhibition of protein synthesis that prevents the loss of proliferation capacity is another tool that allows to distinguish apoptosis from necrosis (Madeo *et al.*, 1999).

In our work we could verify that necrosis phenomenon is not the relevant form of death in the conditions studied, even if some cells appeared with their membrane disintegrated (Figure 25). It is suggested that the turn over between apoptosis and necrosis induced by glucose in *tps1Δ* cells occurs at a glucose concentration higher than 100 mM. This interpretation is supported by: cell number with apoptotic markers, induced by increasing concentrations of glucose, increases with treatments up to 100 mM glucose. Until 100 mM glucose the prevalent death mechanism is apoptosis. More glucose concentrations should be tested and further analyses have to be performed in order to answer at which point necrosis is triggered.

6. CONCLUSIONS

The most accepted explanatory theory for apoptosis in yeast cells states that it is an altruistic event that eliminates those cells that are unable to generate “healthy” descendants (Severin and Hyman, 2002). By succumbing, those cells liberate consumable resources and their “debris” nourish the rare surviving genetic variant (Hardwick and Cheng, 2004), contributing to reproductive success of the population as a whole.

After this study, we are able to affirm that the main differences between *tps1Δ* and *tps1Δ + pPDE2* strains are detected at growth, viability and visualization of apoptotic markers, but its dependency on glucose levels should be better evaluated by quantitative methods. A quantitative assay is required for accurate conclusions. This qualitative limitation did not allow us to have more conclusive results on involvement of necrosis. However, both Annexin-V and TUNEL assay drove us to believe that apoptosis is the predominant cell death mode up to 100 mM glucose. There is no detectable variation on the level of S-nitrosylation of the glyceraldehyde-3-P dehydrogenase at the conditions tested. Different conditions (both concentration and time) need to be investigated. The increase of RAS activation seems to be directly proportional to the glucose increase and to the loss in cell viability in the *tps1Δ* mutant.

S. cerevisiae is the best-researched yeast and probably the best-known eukaryotic organism, which makes it the perfect model to study metazoan, more specifically human cells and diseases linked to deregulations in apoptotic mechanisms. Clinically relevant cytopathological scenarios like accumulation of protein fibrils (Alzheimer, Parkinson) or lipid deregulation can be investigated in yeast for their ability to trigger cell death and for their dependence on apoptotic regulators (reviewed in Fröhlich *et al.*, 2007). With this powerful insight that yeast can provide into novel mammalian apoptotic regulators, valuable therapies development can be launched.

Moreover, yeast has a wide range of industrial application, namely bakery, winery, brewery industries and, most recently, bioethanol production. Thus, more tolerant strains to high sugar concentrations, especially glucose, and also high ethanol concentrations are needed. Apoptosis understanding can be the answer to overcome the limitations in large-scale fermentation processes (Kitagaki *et al.*, 2007).

BIBLIOGRAPHY

- Abdelwahid E., Rolland S., Teng X., Conradt B., Hardwick J. M. and White K.; 2011. "**Mitochondrial involvement in cell death of non-mammalian eukaryotes.**" *Biochimica et Biophysica Acta, BBA - Molecular Cell Research* 1813 (4): 597-607.
- Adachi S., Cross A. R., Babior B. M. and Gottlieb R. A.; 1997. "**Bcl-2 and the outer mitochondrial membrane in the activation of cytochrome c during Fas-mediated apoptosis.**" *J. Biol. chem.* 272: 21878-21882.
- Ahamed M., Akhtar M. J., Siddiqui M., Ahmad J., Musarrat J., Al-Khedhairy A., AlSalhi M. S. and Alrokayan S.; 2011. "**Oxidative stress mediated apoptosis induced by nickel ferrite nanoparticles in cultured A549 cells.**" *Toxicology* 283 (2-3): 101-8.
- Akiyama H., Barger S., Barnum S., Bradt B., Bauer J., Cole G. M., Cooper N. R., Eikelenboom P., Emmerling M., Fiebich B. L., Finch C. E., Frautschy S., Griffin W. S., Hampel H., Hull M., Landreth G., Lue L., Mrak R., Mackenzie I. R., McGeer P. L., O'Banion M. K., Pachter J., Pasinetti G., Plata-Salaman C., Rogers J., Rydel R., Shen Y., Streit W., Strohmeyer R., Tooyoma I., Van Muiswinkel F. L., Veerhuis R., Walker D., Webster S., Wegrzyniak B., Wenk G. and Wyss-Coray T., 2000. "**Inflammation and Alzheimer's disease.**" *Neurobiol. Aging* 21 (9): 383-421.
- Alison M R.; 1999. "**Identifying and quantifying apoptosis: a growth industry in the face of death.**" *The Journal of pathology* 188 (2): 117-8.
- Almeida B., Buttner S., Ohlmeier S., Silva A., Mesquita A., Sampaio-Marques B., Osório N. S., Kollau A., Mayer B., Leão C., Laranjinha J., Rodrigues F., Madeo F. and Ludovico P., 2007. "**NO-mediated apoptosis in yeast.**" *Journal of cell science* 120 (18): 3279-88.
- American Society of Brewing Chemists; 1980.
- Arends M. J., Morris R. G. and Wyllie H.; 1990. "**Apoptosis. The role of the endonuclease.**" *The American journal of pathology* 136 (3): 593-608.
- Avery S. V.; 2011. "**Molecular targets of oxidative stress.**" *The Biochemical journal* 434 (2): 201-10.
- Balzan R., Sapienza H., Galea D. R., Vassallo N., Frey H. and Bannister W. H.; 2004. "**Aspirin commits yeast cells to apoptosis depending on carbon source.**" *Microbiology* 150 (1): 109-115.
- Beullens M, Mbonyi K., Geerts L., Gladines D., Detremerie K., Jans W. and Thevelein J. M.; 1988. "**Studies on the mechanism of the glucose-induced cAMP signal in glycolysis and glucose repression mutants of the yeast *Saccharomyces cerevisiae*.**" *European journal of biochemistry / FEBS* 172 (1): 227-31.

Bevers E. M., Comfurius P., van Rijn J. L., Hemker H. C. and Zwaal R. F.; 1982. "**Generation of prothrombin-converting activity and the exposure of phosphatidylserine at the outer surface of platelets.**" *European journal of biochemistry / FEBS* 122 (2): 429-36.

Bisson L. F., Coons D. M., Kruckeberg A. L. and Lewis D. A.; 1993. "**Yeast sugar transporters.**" *Crit Rev Biochem Mol Biol.* 28 (4): 259-308.

Blázquez M. A., Lagunas R., Gancedo C. and Gancedo J. M.; 1993. "**Trehalose 6-phosphate, a new regulator of yeast glycolysis that inhibits hexokinases.**" *Science* 329 (1): 51-54.

Boles E. and Hollenberg C. P.; 1997. "**The molecular genetics of hexose transport in yeast.**" *FEMS Microbiology Reviews* 21: 85-111.

Bonini B. M., van Vaeck C., Larsson C., Gustafsson L., Ma P., Winderickx J., van Dijck P. and Thevelein J. M.; 2000. "**Expression of *Escherichia coli* otsA in a *Saccharomyces cerevisiae* tps1 mutant restores trehalose 6-phosphate levels and partly restores growth and fermentation with glucose and control of glucose influx into glycolysis.**" *Biochem. J.* 350 (Pt 1): 261-268.

Bonini B. M., van Dijck P. and Thevelein J. M.; 2004. "**Trehalose metabolism: enzymatic pathway and physiological functions.**" *B. R. GA The Mycota*: 291-332.

Bossy-Wetzel E, Newmeyer D. D. and Green D. R.; 1998. "**Mitochondrial cytochrome c release in apoptosis occurs upstream of DEVD-specific caspase activation and independently of mitochondrial transmembrane depolarization.**" *The EMBO journal* 17 (1): 37-49.

Bretscher M. S.; 1972. "**Asymmetrical lipid bilayer structure for biological membranes.**" *Nat. New Biol.* 236 (61): 11-2.

Burhans W. C. and Weinberger M.; 2007. "**Yeast endonuclease G: complex matters of death and of life.**" *Molecular cell* 25 (3): 323-5.

Bustamante E. and Pedersen P. L.; 1977. "**High aerobic glycolysis of rat hepatoma cells in culture: role of mitochondrial hexokinase.**" *Proceedings of the National Academy of Sciences of the United States of America* 74 (9): 3735-9.

Büttner S., Eisenberg T., Carmona-Gutierrez D., Ruli D., Knauer H., Ruckenstein C., Sigrist C., Wissing S., Kollroser M., Fröhlich K.-U., Sigrist S. and Madeo F., 2007. "**Endonuclease G regulates budding yeast life and death.**" *Molecular cell* 25 (2): 233-46.

Cameron S, Levin L., Zoller M. and Wigler M.; 1988. "**cAMP-independent control of sporulation, glycogen metabolism, and heat shock resistance in *S. cerevisiae*.**" *Cell.* 53 (4): 555-66.

Carlson M.; 1987. "MINIREVIEW Regulation of Sugar Utilization in *Saccharomyces* Species." *Microbiology* 169 (11): 4873-4877.

Carmona-Gutierrez D, Ruckenstein C., Bauer M., Eisenberg T., Büttner S. and Madeo F.; 2010. "Cell death in yeast: growing applications of a dying buddy." *Cell death and differentiation* 17 (5): 733-4.

Cheng J., Park T. S., Chio L. C., Fischl A. S. and Ye X. S.; 2003. "Induction of apoptosis by sphingoid long-chain bases in *Aspergillus nidulans*." *Mol. Cell Biol.* 23 (1): 163-177.

Chevtzoff C., Vallortigara J., Avéret N., Rigoulet M. and Devin A.; 2005. "The yeast cAMP protein kinase Tpk3p is involved in the regulation of mitochondrial enzymatic content during growth." *Biochim. Biophysica Acta* 1706 (1-2): 117-25.

Colombo S., Ma P., Cauwenberg L., Winderickx J., Crauwels M., Teunissen A., Nauwelaers D., de Winde J. H., Gorwa M. F., Colavizza D. and Thevelein J. M.; 1998. "Involvement of distinct G-proteins, Gpa2 and Ras, in glucose- and intracellular acidification-induced cAMP signalling in the yeast *Saccharomyces cerevisiae*." *The EMBO journal* 17 (12): 3326-41.

Colombo S., Ronchetti D., Thevelein J. M., Winderickx J. and Martegani E.; 2004. "Activation state of the Ras2 protein and glucose-induced signaling in *Saccharomyces cerevisiae*." *The Journal of biological chemistry* 279 (45): 46715-22.

Crow J. P.; 1997. "Dichlorodihydrofluorescein and dihydrorhodamine 123 are sensitive indicators of peroxynitrite in vitro: implications for intracellular measurement of reactive nitrogen and oxygen species." *Nitric oxide: biology and chemistry / official journal of the Nitric Oxide Society* 1 (2): 145-57.

van Dijck P., Colavizza D., Smet P. and Thevelein J. M.; 1995. "Differential importance of trehalose in stress resistance in fermenting and nonfermenting *Saccharomyces cerevisiae* cells." *Applied and environmental microbiology* 61 (1): 109-15.

Dinsdale M. G., Lloyd D. and Jarvis B.; 1995. "Yeast vitality during cider fermentation: two approaches to the measurement of membrane potential." *J. Inst. Brew.* 101: 453-458.

Downward J.; 2003. "Targeting RAS signalling pathways in cancer therapy." *Nat. Rev. Cancer* 3 (1): 11-22.

Eisenberg T., Carmona-Gutierrez D., Büttner S., Tavernarakis N. and Madeo F.; 2010. "Necrosis in yeast." *Apoptosis: an international journal on programmed cell death* 15: 257-268.

van Engeland M., Nieland L. J., Ramaekers F. C., Schutte B. and Reutelingsperger C. P.; 1998. "Annexin V-affinity assay: a review on an apoptosis detection system based on phosphatidylserine exposure." *Cytometry* 31 (1): 1-9.

Epps D. E., Wolfe M. L. and Groppib V.; 1994. “**Characterization of the steady-state and dynamic fluorescence properties of the potential-sensitive dye bis-(1,3-dibutylbarbituric acid)trimethine oxonol (Dibac4(3)) in model systems and cells.**” *Chemistry and Physics of Lipids* 69 (2): 137-150.

Ernandes J. R., De Meirman C., Rolland F., Winderickx J., de Winde J., Brandão R. L. and Thevelein J. M.; 1998. “**During the initiation of fermentation overexpression of hexokinase PII in yeast transiently causes a similar deregulation of glycolysis as deletion of Tps1.**” *Yeast* 14 (3): 255-69.

Fabrizio P., Battistella L., Vardavas R., Gattazzo C., Liou L.-L., Diaspro A., Dossen J. W., Gralla E. B. and Longo V. D.; 2004. “**Superoxide is a mediator of an altruistic aging program in *Saccharomyces cerevisiae*.**” *The Journal of cell biology* 166 (7): 1055-67.

Fadok V. A., Voelker D. R., Campbell P. A., Cohen J. J., Bratton D. L. and Henson P. M.; 1992. “**Exposure of phosphatidylserine on the surface of apoptotic lymphocytes triggers specific recognition and removal by macrophages.**” *J Immunol.* 148 (7): 2207-16.

Fahrenkrog B.; 2011. “**Nma111p, the pro-apoptotic HtrA-like nuclear serine protease in *Saccharomyces cerevisiae*: a short survey.**” *Biochem Soc Trans.* 39 (5): 1499-501.

Fahrenkrog B., Sauder U. and Aebi U.; 2004. “**The *S. cerevisiae* HtrA-like protein Nma111p is a nuclear serine protease that mediates yeast apoptosis.**” *Journal of cell science* 117 (Pt 1): 115-26.

Festjens N., Berghe T. V. and Vandenebeele P.; 2006. “**Necrosis, a well-orchestrated form of cell demise: signalling cascades, important mediators and concomitant immune response.**” *Biochimica et biophysica acta* 1757 (9-10): 1371-87.

Fraser A. and James C.; 1998. “**Fermenting debate: do yeast undergo apoptosis□?**” *Cell* 8924 (98): 219-221.

Fröhlich K.-U., Fussi H. and Ruckenstein C.; 2007. “**Yeast apoptosis — From genes to pathways.**” *Seminars in Cancer Biology* 17: 112-121.

Fröhlich K.-U. and Madeo F.; 2000. “**Apoptosis in yeast - a monocellular organism exhibits altruistic behaviour.**” *FEBS letters* 473: 7-10.

Fröhlich K.-U. and Madeo F.; 2001. “**Apoptosis in yeast: a new model for aging research.**” *Experimental Gerontology* 37: 1997-2001.

Galluzzi L., Larochette N., Zamzami N. and Kroemer G.; 2006. “**Mitochondria as therapeutic targets for cancer chemotherapy.**” *Oncogene* 25 (34): 4812-30.

Gancedo J. M.; 2008. “**The early steps of glucose signalling in yeast.**” *FEMS microbiology reviews* 32 (4): 673-704.

Gogvadze V., Orrenius S. and Zhivotovsky B.; 2006. “**Multiple pathways of cytochrome c release from mitochondria in apoptosis.**” *Biochimica et biophysica acta* 1757 (5-6): 639-47.

Golstein P. and Kroemer G.; 2007. “**Cell death by necrosis: towards a molecular definition.**” *Trends in biochemical sciences* 32 (1): 37-43.

Gombault A., Godin F., Sy D., Legrand B., Chautard H., Vallée B., Vovelle F. and Bénédetti H.; 2007. “**Molecular basis of the Tfs1/Ira2 interaction: a combined protein engineering and molecular modelling study.**” *Journal of Molecular Biology* 374 (3): 604-617.

Gourlay C. W. and Ayscough K. R.; 2006. “**Actin-induced hyperactivation of the Ras signaling pathway leads to apoptosis in *Saccharomyces cerevisiae*.**” *Molecular and cellular biology* 26 (17): 6487-501.

Gourlay C. W., Carpp L. N., Timpson P., Winder S. J. and Ayscough K. R.; 2004. “**A role for the actin cytoskeleton in cell death and aging in yeast.**” *The Journal of cell biology* 164 (6): 803-9.

Granot D., Levine A. and Dor-Hefetz E.; 2003. “**Sugar-induced apoptosis in yeast cells.**” *FEMS Yeast Research* 4: 7-13.

Hamann A., Brust D. and Osiewacz H. D.; 2008. “**Apoptosis pathways in fungal growth , development and ageing.**” *Trends in Microbiology* 16 (6): 276-83.

Hardwick J. M. and Cheng W.-C.; 2004. “**Mitochondrial Programmed Cell Death Pathways in Yeast.**” *Developmental Cell* 7 (5): 630-632.

Haugland R. P.; 2005. “**A guide to fluorescent probes and labeling technologies.**” *The Handbook, Invitrogen.*

Hayflick L.; 1965. “**The limited *in vitro* lifetime of human diploid cell strains.**” *Exp Cell Res.* 37: 614-36.

van Heerde W. L., Robert-Offerman S., Dumont E., Hofstra L., Doevedans P., Smits J. F., Daemen M. J. and Reutelingsperger C. P.; 2000. “**Markers of apoptosis in cardiovascular tissues: focus on Annexin V.**” *Cardiovascular research* 45 (3): 549-59.

Held, P.; 2010. “**Monitoring growth of beer brewing strains of *Saccharomyces cerevisiae*: the utility of Synergy H1 for providing high quality kinetic data for yeast growth applications.**” *BioTek Instruments, Inc.*

Held, P.; 2010. "An Introduction to Reactive Oxygen Species: Measurement of ROS in Cells." *BioTek Instruments, Inc.*

Higgins C. F.; 1994. "Flip-flop: the transmembrane translocation of lipids." *Cell* 79 (3): 393-5.

Hlavatá L., Aguilaniu H., Pichová A. and Nyström T.; 2003. "The oncogenic RAS2(val19) mutation locks respiration, independently of PKA, in a mode prone to generate ROS." *The EMBO journal* 22 (13): 3337-45.

Hlavatá L., Nachin L., Jezek P. and Nyström T.; 2008. "Elevated Ras/protein kinase A activity in *Saccharomyces cerevisiae* reduces proliferation rate and lifespan by two different reactive oxygen species-dependent routes." *Aging cell* 7 (2): 148-57.

Hohmann S., Neves M. J., de Koning W., Alijo R., Ramos J. and Thevelein J. M.; 1993. "The growth and signalling defects of the ggs1 (fdp1/byp1) deletion mutant on glucose are suppressed by a deletion of the gene encoding hexokinase PII." *Curr Genet.* 23 (4): 281-9.

Hohmann S., Winderickx J., de Winde J. H., Valckx D., Cobbaert P., Luyten K., de Meirsman C., Ramos J. and Thevelein J. M.; 1999. "Novel alleles of yeast hexokinase PII with distinct effects on catalytic activity and catabolite repression of SUC2." *Microbiology* 145 (Pt 3): 703-14.

Holden H. M., Thoden J. B., Timson D. J. and Reece R. J.; 2004. "Galactokinase: structure, function and role in type II galactosemia." *Cellular and molecular life science* 61 (19-20): 2471-84.

Hug H., Enari M. and Nagata S.; 1994. "No requirement of reactive oxygen intermediates in Fas-mediated apoptosis." *FEBS Letters* 351 (3): 311-313.

Hug H., Strand S., Grambihler A., Galle J., Hack V., Stremmel W., Krammer P. H. and Galle P. R.; 1997. "Reactive oxygen intermediates are Involved in the Induction of CD95 Ligand mRNA Expression by Cytostatic Drugs in Hepatoma Cells." *J. Biol. Chem.* 272(45): 28191-28193.

Kharbanda, S., Pandey O., Schofield L., Israels S., Roncinske R., Yoshida K., Bharti A., Yuan Z. M., Saxena S., Weichselbaum R., Nalin C. and Kufe D., 1997. "Role of Bcl-xL as an inhibitor of cytosolic cytochrome c accumulation in DNA damage-induced apoptosis." *Proceedings of the National Academy of Sciences of the United States of America* 94 (13): 6939-6942.

Kim C. N., Wang X., Huang Y., Ibrado A. M., Liu L., Fang G. and Bhalla K.; 1997. "Overexpression of Bcl-xL inhibits Ara-c-induced mitochondrial loss of cytochrome c and other perturbations that activate the molecular cascade of apoptosis." *Cancer Res.* 57 (15): 3115-3120.

King D. A., Hannum D. M., Qi J. S. and Hurst J. K.; 2004. "**HOCI-mediated cell death and metabolic dysfunction in the yeast *Saccharomyces cerevisiae*.**" *Arch. Biochem. Biophys.* 423 (1): 170-81.

Kitagaki H., Araki Y., Funato K. and Shimoi H.; 2007. "**Ethanol-induced death in yeast exhibits features of apoptosis mediated by mitochondrial fission pathway.**" *FEBS Lett.* 581 (16): 2935-42.

Kluck R. M., Bossy-Wetzel E., Green D. R. and Newmeyer D. D.; 1997. "**The release of cytochrome c from mitochondria: a primary site for Bcl-2 regulation of apoptosis.**" *Science* 275: 1132-1136.

Knorre D., Smirnova E. and Severin F. F.; 2005. "**Natural conditions inducing programmed cell death in the yeast *Saccharomyces cerevisiae*.**" *Biochemistry*. 70 (2): 264-6.

Kraakman L., Lemaire K., Ma P., Teunissen W., Donaton M. C., Van Dijck P., Winderickx J., de Winde J. H. and Thevelein J. M.; 1999. "**A *Saccharomyces cerevisiae* G-protein coupled receptor, Gpr1, is specifically required for glucose activation of the cAMP pathway during the transition to growth on glucose.**" *Molecular microbiology* 32 (5): 1002-12.

Kruckeberg A. L., Walsh M. C. and Van Dam K.; 1998. "**How do yeast cells sense glucose?**" *BioEssays: news and reviews in molecular, cellular and developmental biology* 20 (12): 972-6.

Lagunas R.; 1993. "**Sugar transport in *Saccharomyces cerevisiae*.**" *FEMS Microbiol Rev.* 10 (3-4): 229-42.

Leadsham J. E., Kotiadis V. N., Tarrant D. J. and Gourlay C. W.; 2010. "**Apoptosis and the yeast actin cytoskeleton.**" *Cell Death and Differentiation* 17 (5): 754-762.

Leadsham J. E., Miller K., Ayscough K. R., Colombo S., Martegani E., Sudbery P. and Gourlay C. W.; 2009. "**Whi2p links nutritional sensing to actin-dependent Ras-cAMP-PKA regulation and apoptosis in yeast.**" *Journal of cell science* 122 (Pt 5): 706-15.

Leandro M. J., Fonseca C. and Gonçalves P.; 2009. "**Hexose and pentose transport in ascomycetous yeasts: an overview.**" *FEMS yeast research* 9 (4): 511-25.

Liu X., Kim C. N., Yang J., Jemmerson R. and Wang X.; 1999. "**Induction of apoptotic program in cell-free extracts: requirement for dATP and cytochrome c.**" *Cell.* 86 (1): 147-57.

Longo V. D.; 2004. "**Ras: The Other Pro-Aging Pathway.**" *Sci. Aging Knowl. Environ* 29 (39): 36.

Longo V. D.; 2003. "**The Ras and Sch9 pathways regulate stress resistance and longevity.**" *Experimental Gerontology* 38 (7): 807-811.

Ludovico P, Madeo F. and Silva M. T.; 2005. "Yeast programmed cell death: an intricate puzzle." *IUBMB life* 57 (3): 129-35.

Ludovico P, Sousa M. J., Silva M. T., Leão C. and Côrte-Real M.; 2001. "Saccharomyces cerevisiae commits to a programmed cell death process in response to acetic acid." *Microbiology* 147 (Pt 9): 2409-15.

Madeo F., Fröhlich E., Ligr M., Grey M., Sigrist S. J., Wolf D. H. and Fröhlich K.-U.; 1999. "Oxygen Stress: A Regulator of Apoptosis in Yeast." *The Journal of cell biology* 145 (4): 757-67.

Madeo F., Fröhlich E. and Fröhlich K.-U.; 1997. "A yeast mutant showing diagnostic markers of early and late apoptosis." *The Journal of cell biology* 139 (3): 729-34.

Martinou J. C., Desagher S. and Antonsson B.; 2000. "Cytochrome c release from mitochondria: all or nothing." *Nature cell biology* 2 (3): E41-3.

Mazzoni, C. and Falcone C.; 2008. "Caspase-dependent apoptosis in yeast." *Biochim Biophys Acta*. 1783 (7): 1320-7.

Mousavi S. A. and G. Robson D.; 2003. "Entry into the stationary phase is associated with a rapid loss of viability and an apoptotic-like phenotype in the opportunistic pathogen Aspergillus fumigatus." *Fungal Genet. Biol.* 39 (3): 221-229.

Narasimhan M. L., Damsz B., Coca M. A., Ibeas J. I., Yun D. J., Pardo J. M., Hasegawa P. M. and Bressan R. A.; 2001. "A plant defense response effector induces microbial apoptosis." *Mol. Cell* 8 (4): 921-930.

Neves M. J., Hohmann S., Bell W., Dumortier F., Luyten K., Ramos J., Cobbaert P., de Koning W., Kaneva Z., Thevelein J. M.; 1995. "Control of glucose influx into glycolysis and pleiotropic effects studied in different isogenic sets of Saccharomyces cerevisiae mutants in trehalose biosynthesis." *Curr Genet.* 27 (2): 110-22.

Noubhani A., Bunoust O., Bonini B. M., Thevelein J. M., Devin A. and Rigoulet M.; 2009. "The trehalose pathway regulates mitochondrial respiratory chain content through hexokinase 2 and cAMP in Saccharomyces cerevisiae." *The Journal of biological chemistry* 284 (40): 27229-34.

Asaduzzaman M. D. and Oteborg C. G.; 2007. "Standardization of Yeast Growth Curves from Several Curves with Different Initial Sizes." *Master Thesis*.

Otterstedt K., Boles E., Hohmann S., Larsson C., Bill R. M., Sta A. and Gustafsson L.; 2004. "Switching the mode of metabolism in the yeast Saccharomyces cerevisiae." *EMBO Reports* 5 (5):532-7.

Özcan S., Dover J. and Johnston M.; 1998. “**Glucose sensing and signaling by two glucose receptors in the yeast *Saccharomyces cerevisiae***” 17 (9): 2566-2573.

Pereira C., Silva R. D., Saraiva L., Johansson B., Sousa M. J. and Côrte-Real M.; 2008. “**Mitochondria-dependent apoptosis in yeast.**” *Biochimica et biophysica acta* 1783 (7): 1286-302.

Phillips A. J., Sudbery I. and Ramsdale M.; 2003. “**Apoptosis induced by environmental stresses and amphotericin B in *Candida albicans*.**” *Proc. Natl. Acad. Sci. U.S.A.* 100 (24): 14327-14332.

Phillips A. J., Crowe J. D. and Ramsdale M.; 2006. “**Ras pathway signaling accelerates programmed cell death in the pathogenic fungus *Candida albicans*.**” *Proceedings of the National Academy of Sciences of the United States of America* 103 (3): 726-31.

Powers S., Kataoka T., Fasano O., Goldfarb M., Strathern J., Broach J. and Wigler M.; 1984. “**Genes in *S. cerevisiae* encoding proteins with domains homologous to the mammalian ras proteins.**” *Cell* 36 (3): 607-12.

Proskuryakov S. Y., Konoplyannikov A. G. and Gabai V. L.; 2003. “**Necrosis: a specific form of programmed cell death?**” *Experimental Cell Research* 283 (1): 1-16.

Purdy J. B.; 1997. “**Suicide: A Strategy for Life.**” *University of Georgia Research Magazine*.

Querin L., Sanvito R., Magni F., Busti S., Van Dorsselaer A., Alberghina L. and Vanoni M.; 2008. “**Proteomic analysis of a nutritional shift-up in *Saccharomyces cerevisiae* identifies Gvp36 as a BAR-containing protein involved in vesicular traffic and nutritional adaptation.**” *The Journal of biological chemistry* 283 (8): 4730-43.

Rintala E., Wiebe M. G., Tamminen A., Ruohonen L. and Penttilä M.; 2008. “**Transcription of hexose transporters of *Saccharomyces cerevisiae* is affected by change in oxygen provision.**” *BMC microbiology* 8: 53.

Rolland F., De Winde J. H., Lemaire K., Boles E., Thevelein J. M. and Winderickx J.; 2000. “**Glucose-induced cAMP signalling in yeast requires both a G-protein coupled receptor system for extracellular glucose detection and a separable hexose kinase-dependent sensing process.**” *Molecular Microbiology* 38 (2): 348-358.

Rolland F., Winderickx J. and Thevelein J. M.; 2001. “**Glucose-sensing mechanisms in eukaryotic cells.**” *Trends in biochemical sciences* 26 (5): 310-317.

Rolland F., Winderickx J. and Thevelein J. M.; 2002. “**Glucose-sensing and -signalling mechanisms in yeast.**” *FEMS Yeast Research* 2 (2):183-201.

Roucou X., Prescott M., Devenish R. J., Nagley P.; 2000. "A cytochrome c-GFP fusion is not released from mitochondria into the cytoplasm upon expression of Bax in yeast cells." *FEBS Letters* 471: 235-239.

Ruckenstuhl C., Carmona Gutierrez D. and Madeo F.; 2010. "The sweet taste of death: glucose triggers apoptosis during yeast chronological aging." *Review Literature And Arts Of The Americas* 2 (10): 643-649.

Santangelo G. M.; 2006. "Glucose Signaling in *Saccharomyces cerevisiae*." *Society* 70 (1): 253-282.

Schneper L., Krauss A., Miyamoto R., Fang S. and Broach J. R.; 2004. "The Ras / Protein Kinase A Pathway Acts in Parallel with the Mob2 / Cbk1 Pathway To Effect Cell Cycle Progression and Proper Bud Site Selection." *Society* 3 (1): 108-120.

Severin F. F. and Hyman A. A.; 2002. "Pheromone induces programmed cell death in *S. cerevisiae*." *Curr Biol*. 12 (7): 233-5.

Sharon A., Finkelstein A., Shlezinger N. and Hatam I.; 2009. "Fungal apoptosis: function , genes and gene function." *FEMS Microbiology Reviews* 33(5):833-54.

De Silva-udawatta M. N. and Cannon J. F.; 2001. "Roles of trehalose phosphate synthase in yeast glycogen metabolism and sporulation." *Molecular Microbiology* 40: 1345-1356.

Smith A., Ward M. P. and Garrett S.; 1998. "Yeast PKA represses Msn2p/Msn4p-dependent gene expression to regulate growth, stress response and glycogen accumulation." *The EMBO journal* 17 (13): 3556-64.

Syntichaki P. and Tavernarakis N.; 2003. "The biochemistry of neuronal necrosis: rogue biology?" *Nature Reviews Neuroscience* 4 (8): 672-684.

Tamaki H.; 2007. "Glucose-stimulated cAMP-protein kinase A pathway in yeast *Saccharomyces cerevisiae*." *Journal of bioscience and bioengineering* 104 (4): 245-50.

Tamanoi F.; 2011. "Ras Signaling in Yeast." *Vital And Health Statistics. Series 20* (3): 210 -215.

Tanaka, K., Nakafuku M., Tamanoi F., Kaziro Y., Matsumoto K. and Toh-el A.; 1990. "IRA2 , a Second Gene of *Saccharomyces cerevisiae* That Encodes a Protein with a Domain Homologous to Mammalian ras GTPase-Activating Protein." *Society* 10 (8): 4303-4313.

Tarpey M. M., Wink D. A. and Grisham M. B.; 2004. "Methods for detection of reactive metabolites of oxygen and nitrogen: in vitro and in vivo considerations." *American journal of physiology. Regulatory, integrative and comparative physiology* 286 (3): R431-44.

Tavernarakis N.; 2007. "Cardiomyocyte necrosis: alternative mechanisms, effective interventions." *Biochimica et biophysica acta* 1773 (4): 480-2.

Thevelein J. M., Cauwenberg L., Colombo S., De Winde J. H., Donation M., Dumortier F., Kraakman L., Lemaire K., Ma P., Nauwelaers D., Rolland F., Teunissen A., Van Dijck P., Versele M., Wera S., Winderickx J.; 2000. "Nutrient-induced signal transduction through the protein kinase A pathway and its role in the control of metabolism, stress resistance, and growth in yeast." *Enzyme Microb Technol.* 26 (9-10): 819-825.

Thevelein J. M.; 1984. "Regulation of Trehalose Mobilization in Fungi." *Regulation* 48 (1): 42-59.

Thevelein J. M. and De Winde J. H.; 1999. "MicroReview Novel sensing mechanisms and targets for the cAMP ± protein kinase A pathway in the yeast *Saccharomyces cerevisiae*." *Molecular Microbiology* 33: 904-918.

Thevelein J. M. and Hohmann S.; 1995. "TALKING POINT Trehalose synthase: guard to the gate of glycolysis in yeast?" *Trends Biochem. Science* 20(1):3-10.

Toda T., Broek D., Field J., Michaeli T., Cameron S., Nikawa J., Sass P., Birchmeier C., Powers S. and Wigler M.; 1986. "Exploring the function of RAS oncogenes by studying the yeast *Saccharomyces cerevisiae*." *Cold Spring Harbor Laboratory* 17: 253-60.

Tzagoloff A., Akai A. and Needleman R. B.; 1975. "Assembly of the Mitochondrial Membrane System: Characterization of nuclear mutants of *Saccharomyces cerevisiae* with defects in mitochondrial ATPase and respiratory enzymes." *The Journal of Biological Chemistry* 250 (20): 8228-8235.

Vanlangenakker N., Berghe T. V., Krysko D. V., Festjens N. and Vandenabeele P.; 2008. "Molecular Mechanisms and Pathophysiology of Necrotic Cell Death." *Current Molecular Medicine* 8 (3): 207-220.

Vermeulen K., Van Bockstaele D. R. and Berneman Z. N.; 2005. "Apoptosis: mechanisms and relevance in cancer." *Ann. Hematol.* 84: 627-639.

Wang Y., Pierce M., Schneper L., Güldal C. G., Zhang X., Tavazoie S. and Broach J. R.; 2004. "Ras and Gpa2 mediate one branch of a redundant glucose signaling pathway in yeast." *PLoS biology* 2 (5): E128

Williamson P., Bevers E. M., Smeets E. F., Comfurius P., Schlegel R. A. and Zwaal R. F.; 1995. "Continuous analysis of the mechanism of activated transbilayer lipid movement in platelets." *Biochemistry* 34 (33): 10448-55.

Wood M. D. and Sanchez Y.; 2010. "Deregulated Ras signaling compromises DNA damage checkpoint recovery in *S. cerevisiae*." *Cell Cycle* 9: 3353-63.

Yang H., Ren Q. and Zhang Z.; 2008. “**Cleavage of Mcd1 by Caspase-like Protease Esp1 Promotes Apoptosis in Budding Yeast.**” *Molecular Biology of the Cell* 19: 2127-2134.

Yang J., Liu X., Bhalla K., Kim C. N., Ibrado A. M., Cai J., Peng T.-I., Jones D. P. and Wang X.; 1997. “**Prevention of apoptosis by Bcl-2: release of cytochrome c from mitochondria blocked.**” *Science* 275: 1129-1132.

Zhu X., Démolis N., Jacquet M. and Michaeli T.; 2000. “**MSI1 suppresses hyperactive RAS via the cAMP-dependent protein kinase and independently of chromatin assembly factor-1.**” *Curr Genet.* 38 (2): 60-70.

ANEXO I – SOLUTIONS

1	TE Buffer	6	ST-PMSF
			<ul style="list-style-type: none">• 10mM Tris-HCl pH 8• 1 mM EDTA
2	TAE Buffer 10x (1% agarose)		<ul style="list-style-type: none">• 1,2 M Sorbitol• 20 mM Tris HCl pH 7,5• 1 mM EDTA• 0,2 M PMSF• 1 tablet Protease inhibitor/10 ml (Roche)
		7	Phosphate buffered saline (PBS)
	<ul style="list-style-type: none">• 0,4M Tris• 0,2 M Acetic acid• 10 mM EDTA		<ul style="list-style-type: none">• 137 mM NaCl• 2,7 mM KCl• 8,1 mM $\text{Na}_2\text{HPO}_4 \cdot 2 \text{ H}_2\text{O}$• 1,76 mM KH_2PO_4 pH 7,4
3	Digestion Buffer (cyt c)	8	Lysis Buffer (Immunoprecipitation)
	<ul style="list-style-type: none">• 1,2 M Sorbitol• 60 mM Potassium Phosphate pH 7,5• 1 mM EDTA• 15 mM Mercaptoethanol• 1 mg Zymolyase 20T		<ul style="list-style-type: none">• 1% Triton X-100• 120 mM NaCl• 50 mM Tris-HCl pH 7,4• 2 mM EDTA• 10% Glycerol• Protease inhibitor• 1 mM PMSF
4	Lyticase Buffer	9	Wash Buffer (Immunoprecipitation)
	<ul style="list-style-type: none">• 1,2 M Sorbitol• 35 mM Potassium buffer pH 6,8• 0,5 mM MgCl_2• Lyticase (120 U/ml Lyticase buffer)		<ul style="list-style-type: none">• 0,1% Triton X-100• 120 mM NaCl• 50 mM Tris-HCl pH 7,4• 2 mM EDTA• 10% Glycerol
5	Annexin Buffer		
	<ul style="list-style-type: none">• 1,2 M Sorbitol• 10 mM HEPES/NaOH pH 7,4• 140 mM NaCl• 5 mM CaCl_2		

10	Protein sample buffer 5x	15	Milk solution
	<ul style="list-style-type: none"> • 250 mM Tris pH 8 • 50 mM β-mercapto-ethanol • 10% SDS • 0.5% bromophenol blue • 50% glycerol 		<ul style="list-style-type: none"> • 5% powdered skimmed milk • TBST (see 3.12)
11	TBS 10x	16	Lysis buffer (RAS)
	<ul style="list-style-type: none"> • 200 mM Tris HCl pH 8 • 1.5 M NaCl 		<ul style="list-style-type: none"> • 25mM HEPES • 150mM sodium chloride • 1% Non-Idet P-40 • 0.25% sodium deoxycholate • 1mM EDTA • 1mM sodium vanadate • 10% glycerol • 25mM sodium fluoride • 10mM magnesium chloride • 1 tablet of protease inhibitor (Roche)
12	TBST	17	Wash buffer (RAS)
	<ul style="list-style-type: none"> • 1 x TBS (see 3.11) • 0.05% v/v Tween 20 		<ul style="list-style-type: none"> • 1 x PBS • 0.1% Triton • 2 mM magnesium chloride • 1 mM EDTA • 1 mM DDT
13	MOPS Running buffer (NuPage® 20x, Invitrogen)	14	MOPS Blotting buffer
	<ul style="list-style-type: none"> • 50 mM MOPS • 50 mM Tris Base • 0.1% SDS • 1 mM EDTA, pH 7.7 		<ul style="list-style-type: none"> • 20% methanol • 1x MOPS running buffer (see 3.13)